PHYSICAL REVIEW D **92,** 125032 (2015)

Eikonal approximation, Finsler structures, and implications for Lorentz-violating photons in weak gravitational fields

M. Schreck*

Indiana University Center for Spacetime Symmetries, Indiana University, Bloomington, Indiana 47405-7105, USA

(Received 13 August 2015; published 29 December 2015)

In the current article, the classical analog of the minimal photon sector in the Lorentz-violating Standard-Model extension (SME) is investigated. The analysis is based on describing a photon classically by a geometric ray that satisfies the eikonal equation. The action principle, which leads to the eikonal equation in conventional optics, is demonstrated to work in most (but not all) Lorentz-violating cases as well. Furthermore it is found that the integrands of the action functional correspond to Finsler structures. Based on these results, Lorentz-violating light rays in a weak gravitational background are treated through the use of the minimal-coupling principle. This allows for obtaining sensitivities on Lorentz violation in the photon sector by measurements of light bending at massive bodies such as the Sun. The computations are carried out for the currently running ESA mission GAIA and the planned NASA/ESA mission LATOR. Finally, a range of aspects of explicit Lorentz violation for photons is discussed in the Finsler setting.

DOI: 10.1103/PhysRevD.92.125032 PACS numbers: 11.30.Cp, 02.40.-k, 11.80.Fv, 42.15.-i

I. INTRODUCTION

During the past 15 years, plenty of progress has been made in understanding *CPT* and Lorentz violation and its possible implications on physics from both a theoretical and a phenomenological point of view. This was made possible by establishing the Standard-Model extension (SME) in 1998 [1] and by the subsequent tireless work of people in our community eager to study imprints of Planck-scale physics detectable by experiments operating at much smaller energies. The SME is a powerful framework incorporating all Lorentz-violating operators into the Standard Model of elementary particles and general relativity. It neither modifies the gauge structure of the Standard Model nor does it introduce new particles. The power-counting renormalizable contributions of the SME are grouped into its minimal part where the remaining higher-order operators comprise the nonminimal SME [2–4]. This framework allows for astounding experimental tests of Lorentz invariance and some present experiments even reach a sensitivity of the Planck scale square (see [5] for a yearly updated compilation of experimental constraints on Lorentz-violating coefficients). Since *CPT* violation implies Lorentz violation according to a theorem by Greenberg [6], the Standard-Model extension involves all *CPT*-odd operators as a subset. Note that Lorentz violation has been predicted by various prototypes of fundamental theories such as string theory [7–9], loop quantum gravity [10,11], noncommutative spacetime [12,13], spacetime foam [14–16], and models with nontrivial spacetime topology [17,18].

In the recent past, profound studies of modified quantum field theories based on the SME were performed at tree-level and beyond, i.e., including quantum corrections. The result of these studies is that most sectors are free of any inconsistencies [19–33]. Furthermore, parts of the SME were explicitly shown to be renormalizable at one loop [34–38]. Latest computations have even demonstrated renormalizability of the modified quantum electrodynamics [39] and the pure Yang-Mills sector [40] at infinite-loop order using algebraic techniques. Therefore as long as the SME is restricted to Minkowski spacetime, it seems to be a reasonable, well-behaved, and model-independent test framework for Planck-scale physics.

The gravitational sector of the SME was constructed in the seminal article [41]. In the aftermath, studies of its theory and phenomenology were performed in a series of papers [42–51] with recent investigations of even nonminimal operators in short-range gravity tests [52,53]. One of the most important theoretical results of [41] is a no-go theorem stating that explicit Lorentz violation is incompatible with the geometric framework of general relativity, which is Riemannian geometry. Considering Lorentz-violating matter in a gravitational background results in modified conservation laws of the energy-momentum tensor based on Noether's theorem. However, Lorentz violation does *a priori* not modify the geometrical base such as the Bianchi identities of the Riemann curvature tensor. Due to the Einstein equations the second Bianchi identity is tightly bound to the conservation of energy-momentum, which is then incompatible with the modified matter sector.

A possibility of circumventing this clash is to perform phenomenological studies in theories resting on

*mschreck@indiana.edu

spontaneous Lorentz violation. This means that a Lorentz-violating background field arises dynamically as the vacuum expectation value of a vector or tensor field. Such models have been studied since the early 1990s [7,54–58] (even before the SME existed) and they can be considered as one of the motivations that lead to the construction of the SME. The crucial point within models of spontaneous Lorentz violation is to take into account the Nambu-Goldstone modes that are linked to the symmetry breaking. This can lead to arduous perturbative calculations within such a theory.

For these reasons, it would be preferable to have a setup available that allows for incorporating explicit Lorentz violation into a curved background without possible tensions with the underlying geometrical properties. A suggestion was already given in [41] along the same lines as the no-go theorem: introducing an alternative geometrical framework that can include preferred directions naturally. Such an extension of Riemannian geometry has been known in the mathematics community for almost 100 years. It is named Finsler geometry in reference to the famous mathematician Finsler who studied generalized path length functionals in his Ph.D. thesis [59,60] (cf. [61] for a comprehensive mathematical overview on the subject).

Finsler geometry has been applied to various fields of physics [62]. In the context of the Standard-Model extension, it found its use just a couple of years ago when it was shown that the minimal Lorentz-violating fermion sector can be mapped to classical-particle descriptions [63–67]. The corresponding Lagrange functions are closely linked to Finsler structures, i.e., generalized path length functionals. Recently a nonminimal case was studied [68] as well as classical-particle trajectories in electromagnetic fields and modified spin precession based on an isotropic set of minimal fermion coefficients [69]. In [70] a particular class of Finsler spaces known as bipartite is investigated closer from a physics point of view and [71] suggests classical-mechanics systems that are linked to three-dimensional versions of Finsler b space [64]. In a very recent paper [72] b space is discussed from a mathematical point of view. Its indicatrix (surface of constant value of the Finsler structure) is a two-valued deformation from a sphere that is characterized by singularities with ambiguous derivatives. Considering the indicatrix as an algebraic variety, the Hironaka theorem says that such singularities can be removed [73]. In [72] a coordinate transformation was found, which allows one to remove the singular sets and to glue the remaining parts together appropriately. This results in a well-defined mathematical description of b space that can be used for future physical investigations.

The goals of the current article are threefold. First, analogous classical equivalents for the minimal CPT-even photon sector of the SME will be found. Second, with these equivalents at hand we study phenomenological aspects of Lorentz-violating photons in weak gravitational fields. Last but not least various consequences of this approach will be drawn based on Finsler geometry. The procedures to be developed will differ extensively from the SME fermion counterparts.

The paper is organized as follows. In Sec. II the Lorentz-violating framework, which all investigations are based on, is introduced. A brief review on Finsler geometry and Finsler structures in the SME fermion sector is given in Sec. III, followed by an explanation of the method to constructing Finsler structures in the photon sector. In that section we investigate different cases that are the most interesting ones from a physics point of view. In the geometric-optics approximation photons are described by the eikonal equation, which forms the cornerstone of Sec. IV. It is demonstrated how the Finsler structures obtained are linked to the eikonal equation for the different sectors analyzed in the previous section. Since the isotropic modification of the CPT-even sector can be considered to be the most important one, all forthcoming studies will be based on the latter. Section V is dedicated to investigating the isotropic eikonal equation in a weak gravitational background. We develop a phenomenological framework to study light bending at massive bodies within such a theory. In this context, prospects are given on detecting isotropic Lorentz violation of photons propagating in a gravitational background. This is carried out for two space-based missions: GAIA and LATOR. The final part of the paper is more theoretical. In Sec. VI the modified conservation law of the energy-momentum tensor is investigated, interpreting the results from the point of view of explicit versus spontaneous Lorentz violation. Last but not least, in Sec. VII we examine the properties of the isotropic spacetime studied in Sec. V from a Finsler-geometric point of view. The most important findings in total are concluded on and discussed in Sec. VIII. Essential calculational details can be found in Appendixes A to C. Throughout the article natural units with $\hbar = c = 1$ are chosen unless otherwise stated.

II. CONSTRUCTION OF CLASSICAL LAGRANGIANS

The base of the current article is formed by the minimal SME photon sector whose action S_γ is comprised of CPT-even modified Maxwell (mM) [1,74,75] theory and CPT-odd Maxwell-Chern-Simons (MCS) theory [1,74–76]:

$$S_\gamma = \int_{\mathbb{R}^4} \mathrm{d}^4x[\mathcal{L}_{\mathrm{mM}}(x) + \mathcal{L}_{\mathrm{MCS}}(x) + \mathcal{L}_{\mathrm{mass}}(x)], \tag{2.1a}$$

$$\mathcal{L}_{\mathrm{mM}}(x) = -\frac{1}{4}\eta^{\mu\rho}\eta^{\nu\sigma}F_{\mu\nu}(x)F_{\rho\sigma}(x) - \frac{1}{4}(k_F)^{\mu\nu\varrho\sigma}F_{\mu\nu}(x)F_{\varrho\sigma}(x), \tag{2.1b}$$

$$\mathcal{L}_{\mathrm{MCS}}(x) = \frac{1}{2}m_{\mathrm{CS}}(k_{AF})^\kappa\varepsilon_{\kappa\lambda\mu\nu}A^\lambda(x)F^{\mu\nu}(x), \tag{2.1c}$$

$$\mathcal{L}_{\text{mass}}(x) = \frac{1}{2} m_\gamma^2 A_\mu(x) A^\mu(x). \tag{2.1d}$$

Here $F_{\mu\nu}(x) \equiv \partial_\mu A_\nu(x) - \partial_\nu A_\mu(x)$ is the electromagnetic field strength tensor that involves the $U(1)$ gauge field $A_\mu(x)$. The fields are defined in Minkowski spacetime with metric $(\eta_{\mu\nu}) = \text{diag}(1, -1, -1, -1)$. The totally antisymmetric Levi-Civita symbol in four spacetime dimensions is denoted as $\varepsilon^{\mu\nu\varrho\sigma}$ with $\varepsilon^{0123} = 1$. The controlling coefficients characteristic for the framework considered are comprised in the fourth-rank observer tensor $(k_F)^{\mu\nu\varrho\sigma}$ and the observer vector $(k_{AF})^\kappa$. Both have dimensionless components and they do not transform covariantly with respect to particle Lorentz transformations, which renders this theory explicitly Lorentz-violating. The field operator of modified Maxwell theory is of dimension four, whereas the operator of MCS theory has mass dimension three. Therefore, MCS theory involves the Chern-Simons mass scale m_{CS} for dimensional consistency.

It is well known that a photon mass term encoded in $\mathcal{L}_{\text{mass}}$ (with the photon mass m_γ) violates $U(1)$ gauge invariance. It has been introduced here for certain purposes that will be explained below, but for most occasions m_γ will be set to zero. Anyhow in [26] it was demonstrated that certain birefringent cases of modified Maxwell theory require a nonvanishing photon mass (at least in intermediate calculations) to have a consistent Gupta-Bleuler quantization. Finally, a gauge fixing term will be omitted in the action, since all considerations will be carried out at the classical level.

In the first years of the SME, several people demonstrated that an MCS term can arise radiatively at one-loop level by imposing a nonvanishing CPT-odd b_μ-term in the fermion sector. The generated contribution is ambiguous, i.e., its global prefactor depends on the regularization scheme [77–82]. Similarly, more recent developments show that modified-Maxwell terms arise through radiative corrections based on a CPT-odd Yukawa-type coupling in the fermion sector with what is known as an "aether field" [83,84].

A. Classical Lagrangians and Finsler structures

The major goal is to understand how Lorentz-violating photons can be described in the context of gravity. Since Einstein's relativity is a classical theory, it is reasonable to obtain a classical analog of the quantum field theory based on the action of Eq. (2.1). With such an analog at hand, it should be possible to study how an explicitly Lorentz-violating theory of gravity could be constructed consistently. As an introduction to the topic, the mapping procedure of the SME fermion sector to a classical point-particle description [63] shall be reviewed. From a quantum theoretical point of view a particle can be understood as a suitable superposition of free-field solutions with dispersion relation

$$f(p_\mu, m_\psi, k_x) = 0, \qquad (p_\mu) = \begin{pmatrix} p_0 \\ \mathbf{p} \end{pmatrix}, \tag{2.2}$$

such that its probability density is nonzero in a localized region and drops off to zero sufficiently fast outside. Here p_0 is the particle energy, $\mathbf{p}$ its three-momentum, m_ψ the fermion mass, and k_x denotes a particular set of Lorentz-violating coefficients where x represents a Lorentz index structure. The physical propagation velocity of such a wave packet is the group velocity

$$\mathbf{v}_{\text{gr}} \equiv \frac{\partial p_0}{\partial \mathbf{p}}. \tag{2.3}$$

A classical, relativistic pointlike particle is assumed to propagate with four-velocity $u^\mu = \gamma(1, \mathbf{v})$ where $\mathbf{v}$ is the three-velocity. To map the wave packet to such a classical particle, it makes sense to identify the group velocity components with the appropriate spatial four-velocity components:

$$\mathbf{v}_{\text{gr}} \stackrel{!}{=} -\frac{\mathbf{u}}{u^0}. \tag{2.4}$$

The minus sign has its origin in the different position of the spatial index on both sides of the equation. Since the physics of the classical particle rests on a Lagrange function $L = L(u^0, \mathbf{u})$, its construction is of paramount importance. If the Lagrange function is positively homogeneous of degree one, i.e., $L(\lambda u^0, \lambda \mathbf{u}) = \lambda L(u^0, \mathbf{u})$ for $\lambda > 0$, the action is parametrization-invariant. In this case, the physics does not depend on the way the particle trajectory is parametrized, which is a very reasonable property to have. Positive homogeneity gives the following condition on the Lagrange density according to Euler's theorem [61]:

$$L = -p_\mu u^\mu, \qquad p_\mu = -\frac{\partial L}{\partial u^\mu}, \tag{2.5}$$

with the conjugate momentum p_μ. The latter is identified with the momentum that appears in the quantum theoretical dispersion relation of Eq. (2.2). The global minus sign in its definition has been introduced such that the nonrelativistic kinetic energy is positive. Now Eqs. (2.2), (2.4), and (2.5) comprise a set of five conditions that shall be used to determine p_μ and L. Hence, all four-momentum components and the Lagrange function are supposed to be solely expressed in terms of four-velocity components.

The Lagrange functions corresponding to the standard fermion dispersion law $p_0^2 - \mathbf{p}^2 - m_\psi^2 = 0$ read $L = \pm m_\psi \sqrt{(u^0)^2 - \mathbf{u}^2}$. The two signs are the classical counterparts of the particle-antiparticle solutions at the level of quantum field theory. It can be checked that the five equations above are fulfilled for this choice of L. The latter can also be written in the form $L = \pm m_\psi \sqrt{r_{\mu\nu} u^\mu u^\nu}$

with $r_{\mu\nu}$ known as the intrinsic metric. This metric is essential to determine lengths of vectors and angles enclosed by vectors. In the particular case considered it corresponds to the (indefinite) Minkowski metric: $r_{\mu\nu} = \eta_{\mu\nu}$. This is not surprising since the starting point to obtaining the Lagrange function was a field theory defined in Minkowski spacetime. By a Wick rotation the Lagrange function is related to a new function F based on a positive definite intrinsic metric:

$$F(y) \equiv F(\mathbf{y}, y^4) \equiv \frac{\mathrm{i}}{m_\psi} L(\mathrm{i}y^4, \mathbf{y}) = \sqrt{r_{ij} y^i y^j},$$
$$r_{ij} = \mathrm{diag}(1,1,1,1)_{ij}. \tag{2.6}$$

Promoting r_{ij} to an arbitrary position-dependent metric $r_{ij}(x)$, the function F becomes dependent on x: $F(y) \mapsto F(x,y)$. It can then be interpreted as the integrand of a path length functional of a Riemannian manifold M where $y \in T_x M$. A Finsler structure is a generalization of that obeying the following properties:

(1) $F(x,y) > 0$,
(2) $F(x,y) \in C^\infty$ for all $y \in T_x M \backslash \{\text{slits}\}$,
(3) positive homogeneity in y, i.e., $F(x,\lambda y) = \lambda F(x,y)$ for $\lambda > 0$, and
(4) the derived metric (Finsler metric)

$$g_{ij} \equiv \frac{1}{2} \frac{\partial^2 F^2}{\partial y^i \partial y^j}, \tag{2.7}$$

is positive definite.

Prominent examples for Finsler structures that are outside the scope of Riemannian geometry are Randers structures, $F(y) = \alpha + \beta$, and Kropina structures, $F(y) = \alpha^2/\beta$, with $\alpha = \sqrt{a_{ij} y^i y^j}$ and $\beta = b_i y^i$ where a_{ij} is a Riemannian metric and b_i a one-form. There are certain theorems available to classify Finsler structures using various kinds of torsions. The most important one is the Cartan torsion C_{ijk}, which is given by [85]

$$C_{ijk} \equiv \frac{1}{2} \frac{\partial g_{ij}}{\partial y^k} = \frac{1}{4} \frac{\partial^3 F^2}{\partial y^i \partial y^j \partial y^k}. \tag{2.8}$$

In some books, C_{ijk} is defined with an additional prefactor F (see, e.g., [61]). The mean Cartan torsion reads as follows:

$$I_i \equiv g^{jk} C_{ijk}, \qquad (g^{ij}) \equiv (g_{ij})^{-1}, \tag{2.9}$$

with the inverse derived metric g^{ij}. Deicke's theorem says that a Finsler space is Riemannian if and only if I_i vanishes [86]. The Matsumoto torsion provides a further set of quantities that are very useful to classify Finsler structures:

$$M_{ijk} \equiv C_{ijk} - \frac{1}{n+1}(I_i h_{jk} + I_j h_{ik} + I_k h_{ij}),$$
$$h_{ij} \equiv F \frac{\partial^2 F}{\partial y^i \partial y^j}. \tag{2.10}$$

Here n is the dimension of the Finsler structure considered [85]. According to the Matsumoto-Hōjō theorem, a Finsler structure is either of Randers or Kropina type if and only if the Matsumoto torsion is equal to zero [87]. These theorems will be used frequently throughout the paper to classify Finsler structures encountered.

Following the rules recalled at the beginning of the current section classical Lagrange functions of the SME fermion sector were derived in [63,66–69]. In the articles [64–66,68] their corresponding Finsler structures were examined. In this paper, analogous investigations shall be performed for the minimal SME photon sector based on the action of Eq. (2.1). It will become evident that the possible techniques used differ from the procedures adopted for the fermion sector.

B. Maxwell-Chern-Simons theory

In the current section, the CPT-even photon sector components $(k_F)^{\mu\nu\varrho\sigma}$ in Eq. (2.1b) will be set to zero restricting our considerations to the MCS term of Eq. (2.1c) only. Furthermore, the photon mass m_γ will be set to zero as well. In the seminal article [76] the magnitude of $m_{\mathrm{CS}}(k_{AF})^\kappa$ was constrained tightly due to the absence of astrophysical birefringence. A collection of all constraints on components of $m_{\mathrm{CS}}(k_{AF})^\kappa$ can be found in the data tables [5]. In spite of the tight bounds, MCS theory is very interesting from a theoretical point of view. The structure of the quantum field theory based on MCS theory is quite involved, which was shown by extensive investigations carried out in [20].[1] The smoking-gun results of the latter reference are that MCS theory is well behaved as long as the preferred spacetime direction $(k_{AF})^\kappa$ is spacelike. Issues with either microcausality or unitarity arise for timelike $(k_{AF})^\kappa$, though. Interestingly, this behavior mirrors in the classical Finsler structure of MCS theory that will be derived as follows. First of all spacelike MCS theory shall be considered. The modified field equations in momentum space read as follows [1]:

$$M^{\alpha\delta}(p) A_\delta = 0, \tag{2.11a}$$

$$M^{\alpha\delta}(p) = \eta^{\alpha\delta} k^2 - k^\alpha k^\delta - 2\mathrm{i} m_{\mathrm{CS}} (k_{AF})_\beta \varepsilon^{\alpha\beta\gamma\delta} k_\gamma, \tag{2.11b}$$

where k_μ is the four-momentum to be distinguished from the four-momentum p_μ used for fermions. Imposing Lorenz gauge $k^\delta A_\delta = 0$, the condition of a vanishing determinant of M results in

[1]Note that the global prefactor of MCS theory is different in the latter reference.

$$k^4 + 4m_{\mathrm{CS}}^2[k^2(k_{AF})^2 - (k\cdot k_{AF})^2] = 0, \tag{2.12}$$

leading to the following dispersion relations:

$$\omega_{1,2} = \sqrt{\mathbf{k}^2 + 2m_{\mathrm{CS}}^2(\mathbf{k}_{AF})^2 \pm 2m_{\mathrm{CS}}\sqrt{m_{\mathrm{CS}}^2(\mathbf{k}_{AF})^4 + (\mathbf{k}\cdot\mathbf{k}_{AF})^2}}. \tag{2.13}$$

Here the spatial momentum $\mathbf{k}$ is not to be confused with the spatial part $\mathbf{k}_{AF}$ of the MCS vector. Following the procedure outlined in Appendix A 2 leads to the Lagrange function

$$L|^{\pm}_{\mathrm{MCS}} = \pm m_{\mathrm{CS}}(\sqrt{-(k_{AF})^2u^2} \pm \sqrt{(k_{AF}\cdot u)^2 - (k_{AF})^2u^2}). \tag{2.14}$$

First of all, this result matches the Lagrange function first obtained in [88]. For spacelike k_{AF} it corresponds to the Lagrangian of the minimal fermionic b^μ coefficient where here $(k_{AF})^\mu$ takes the role of b^μ and the Chern-Simons mass m_{CS} takes the role of the fermion mass m_ψ. This is because there exists a correspondence between MCS theory and the fermion theory involving the b^μ coefficient whose Lagrange density has the form $b^\mu\bar{\psi}\gamma_5\gamma_\mu\psi$. The associated field operator is of dimension three and it is CPT-odd [2], which parallels some of the properties of MCS theory. Therefore the Wick-rotated version of Eq. (2.14) can be interpreted as a b space. The form of the Lagrangian of Eq. (2.14) remains the same even for MCS theory with a timelike k_{AF}, which can be shown by direct computation. Undoubtedly, issues arise for timelike k_{AF}, since in this case the Lagrange function is not a real function anymore.

A classical Lagrange function is of mass dimension one, which is why Eq. (2.14) is directly proportional to the single mass scale m_{CS} that appears in this framework. In the limit $m_{\mathrm{CS}} \mapsto 0$ the Lagrange function vanishes, which reveals the challenge in deriving appropriate Lagrange functions corresponding to Lorentz-violating frameworks that do not have a dimensional scale associated with them. This is especially the case for a photon theory based on modified Maxwell theory, which will be discussed as follows.

C. Modified Maxwell theory

In the remainder of the paper, the Chern-Simons mass m_{CS} will be set to zero and the Lagrange density of MCS theory, Eq. (2.1c), will not be taken into account anymore. The observer four-tensor $(k_F)^{\mu\nu\varrho\sigma}$ in Eq. (2.1b) will be decomposed into contributions involving the Minkowski metric and a (4×4) matrix $\tilde{\kappa}^{\mu\nu}$ according to the nonbirefringent *Ansatz* [75,89]

$$(k_F)^{\mu\nu\varrho\sigma} = \frac{1}{2}(\eta^{\mu\varrho}\tilde{\kappa}^{\nu\sigma} - \eta^{\mu\sigma}\tilde{\kappa}^{\nu\varrho} - \eta^{\nu\varrho}\tilde{\kappa}^{\mu\sigma} + \eta^{\nu\sigma}\tilde{\kappa}^{\mu\varrho}). \tag{2.15}$$

The matrix $\tilde{\kappa}^{\mu\nu}$ is supposed to be symmetric and traceless. Its particular choice amounts to different Lorentz-violating cases in the minimal, CPT-even photon sector characterized by nonbirefringent photon dispersion laws at first order in the Lorentz-violating coefficients. This means that resulting dispersion relations for the two physical photon polarization states coincide with each other at first order in Lorentz violation. The notation—especially for the controlling coefficients—is mainly based on [74].

First of all the photon mass is kept. The equations of motion for the photon field A_μ in momentum space then take the following form [1,88]:

$$M^{\alpha\delta}(k)A_\delta = 0, \tag{2.16a}$$

$$M^{\alpha\delta}(k) = \eta^{\alpha\delta}(k^2 - m_\gamma^2) - k^\alpha k^\delta - 2(k_F)^{\alpha\beta\gamma\delta}k_\beta k_\gamma. \tag{2.16b}$$

Now different interesting cases of modified Maxwell theory (including a photon mass term) will be examined. The simplest case is undoubtedly the isotropic one, which is characterized by a single controlling coefficient $\tilde{\kappa}_{\mathrm{tr}}$ and one preferred timelike spacetime direction ξ^μ. The matrix $\tilde{\kappa}^{\mu\nu}$ is then diagonal and it is given as follows:

$$\tilde{\kappa}^{\mu\nu} = 2\tilde{\kappa}_{\mathrm{tr}}\left(\xi^\mu\xi^\nu - \frac{1}{4}\xi^2\eta^{\mu\nu}\right) = \frac{3}{2}\tilde{\kappa}_{\mathrm{tr}}\mathrm{diag}\left(1,\frac{1}{3},\frac{1}{3},\frac{1}{3}\right)^{\mu\nu}, \tag{2.17a}$$

$$(\xi^\mu) = (1,0,0,0)^T. \tag{2.17b}$$

The dispersion equation, which follows from claiming a vanishing determinant of $M^{\alpha\delta}$ in Eq. (2.16) using Lorenz gauge $k^\delta A_\delta = 0$, results in

$$m_\gamma^2 = a^{\mu\nu}k_\mu k_\nu, \tag{2.18a}$$

$$a^{\mu\nu} = \mathrm{diag}(1+\tilde{\kappa}_{\mathrm{tr}}, -[1-\tilde{\kappa}_{\mathrm{tr}}], -[1-\tilde{\kappa}_{\mathrm{tr}}], -[1-\tilde{\kappa}_{\mathrm{tr}}])^{\mu\nu}. \tag{2.18b}$$

The next case to be considered is a nonbirefringent, anisotropic one that is characterized by a single (parity-even) controlling coefficient $\tilde{\kappa}_{e-}^{11}$ and one spacelike direction ζ^μ. Furthermore $\tilde{\kappa}_{e-}^{22} = \tilde{\kappa}_{e-}^{11}$, $\tilde{\kappa}_{e-}^{33} = -2\tilde{\kappa}_{e-}^{11}$ and all remaining ones vanish. The matrix $\tilde{\kappa}^{\mu\nu}$ for the nonbirefringent *Ansatz* is given as follows:

$$\tilde{\kappa}^{\mu\nu} = 3\tilde{\kappa}_{e-}^{11}\left(\zeta^\mu\zeta^\nu - \frac{1}{4}\zeta^2\eta^{\mu\nu}\right) = \frac{3}{4}\tilde{\kappa}_{e-}^{11}\mathrm{diag}(1,-1,-1,3)^{\mu\nu}, \tag{2.19a}$$

$$(\zeta^\mu) = (0,0,0,1)^T. \tag{2.19b}$$

The latter has a similar structure compared to Eq. (2.17a) and it is again diagonal. However, its spatial coefficients differ from each other revealing the anisotropy. The modified photon dispersion equation can be written in the same form as for the isotropic case:

$$m_\gamma^2 = b^{\mu\nu}k_\mu k_\nu, \tag{2.20a}$$

$$b^{\mu\nu} = \mathrm{diag}\left(1+\frac{3}{2}\tilde{\kappa}_{e-}^{11}, -\left[1+\frac{3}{2}\tilde{\kappa}_{e-}^{11}\right], -\left[1+\frac{3}{2}\tilde{\kappa}_{e-}^{11}\right], -\left[1-\frac{3}{2}\tilde{\kappa}_{e-}^{11}\right]\right)^{\mu\nu}. \tag{2.20b}$$

The third particular case of modified Maxwell theory to be examined in this context is characterized by three (parity-odd) controlling coefficients $\tilde{\kappa}_{o+}^{23}$, $\tilde{\kappa}_{o+}^{31}$, and $\tilde{\kappa}_{o+}^{12}$ where all remaining ones that are not related by symmetries vanish. Furthermore, there are two preferred spacetime directions: a timelike direction ξ^μ and a spacelike one ζ^μ. The matrix $\tilde{\kappa}^{\mu\nu}$ in the nonbirefringent *Ansatz* can be cast into

$$\tilde{\kappa}^{\mu\nu} = \frac{1}{2}(\xi^\mu\zeta^\nu + \zeta^\mu\xi^\nu) - \frac{1}{4}(\xi\cdot\zeta)\eta^{\mu\nu}, \tag{2.21a}$$

$$(\xi^\mu) = (1,0,0,0)^T, \qquad (\zeta^\mu) = -2(0,\boldsymbol{\zeta})^T, \qquad \boldsymbol{\zeta} = (\tilde{\kappa}_{o+}^{23}, \tilde{\kappa}_{o+}^{31}, \tilde{\kappa}_{o+}^{12})^T. \tag{2.21b}$$

Due to observer Lorentz invariance the coordinate system can be set up such that $\boldsymbol{\zeta}$ points along its third axis. The first photon dispersion equation is quadratic and reads as follows:

$$m_\gamma^2 = c^{\mu\nu}k_\mu k_\nu, \tag{2.22a}$$

$$c^{\mu\nu} = \begin{pmatrix} 1 & 0 & 0 & -\mathcal{E} \\ 0 & -1 & 0 & 0 \\ 0 & 0 & -1 & 0 \\ -\mathcal{E} & 0 & 0 & -1 \end{pmatrix}^{\mu\nu}, \qquad \mathcal{E} = \sqrt{(\tilde{\kappa}_{o+}^{23})^2 + (\tilde{\kappa}_{o+}^{31})^2 + (\tilde{\kappa}_{o+}^{12})^2}. \tag{2.22b}$$

Note that the latter has an equivalent structure to Eqs. (2.18a), (2.20a). However, the second dispersion equation is quartic and it is given by

$$0 = (k^2 - m_\gamma^2)^2 - (k\cdot\zeta)(k\cdot\xi)(k^2 - m_\gamma^2) + \frac{1}{4}\{(k\cdot\zeta)^2 + \zeta^2[(k\cdot\xi)^2 - k^2]\}k^2. \tag{2.23}$$

For $m_\gamma = 0$ the right-hand side of the latter factorizes into k^2 and a quadratic dispersion relation that differs from Eq. (2.22) (for $m_\gamma = 0$) at second order in the controlling coefficients. The nonbirefringent *Ansatz* of Eq. (2.15) prevents birefringence to occur only at leading order in Lorentz violation.

Now the classical Lagrange functions for all cases previously introduced are given as follows. The derivation for one particular of those is shown in Appendix A 1 and it works analogously for the remaining ones. For the isotropic case (denoted as ⊙) the Lagrange functions read

$$L|_\odot^\pm = \pm m_\gamma\sqrt{a_{\mu\nu}u^\mu u^\nu}, \tag{2.24a}$$

$$(a_{\mu\nu}) = \mathrm{diag}\left(\frac{1}{1+\kappa_{\mathrm{tr}}}, -\frac{1}{1-\kappa_{\mathrm{tr}}}, -\frac{1}{1-\kappa_{\mathrm{tr}}}, -\frac{1}{1-\kappa_{\mathrm{tr}}}\right) = (a^{\mu\nu})^{-1}. \tag{2.24b}$$

For the nonbirefringent, anisotropic case (⦶) they are given by

$$L|_⦶^\pm = \pm m_\gamma\sqrt{b_{\mu\nu}u^\mu u^\nu}, \tag{2.25a}$$

$$(b_{\mu\nu}) = \mathrm{diag}\left(\frac{1}{1+(3/2)\tilde{\kappa}_{e-}^{11}}, -\frac{1}{1+(3/2)\tilde{\kappa}_{e-}^{11}}, -\frac{1}{1+(3/2)\tilde{\kappa}_{e-}^{11}}, -\frac{1}{1-(3/2)\tilde{\kappa}_{e-}^{11}}\right) = (b^{\mu\nu})^{-1}. \tag{2.25b}$$

Finally for the first dispersion relation of the parity-odd case (⊗) we obtain

$$L|_\otimes^\pm = \pm m_\gamma\sqrt{c_{\mu\nu}u^\mu u^\nu}, \tag{2.26a}$$

$$(c_{\mu\nu}) = \begin{pmatrix} 1/(1+\mathcal{E}^2) & 0 & 0 & -\mathcal{E}/(1+\mathcal{E}^2) \\ 0 & -1 & 0 & 0 \\ 0 & 0 & -1 & 0 \\ -\mathcal{E}/(1+\mathcal{E}^2) & 0 & 0 & -1/(1+\mathcal{E}^2) \end{pmatrix} = (c^{\mu\nu})^{-1}. \tag{2.26b}$$

Finding a classical Lagrangian that corresponds to the quartic dispersion equation of Eq. (2.23) is a challenging task that we leave for the future. The examples for Lagrange functions of Lorentz-violating photons in Eq. (2.24a), Eq. (2.25a), and Eq. (2.26a) reveal the general behavior. When the photon dispersion equation is of the

form $Q^{\mu\nu}k_\mu k_\nu = m_\gamma^2$ with an invertible (4×4) matrix Q the associated Lagrange function generically reads as (see [63] for the fermion analog):

$$L^{\pm} = \pm m_\gamma \sqrt{Q^{-1}_{\mu\nu} u^\mu u^\nu}. \tag{2.27}$$

These Lagrange functions rely on the existence of a nonzero photon mass. In general, Lagrange functions are of mass dimension one, which is why they have to involve some dimensionful scale characteristic for the physical problem considered. For the classical fermionic point-particle analogs studied in [63] this scale corresponds to the particle mass. In MCS theory, the Chern-Simons mass m_{CS} takes the role of the characteristic dimensionful scale as we saw in Eq. (2.14). However, since modified Maxwell theory does not involve a dimensionful scale, a photon mass m_γ had to be introduced to construct Lagrange functions for the classical point-particle analogs.

D. Classical wavefront

A photon mass is undoubtedly not an attractive feature in a theory since the mass term violates gauge invariance. Even if a photon mass has to be introduced as an intermediate ingredient to regularize infrared divergences in quantum corrections or to grant a consistent quantization of a particular Lorentz-violating framework, cf. [26], it should be possible to consider the limit $m_\gamma \mapsto 0$ at the end of any calculation. For this reason, an alternative procedure shall be developed to obtain the classical analog of (Lorentz-violating) photons. Classically, an electromagnetic pulse makes up a wavefront that can be interpreted as a surface in four-dimensional spacetime: $w = w(t,\mathbf{x}) = 0$. In a Lorentz-invariant theory it fulfills the following equation [90]:

$$\left(\frac{\partial w}{\partial t}\right)^2 - (\boldsymbol{\nabla} w)^2 = 0. \tag{2.28}$$

Computing the square root and choosing one particular sign results in:

$$\frac{\partial w}{\partial t} - \sqrt{\left(\frac{\partial w}{\partial x}\right)^2 + \left(\frac{\partial w}{\partial y}\right)^2 + \left(\frac{\partial w}{\partial z}\right)^2} = 0. \tag{2.29}$$

The latter is a Hamilton-Jacobi equation where w is understood as the action S and the expression on the right-hand side as the Hamilton function:

$$\frac{\partial S}{\partial t} + H(\mathbf{x}, \boldsymbol{\nabla} S) = 0, \qquad S(t,\mathbf{x}) = w(t,\mathbf{x}),$$
$$H(\mathbf{x},\mathbf{k}) = -\sqrt{\mathbf{k}^2}, \tag{2.30}$$

where $\mathbf{k}$ is the wave vector (momentum). Examples that obey Eq. (2.29) are

$$w = t - \hat{\mathbf{a}}\cdot\mathbf{x}, \qquad |\hat{\mathbf{a}}| = 1, \tag{2.31a}$$

$$w = t - \sqrt{\mathbf{x}^2}. \tag{2.31b}$$

The first describes a plane wavefront with unit normal vector $\hat{\mathbf{a}}$ and the second a spherical wavefront. This can be seen by equating w with zero and considering a fixed value for t. Introducing λ as a parameter for the trajectory of the wave, both wavefronts can be differentiated with respect to λ, which leads to

$$\frac{\partial w}{\partial \lambda} = u^0 - \hat{\mathbf{a}}\cdot\mathbf{u}, \tag{2.32a}$$

$$\frac{\partial w}{\partial \lambda} = u^0 - \sqrt{\mathbf{u}^2}, \qquad u^0 \equiv \frac{\mathrm{d}t}{\mathrm{d}\lambda}, \qquad \mathbf{u} \equiv \frac{\mathrm{d}\mathbf{x}}{\mathrm{d}\lambda}. \tag{2.32b}$$

At a first glance, it may be assumed that the latter are suitable Lagrange functions since they are positively homogeneous of degree one. However, computing the derived metrics $g_{\mu\nu}$ according to

$$g_{\mu\nu} \equiv \frac{1}{2}\frac{\partial^2 L^2}{\partial u^\mu \partial u^\nu}, \tag{2.33}$$

quickly reveals that their resulting determinants vanish. Therefore, such a $g_{\mu\nu}$ is not invertible and definitely fails to describe a possible (pseudo-)Finsler structure. This is a result that can be shown to hold in general. Assume that a Lagrange function L exists describing the classical wavefront analog of photons. Then the associated conjugated momentum p_μ must be lightlike to obey the photon dispersion relation:

$$p_\mu = -\frac{\partial L}{\partial u^\mu}, \qquad p_\mu = -f(u^0,u)\begin{pmatrix}1\\ \pm 1\end{pmatrix}_\mu. \tag{2.34}$$

Due to rotational symmetry in the Lorentz-invariant case it is sufficient to consider a $(1+1)$-dimensional spacetime, which is why a lightlike p_μ must be of the form stated in Eq. (2.34) with a C^∞ function $f(u^0,u)$ where $u \equiv |\mathbf{u}|$. The derived metric is then given by

$$\begin{aligned} g_{\mu\nu} &= \frac{1}{2}\frac{\partial^2 L^2}{\partial u^\mu \partial u^\nu} = L\frac{\partial^2 L}{\partial u^\mu \partial u^\nu} + \frac{\partial L}{\partial u^\mu}\frac{\partial L}{\partial u^\nu} \\ &= L\begin{pmatrix} f^{(1)} & f^{(2)} \\ \pm f^{(1)} & \pm f^{(2)}\end{pmatrix}_{\mu\nu} + \begin{pmatrix} f^2 & \pm f^2 \\ \pm f^2 & f^2\end{pmatrix}_{\mu\nu} \\ &= \begin{pmatrix} Lf^{(1)} + f^2 & Lf^{(2)} \pm f^2 \\ \pm(Lf^{(1)} + f^2) & \pm(Lf^{(2)} \pm f^2)\end{pmatrix}_{\mu\nu}, \end{aligned} \tag{2.35}$$

where (1) denotes differentiation with respect to u^0 and (2) means differentiation by u. It clearly holds that $\det(g_{\mu\nu}) = 0$ irrespective of the unknown function f.

Therefore, a Lagrange function L with an invertible derived metric cannot exist in the photon case. Because of this an alternative procedure has to be developed to assign a possible (pseudo-)Finsler structure to photons, which will be examined in what follows.

III. FINSLER STRUCTURES OF THE PHOTON SECTOR

In the previous section, it was intimated that the usual method to finding Finsler structures in the fermion sector does not seem to work in the minimal CPT-even photon sector. The reason is the absence of a dimensionful physical scale needed for dimensional consistency of a Lagrange function. Photons must be treated differently from fermions to obtain something like a classical description. This shall be undertaken in the current section.

A. Lorentz-invariant case

To become familiar with our goals, the situation in standard electrodynamics will be described first. In a Lorentz-invariant vacuum Maxwell's equations in momentum space read as follows:

$$\mathbf{k}\times\mathbf{B}+\omega\mathbf{E}=\mathbf{0},\qquad \mathbf{k}\times\mathbf{E}-\omega\mathbf{B}=\mathbf{0}, \tag{3.1a}$$

$$\mathbf{k}\cdot\mathbf{E}=0,\qquad \mathbf{k}\cdot\mathbf{B}=0. \tag{3.1b}$$

Here $\mathbf{E}$ is the electric field, $\mathbf{B}$ the magnetic flux density, $\mathbf{k}$ the wave vector, and ω the frequency. The dispersion relation can be derived directly from the wave equation. The latter is obtained by computing the cross product of the wave vector and, e.g., the first of Eq. (3.1a) where the second equation has to be plugged in subsequently:

$$\begin{aligned}&\mathbf{k}\times(\mathbf{k}\times\mathbf{B})+\omega\mathbf{k}\times\mathbf{E}\\&\quad=\mathbf{k}(\mathbf{k}\cdot\mathbf{B})-\mathbf{k}^2\mathbf{B}+\omega^2\mathbf{B}\\&\quad=(\omega^2-\mathbf{k}^2)\mathbf{B}=\mathbf{0}.\end{aligned} \tag{3.2}$$

Here the second of Eq. (3.1b) is used as well, which says that in a Lorentz-invariant vacuum the magnetic field is transverse. Equation (3.2) has nontrivial solutions for the magnetic field only in case of $\omega^2=\mathbf{k}^2$, which immediately leads to the dispersion relation $\omega=|\mathbf{k}|$ of electromagnetic waves. The dispersion equation

$$\omega^2-\mathbf{k}^2=0 \tag{3.3}$$

is the base to determine the Finsler structure associated with standard Maxwell theory. The method is introduced in [62] and will be described as follows. Let M be a Finsler manifold and $F=F(x,y)$ the corresponding Finsler structure with $x\in M$ and $y\in T_xM$ where T_xM is the tangent space at x. The indicatrix S_xM at a point x of a Finsler space is the set of all y where the Finsler structure takes the constant value 1, i.e., $S_xM=\{y\in T_xM|F(x,y)=1\}$. Note that a Finsler structure defines an indicatrix, but conversely each indicatrix determines a Finsler structure [91].

Finsler himself expressed the idea that an indicatrix might model the phase velocity of light waves in both isotropic and anisotropic materials. Hence, what is needed to associate a Finsler structure to a photon theory is an indicatrix [62]. The phase velocity vector is defined as $\mathbf{v}_{\mathrm{ph}}\equiv\hat{\mathbf{k}}v_{\mathrm{ph}}$ with $v_{\mathrm{ph}}=\omega/|\mathbf{k}|$ and the unit wave vector is $\hat{\mathbf{k}}\equiv\mathbf{k}/|\mathbf{k}|$. Since Eq. (3.3) still depends on both the energy and the momentum components, we divide it by $|\mathbf{k}|^2$. This results in an equation that involves the phase velocity and quantities of zero mass dimension:

$$v_{\mathrm{ph}}^2-1=0. \tag{3.4}$$

Now Eq. (3.4) can be considered as the indicatrix of the associated Finsler structure that is still to be found. This is accomplished using Okubo's technique, which is outlined in [61,62]. Consider a surface within a Finsler manifold M that is described by an equation $f(x,y)=0$. A function $F(y)$ taking a constant value 1 on such a surface can be found by solving the equation $f(x,y/F(y))=0$ with respect to $F(y)$ where the solution does not necessarily have to be unique. Denoting the phase velocity by $v_{\mathrm{ph}}\equiv|\mathbf{u}|$ with $\mathbf{u}\equiv(u^1,u^2,u^3)$ we perform the replacement $u^i\mapsto u^i/F(\mathbf{u})$ and obtain from Eq. (3.3)

$$\frac{\mathbf{u}^2}{F(\mathbf{u})^2}-1=0. \tag{3.5}$$

The latter can be solved for $F(\mathbf{u})$ immediately:

$$F(\mathbf{u})|^{\pm}_{\mathrm{LI}}=\pm\sqrt{\mathbf{u}^2}=\pm\sqrt{r_{ij}u^iu^j},\qquad r_{ij}=\mathrm{diag}(1,1,1)_{ij}. \tag{3.6}$$

As long as the intrinsic metric r_{ij} is positive definite, which is the case for the particular r_{ij} given, $F(\mathbf{u})|^{+}_{\mathrm{LI}}$ fulfills all properties of Sec. II A. Therefore, it can be interpreted as a three-dimensional Finsler structure where the derived metric $g^{\pm}_{\mathrm{LI},ij}$ corresponds to the intrinsic metric. Since the Cartan torsion vanishes, it must be a Riemannian structure according to Deicke's theorem.

B. Isotropic case

In the Lorentz-violating case modified Maxwell's equations can be constructed by using Eqs. (4)–(6) of [74]. A Lorentz-violating vacuum behaves like an effective medium for electromagnetic waves, which is why Maxwell's equations now involve nontrivial permeability and permittivity tensors. In momentum space, they read as

follows (where the spatial indices of $\mathbf{k}$ are understood to be upper ones):

$$\mathbf{k}\times\mathbf{H}+\omega\mathbf{D}=\mathbf{0},\qquad \mathbf{k}\times\mathbf{E}-\omega\mathbf{B}=\mathbf{0}, \tag{3.7a}$$

$$\mathbf{k}\cdot\mathbf{D}=0,\qquad \mathbf{k}\cdot\mathbf{B}=0. \tag{3.7b}$$

The first two of these deliver relationships between the electric displacement $\mathbf{D}$, the magnetic field $\mathbf{H}$, the electric field $\mathbf{E}$, and the magnetic flux density $\mathbf{B}$. The transformation between $(\mathbf{D},\mathbf{H})$ and $(\mathbf{E},\mathbf{B})$ is governed by (3×3) matrices κ_{DE}, κ_{DB}, κ_{HE}, and κ_{HB} comprising the controlling coefficients and they are given by Eq. (4) in the latter reference. In the isotropic case considered here the matrices κ_{DB} and κ_{HE} do not contribute. It then holds that

$$\mathbf{H}=\mu^{-1}\mathbf{B},\qquad \mu^{-1}=\mathbb{1}_3+\kappa_{HB}=\mathbb{1}_3-\kappa_{DE}, \tag{3.8a}$$

$$\mathbf{D}=\varepsilon\mathbf{E},\qquad \varepsilon=\mathbb{1}_3+\kappa_{DE}, \tag{3.8b}$$

$$\kappa_{DE}=\tilde{\kappa}_{\mathrm{tr}}\mathrm{diag}(1,1,1)=-\kappa_{HB}, \tag{3.8c}$$

$$\varepsilon\mu=n^2\mathrm{diag}(1,1,1),\qquad n^{-1}=\mathcal{A}\equiv\sqrt{\frac{1-\tilde{\kappa}_{\mathrm{tr}}}{1+\tilde{\kappa}_{\mathrm{tr}}}}. \tag{3.8d}$$

Maxwell's equations in momentum space will be needed to obtain the dispersion relations. Each of the equations involves different fields. However, to obtain the dispersion relation, a single equation is required that contains one of the four fields only. Since according to Eq. (3.8) the different fields are related by matrices proportional to the unit matrix, the standard procedure outlined in Sec. III A works here:

$$\begin{aligned}&\mathbf{k}\times(\mathbf{k}\times\mathbf{E})-\omega(\mathbf{k}\times\mathbf{B})\\&\quad=\mathbf{k}\times(\mathbf{k}\times\mathbf{E})-\omega\mu(\mathbf{k}\times\mathbf{H})\\&\quad=\mathbf{k}\times(\mathbf{k}\times\mathbf{E})+\omega^2\mu\mathbf{D}=\mathbf{k}\times(\mathbf{k}\times\mathbf{E})+\omega^2\varepsilon\mu\mathbf{E}=\mathbf{0}.\end{aligned} \tag{3.9}$$

Writing the equation explicitly in matrix form leads to

$$\begin{pmatrix} n^2\omega^2-(k_2^2+k_3^2) & k_1k_2 & k_1k_3\\ k_1k_2 & n^2\omega^2-(k_1^2+k_3^2) & k_2k_3\\ k_1k_3 & k_2k_3 & n^2\omega^2-(k_1^2+k_2^2)\end{pmatrix}\times\begin{pmatrix}E^1\\E^2\\E^3\end{pmatrix}=\begin{pmatrix}0\\0\\0\end{pmatrix}, \tag{3.10}$$

where $\mathbf{E}\equiv(E^1,E^2,E^3)^T$ is the electric field strength vector. Lowering the indices of the components of $\mathbf{k}$ does not lead to changes since the components always appear in bilinear combinations. The condition of a vanishing determinant of the coefficient matrix, which is necessary such that nontrivial solutions exist for the electric field, leads to the dispersion equation

$$0=n^2\omega^2(n^2\omega^2-\mathbf{k}^2)^2. \tag{3.11}$$

From this, we obtain the spurious solution $\omega=0$ associated with a nonpropagating wave and the modified dispersion relation $\omega=\mathcal{A}|\mathbf{k}|$. Now we again need an indicatrix. A reasonable choice to start with is Eq. (3.11). Dividing the latter by the prefactor and computing the square root does not change the set of physical zeros for ω, i.e., we can also take

$$n^2\omega^2-\mathbf{k}^2=0. \tag{3.12}$$

A subsequent division by $|\mathbf{k}|^2$ results in the indicatrix of the related Finsler structure:

$$v_{\mathrm{ph}}^2-\mathcal{A}^2=0. \tag{3.13}$$

Using Okubo's technique we obtain $F(\mathbf{u})$ immediately:

$$0=\frac{\mathbf{u}^2}{F(\mathbf{u})^2}-\mathcal{A}^2, \tag{3.14a}$$

$$\begin{aligned}&F(\mathbf{u})|^{\pm}_{\circledcirc}=\pm\frac{1}{\mathcal{A}}\sqrt{\mathbf{u}^2}=\pm\frac{1}{\mathcal{A}}\sqrt{r_{ij}u^iu^j},\\&\quad r_{ij}=\mathrm{diag}(1,1,1)_{ij},\end{aligned} \tag{3.14b}$$

where the symbol $\circledcirc$ denotes "isotropic." Comparing Eq. (3.14b) to Eq. (3.6) we see that the only difference in comparison to the Lorentz-invariant case is the prefactor $1/\mathcal{A}$. This is not surprising, as the case considered is isotropic and the result involves the spatial velocity components only. For a positive definite r_{ij}, $F(\mathbf{u})|^{+}_{\circledcirc}$ fulfills all properties of a Finsler structure where the derived metric is given by $g^{\pm}_{\circledcirc,ij}=r_{ij}/\mathcal{A}^2$. Due to the isotropy the latter is still Riemannian, which can be explicitly checked via the Cartan torsion. In comparison to the Lorentz-invariant case, it involves a global scaling factor.

C. Anisotropic, nonbirefringent case

The anisotropic case with a single modified dispersion relation reveals some peculiar properties. The matrices relating the different electromagnetic fields with each other are given by

$$\kappa_{DE}=\frac{3}{2}\tilde{\kappa}_{e-}^{11}\mathrm{diag}(1,1,-1)=-\kappa_{HB}, \tag{3.15a}$$

$$\kappa_{DB}=\kappa_{HE}=\mathbf{0}_3, \tag{3.15b}$$

with the (3×3) zero matrix $\mathbf{0}_3$. The matrices κ_{DE} and κ_{HB} are diagonal as well, but the difference to the isotropic case is that they are no longer proportional to the identity matrix. This is not surprising due to the preferred spacelike direction $\boldsymbol{\zeta}$ pointing along the third spatial axis where there is a residual isotropy in the plane perpendicular to this axis. Therefore the first two components of the diagonal matrix $\varepsilon\mu$ are equal, but the third differs from those:

$$\varepsilon\mu = \mathrm{diag}(n_1^2, n_2^2, n_3^2), \qquad n_1 = n_2 = \frac{1}{\mathcal{B}},$$
$$n_3 = \mathcal{B}, \qquad \mathcal{B} \equiv \sqrt{\frac{1-(3/2)\tilde{\kappa}_{e-}^{11}}{1+(3/2)\tilde{\kappa}_{e-}^{11}}}. \tag{3.16}$$

Now we again need an equation that can serve as a basis for the indicatrix of the associated Finsler space. Multiplying the second of Eq. (3.7a) with μ^{-1}, computing the cross product with $\mathbf{k}$, and using the first of Eq. (3.7a) leads to an equation for the electric field vector:

$$\mathbf{k}\times[(\mu^{-1}(\mathbf{k}\times\mathbf{E})] + \omega^2\varepsilon\mathbf{E} = \mathbf{0}. \tag{3.17}$$

Multiplying the latter with an appropriate prefactor, in matrix form it reads as follows:

$$\begin{pmatrix} \omega^2-k_2^2-k_3^2n_3^2 & k_1k_2 & k_1k_3n_3^2 \\ k_1k_2 & \omega^2-k_1^2-k_3^2n_3^2 & k_2k_3n_3^2 \\ k_1k_3n_3^2 & k_2k_3n_3^2 & (\omega^2-k_1^2-k_2^2)n_3^2 \end{pmatrix} \times \begin{pmatrix} E^1 \\ E^2 \\ E^3 \end{pmatrix} = \begin{pmatrix} 0 \\ 0 \\ 0 \end{pmatrix}. \tag{3.18}$$

Lowering the components of $\mathbf{k}$ does not produce any changes. The determinant condition for this system of equations leads to

$$0 = \omega^2(\omega^2 - k_\perp^2 - k_\parallel^2 n_3^2)^2, \tag{3.19a}$$

$$k_\parallel \equiv \mathbf{k}\cdot\boldsymbol{\zeta}, \qquad k_\perp \equiv |\mathbf{k} - k_\parallel\boldsymbol{\zeta}|. \tag{3.19b}$$

For convenience, the three-momentum $\mathbf{k}$ is decomposed into a component $k_\parallel$ along the preferred spatial direction $\boldsymbol{\zeta} = (0,0,1)^T$ and into a component $k_\perp$ perpendicular to $\boldsymbol{\zeta}$. This results in the spurious solution $\omega = 0$ and a single dispersion relation for electromagnetic waves:

$$\omega = \sqrt{k_\perp^2 + \mathcal{B}^2 k_\parallel^2}. \tag{3.20}$$

Here the remaining isotropy perpendicular to the preferred direction becomes evident as well. The photon will only be affected by Lorentz violation in case it has a momentum component pointing along the preferred direction. Note that the result of Eq. (3.20) is very interesting from the perspective that the underlying Lorentz-violating framework is anisotropic, but in spite of this anisotropy there is only a single dispersion relation. In contrast, birefringence, i.e., the property of having two different dispersion laws dependent on photon polarization seems to always occur in anisotropic media in nature. The reason that there is a single dispersion relation here only is the extreme fine-tuning of permeability and permittivity [cf. Eq. (3.15a)], which can most probably not be found in any materials.

Now, the equation for the indicatrix follows from

$$\omega^2 - k_\perp^2 - k_\parallel^2 n_3^2 = 0, \tag{3.21}$$

in dividing it by $\mathbf{k}^2$. Introducing the angle ϑ between the wave vector $\mathbf{k}$ and the preferred spatial direction $\boldsymbol{\zeta}$ leads to

$$0 = v_{\mathrm{ph}}^2 - \sin^2\vartheta - \mathcal{B}^2\cos^2\vartheta, \tag{3.22a}$$

$$\cos\vartheta \equiv \hat{\mathbf{k}}\cdot\boldsymbol{\zeta}, \qquad \hat{\mathbf{k}} \equiv \frac{\mathbf{k}}{|\mathbf{k}|}. \tag{3.22b}$$

Thinking of ϑ as the polar angle in spherical coordinates, Eq. (3.22a) can be reinterpreted using

$$v_{\mathrm{ph}}^2 = \mathbf{u}^2, \qquad \cos\vartheta = \frac{u^3}{|\mathbf{u}|}, \qquad \sin\vartheta = \frac{\sqrt{(u^1)^2+(u^2)^2}}{|\mathbf{u}|}, \tag{3.23}$$

as follows:

$$\mathbf{u}^4 - [(u^1)^2 + (u^2)^2 + \mathcal{B}^2(u^3)^2] = 0. \tag{3.24}$$

The latter is the equation that determines the indicatrix. Okubo's technique can again be used to obtain a Finsler structure directly when $\mathbf{u}$ is replaced by $\mathbf{u}/F(\mathbf{u})$ in Eq. (3.24):

$$\mathbf{u}^4 - F(\mathbf{u})^2[(u^1)^2 + (u^2)^2 + \mathcal{B}^2(u^3)^2] = 0. \tag{3.25}$$

This leads to the result

$$F(\mathbf{u})|_{\oplus}^{\pm} = \pm\frac{\mathbf{u}^2}{\sqrt{(u^1)^2+(u^2)^2+\mathcal{B}^2(u^3)^2}}, \tag{3.26}$$

which can also be written in the form

$$F(\mathbf{u})|_{\oplus}^{\pm} = \pm\frac{r_{ij}u^iu^j}{\sqrt{s_{ij}u^iu^j}}, \qquad r_{ij} = \mathrm{diag}(1,1,1)_{ij},$$
$$s_{ij} = \mathrm{diag}(1,1,\mathcal{B}^2)_{ij}. \tag{3.27}$$

Here $\oplus$ means "anisotropic." In principle, the Finsler structure can be interpreted to involve an intrinsic metric

r_{ij} and a second metric s_{ij}. Since the background considered is flat, it is reasonable to take r_{ij} as the metric that determines the lengths of vectors and the angles between vectors. For general r_{ij} and s_{ij} the derived metric is given by

$$g_{ij} = F(\mathbf{u})|^{\pm}_{\oplus}\frac{\partial^2 F(\mathbf{u})|^{\pm}_{\oplus}}{\partial u^i \partial u^j} + \frac{\partial F(\mathbf{u})|^{\pm}_{\oplus}}{\partial u^i}\frac{\partial F(\mathbf{u})|^{\pm}_{\oplus}}{\partial u^j}, \tag{3.28a}$$

$$\frac{\partial F(\mathbf{u})|^{\pm}_{\oplus}}{\partial u^i} = \pm\frac{1}{(s_{ab}u^a u^b)^{3/2}}\mathcal{Q}_{iklm}u^k u^l u^m, \tag{3.28b}$$

$$\begin{aligned}\frac{\partial^2 F(\mathbf{u})|^{\pm}_{\oplus}}{\partial u^i \partial u^j} = {} & \mp\frac{3s_{jn}}{(s_{ab}u^a u^b)^{5/2}}\mathcal{Q}_{iklm}u^k u^l u^m u^n \\ & \pm\frac{1}{(s_{ab}u^a u^b)^{3/2}}\mathcal{Q}_{iklm} \\ & \times(\delta^{kj}u^l u^m + \delta^{jl}u^k u^m + \delta^{mj}u^k u^l),\end{aligned} \tag{3.28c}$$

$$\mathcal{Q}_{iklm} = 2s_{kl}r_{im} - r_{kl}s_{im}. \tag{3.28d}$$

This result is not very illuminating. When contracted with appropriate velocity components it collapses to $(F(\mathbf{u})|^{\pm}_{\oplus})^2$, which follows from its homogeneity of degree 2:

$$g^{\pm}_{\oplus,ij}u^i u^j = (F(\mathbf{u})|^{\pm}_{\oplus})^2, \qquad g^{\pm}_{\oplus,ij} \equiv \frac{1}{2}\frac{\partial^2 (F(\mathbf{u})|^{\pm}_{\oplus})^2}{\partial u^i \partial u^j}. \tag{3.29}$$

Now the following properties of $F(\mathbf{u})|^{\pm}_{\oplus}$ can be deduced:

(1) $F(\mathbf{u})|^{+}_{\oplus} > 0$ for $\mathbf{u} \in TM\backslash\{0\}$ if r_{ij} and s_{ij} are positive definite,
(2) $F(\mathbf{u})|^{\pm}_{\oplus} \in C^\infty$ for $\mathbf{u} \in TM\backslash\{0\}$ as well as positive definite s_{ij},
(3) $F(\lambda\mathbf{u})|^{\pm}_{\oplus} = \lambda F(\mathbf{u})|^{\pm}_{\oplus}$ for $\lambda > 0$, i.e., positive homogeneity,
(4) and the derived metric g_{ij} is positive definite for $\mathbf{u} \in TM\backslash\{0\}$ as long as both r_{ij} and s_{ij} are sufficiently small perturbations from the identity matrix.

Therefore as long as both r_{ij} and s_{ij} are perturbations from the identity matrix, which, in particular, is the case for r_{ij} and s_{ij} given in Eq. (3.27), $F(\mathbf{u})|^{+}_{\oplus}$ defines a three-dimensional Finsler structure, indeed. Furthermore, both the Cartan and the Matsumoto torsion can be computed to be able to classify this Finsler structure. The results are complicated and they do not provide further insight, which is why they will be omitted. However, they are nonzero in general whereby according to Deicke's theorem, Eq. (3.27) is not a Riemannian structure and according to the Matsumoto-Hōjō theorem it is neither a Randers nor a Kropina structure. The result corresponds to Eq. (4.2.2.6) of [62] where $a = \mathcal{B}$ and $b = 1$ in their notation. They denote this type of Finsler structure as a second-order Kropina structure in resemblance to a Kropina structure $F(\mathbf{u}) = \alpha^2/\beta$ with $\alpha = \sqrt{a_{ij}u^i u^j}$ and $\beta = b_i u^i$. In the latter reference Eq. (3.27) appears in the context of light propagation in uniaxial media. The numerator involves the Euclidean intrinsic metric r_{ij} only, whereas the denominator is characterized by another metric s_{ij}. The latter could be thought of as the metric governing physics since it comprises the physical quantity $\mathcal{B}$.

D. Anisotropic, birefringent (at second order) case

The penultimate example provides a case of modified Maxwell theory that has not been considered in Sec. II C. It is parity-even and characterized by two preferred spacelike directions:

$$(\zeta_1^\mu) = \begin{pmatrix}0\\ \boldsymbol{\zeta}_1\end{pmatrix}, \qquad (\zeta_2^\mu) = \begin{pmatrix}0\\ \boldsymbol{\zeta}_2\end{pmatrix},$$
$$\boldsymbol{\zeta}_1 = \begin{pmatrix}\sin\eta\\ 0\\ \cos\eta\end{pmatrix}, \qquad \boldsymbol{\zeta}_2 = \begin{pmatrix}-\sin\eta\\ 0\\ \cos\eta\end{pmatrix}. \tag{3.30}$$

They are normalized and enclose an angle of 2η. We consider an observer frame with one nonzero controlling coefficient $\mathcal{G}$. Then the (4×4) matrix employed in the nonbirefringent *Ansatz* reads

$$\tilde{\kappa}^{\mu\nu} = \mathcal{G}\left(\zeta_1^\mu\zeta_2^\nu + \zeta_1^\nu\zeta_2^\mu - \frac{1}{2}(\zeta_1\cdot\zeta_2)\eta^{\mu\nu}\right). \tag{3.31}$$

This corresponds to the following choices for the matrices that appear in Maxwell's equations:

$$\kappa_{DE} = \mathcal{G}\mathrm{diag}(1, \cos(2\eta), -1) = -\kappa_{HB}, \tag{3.32a}$$

$$\kappa_{DB} = \kappa_{HE} = \mathbf{0}_3. \tag{3.32b}$$

Thus, there are nontrivial permeability and permittivity tensors, but the electric and magnetic fields do still not mix. Using these matrices, modified Maxwell's equations can be obtained according to the procedure used in Sec. III C. The condition of a vanishing coefficient determinant for nontrivial solutions results in an equation for the dispersion relation:

$$\begin{aligned}0 = {} & \omega^2[(1-\mathcal{G}^2)\omega^2 - (1+\mathcal{G})[1-\mathcal{G}\cos(2\eta)]k_1^2 \\ & - (1-\mathcal{G}^2)k_2^2 - (1-\mathcal{G})[1-\mathcal{G}\cos(2\eta)]k_3^2] \\ & \times\{\omega^2[1+\mathcal{G}\cos(2\eta)] - (1+\mathcal{G})k_1^2 \\ & - [1+\mathcal{G}\cos(2\eta)]k_2^2 - (1-\mathcal{G})k_3^2\}.\end{aligned} \tag{3.33}$$

In contrast to the anisotropic case considered in Sec. III C the current framework is characterized by two distinct modified dispersion relations. They can be written in the form

$$\omega_1 = \sqrt{\mathcal{G}_1 k_1^2 + k_2^2 + \mathcal{G}_2 k_3^2}, \tag{3.34a}$$

$$\omega_2 = \sqrt{\tilde{\mathcal{G}}_1 k_1^2 + k_2^2 + \tilde{\mathcal{G}}_2 k_3^2}, \tag{3.34b}$$

$$\mathcal{G}_1 \equiv \frac{1-\mathcal{G}\cos(2\eta)}{1-\mathcal{G}}, \qquad \mathcal{G}_2 \equiv \frac{1-\mathcal{G}\cos(2\eta)}{1+\mathcal{G}}, \tag{3.34c}$$

$$\tilde{\mathcal{G}}_1 \equiv \frac{1+\mathcal{G}}{1+\mathcal{G}\cos(2\eta)}, \qquad \tilde{\mathcal{G}}_2 \equiv \frac{1-\mathcal{G}}{1+\mathcal{G}\cos(2\eta)}. \tag{3.34d}$$

Evidently the contribution associated with the second three-momentum component stays unmodified which is reasonable, since the preferred directions of Eq. (3.30) do not point along the second spatial axis. Each dispersion relation can be expanded for $\mathcal{G} \ll 1$ showing that they differ at second order in Lorentz violation. In general the non-birefringent *Ansatz* of Eq. (2.15) works at leading order only. Besides, the dispersion relations depend on the angle 2η enclosed by the two preferred directions. With the normalized propagation direction of the electromagnetic wave given by $\hat{\mathbf{k}}$, the latter encloses the angles θ_1, θ_2 with the first and the second preferred direction, respectively. These are given by

$$\cos\theta_1 = \hat{\mathbf{k}} \cdot \boldsymbol{\zeta}_1 = \hat{k}^1 \sin\eta + \hat{k}^3 \cos\eta, \tag{3.35a}$$

$$\cos\theta_2 = \hat{\mathbf{k}} \cdot \boldsymbol{\zeta}_2 = -\hat{k}^1 \sin\eta + \hat{k}^3 \cos\eta. \tag{3.35b}$$

The components of the propagation direction vector $\hat{\mathbf{k}}$ can now be expressed in terms of the angles θ_1, θ_2, and η. Note that $\hat{\mathbf{k}}$ is a unit vector by construction:

$$\hat{k}^1 = \frac{\cos\theta_1 - \cos\theta_2}{2\sin\eta}, \qquad \hat{k}^3 = \frac{\cos\theta_1 + \cos\theta_2}{2\cos\eta},$$
$$\hat{k}^2 = \sqrt{1 - (\hat{k}^1)^2 - (\hat{k}^3)^2}. \tag{3.36}$$

Now the two individual factors of Eq. (3.33) are considered giving the modified dispersion relations. Dividing each by the wave-vector magnitude $|\mathbf{k}|$, introducing the phase velocity, and expressing all propagation direction components by the angles of Eq. (3.36), equations for the phase velocities are obtained as before:

$$0 = (1-\mathcal{G}^2) v_{\mathrm{ph}}^2 + \frac{\mathcal{G}}{2}\{4\cos(\theta_1)\cos(\theta_2) - \mathcal{G}[\cos(2\theta_1) + \cos(2\theta_2)]\} - 1, \tag{3.37a}$$

$$0 = [1 + \mathcal{G}\cos(2\eta)](1 - v_{\mathrm{ph}}^2) - 2\mathcal{G}\cos(\theta_1)\cos(\theta_2). \tag{3.37b}$$

In dividing the second equation by $-[1+\mathcal{G}\cos(2\eta)]$ and expanding both equations to linear order in $\mathcal{G}$, these results correspond to each other as expected. Now we are in a position to interpret the latter equations geometrically, which will lead us directly to the Finsler structures associated with this particular sector. In doing so, the velocity $\mathbf{u}$ is introduced and both the phase velocity and the angles θ_1, θ_2 are expressed by the magnitude or components of $\mathbf{u}$ as follows:

$$v_{\mathrm{ph}} = |\mathbf{u}|, \tag{3.38a}$$

$$\cos\theta_1 = \frac{u^1}{|\mathbf{u}|}\sin\eta + \frac{u^3}{|\mathbf{u}|}\cos\eta, \tag{3.38b}$$

$$\cos\theta_2 = -\frac{u^1}{|\mathbf{u}|}\sin\eta + \frac{u^3}{|\mathbf{u}|}\cos\eta. \tag{3.38c}$$

Inserting those into Eq. (3.37a) and using Okubo's technique leads to two distinct Finsler structures. The first is given by

$$F(\mathbf{u})|^{(1)\pm}_{\text{Ⓥ}} = \pm\frac{r_{ij}u^i u^j}{\sqrt{s_{ij}u^i u^j}}, \qquad r_{ij} = \mathrm{diag}(1,1,1)_{ij},$$
$$s_{ij} = \mathrm{diag}(\mathcal{G}_1, 1, \mathcal{G}_2)_{ij}, \tag{3.39}$$

and the second reads as

$$F(\mathbf{u})|^{(2)\pm}_{\text{Ⓥ}} = \pm\frac{r_{ij}u^i u^j}{\sqrt{s_{ij}u^i u^j}}, \qquad r_{ij} = \mathrm{diag}(1,1,1)_{ij},$$
$$s_{ij} = \mathrm{diag}(\tilde{\mathcal{G}}_1, 1, \tilde{\mathcal{G}}_2)_{ij}. \tag{3.40}$$

Here Ⓥ means "anisotropic and birefringent (at second order)." The four Finsler structures obtained have a form analogous to the Finsler structure found in Eq. (3.27) of Sec. III C. This is not surprising since both sectors are anisotropic but parity-even. Having birefringence at second order in Lorentz violation obviously does not affect the form of the Finsler structure. In such a case, we can obtain several distinct Finsler structures that differ from each other at second order in the controlling coefficients via the metrics s_{ij}.

In Eq. (3.27) the latter s_{ij} differs from the standard Euclidean metric only by the component s_{33}. Here both s_{11} and s_{33} are modified by Lorentz violation where they also depend on the angle η enclosed by the two preferred directions. The component s_{22} is standard, which again reflects the fact that the preferred directions have a vanishing second component. Since s_{ij} involves the physical (dimensionless) constants $\mathcal{G}_i$ and $\tilde{\mathcal{G}}_i$ for $i = 1\ldots2$, it is reasonable to say that s_{ij} seems to govern the physical properties of photon propagation in these cases.

E. Parity-odd case

The final interesting sector considered involves the three parity-odd coefficients $\tilde{\kappa}^{12}_{o+}$, $\tilde{\kappa}^{31}_{o+}$, and $\tilde{\kappa}^{23}_{o+}$ and it will turn out to be the most complicated one. The preferred spacetime directions are given in Eq. (2.21b) and the matrices relating the electromagnetic fields to each other read

$$\kappa_{DE} = \mathbf{0}_3, \qquad \kappa_{HB} = \mathbf{0}_3, \tag{3.41a}$$

$$\kappa_{DB} = \begin{pmatrix} 0 & \tilde{\kappa}^{12}_{o+} & -\tilde{\kappa}^{31}_{o+} \\ -\tilde{\kappa}^{12}_{o+} & 0 & \tilde{\kappa}^{23}_{o+} \\ \tilde{\kappa}^{31}_{o+} & -\tilde{\kappa}^{23}_{o+} & 0 \end{pmatrix}, \qquad \kappa_{HE} = -\kappa^T_{DB} = \kappa_{DB}. \tag{3.41b}$$

The relationships between the fields are given by

$$\mathbf{D} = \mathbf{E} + \kappa_{DB}\mathbf{B}, \tag{3.42a}$$

$$\mathbf{H} = \kappa_{HE}\mathbf{E} + \mathbf{B} = \kappa_{DB}\mathbf{E} + \mathbf{B}. \tag{3.42b}$$

In contrast to the aforementioned cases, the parity-odd case has the peculiarity that the electric fields mix with the magnetic fields. Therefore obtaining an equation for the electric field from Maxwell's equations is more involved here. Nevertheless it can be accomplished along the following chain of steps:

$$\mathbf{0} = \kappa_{DB}(\mathbf{k}\times\mathbf{E}) - \omega\kappa_{DB}\mathbf{B}, \tag{3.43a}$$

$$\mathbf{0} = \kappa_{DB}(\mathbf{k}\times\mathbf{E}) - \omega(\mathbf{D}-\mathbf{E}), \tag{3.43b}$$

$$\mathbf{0} = \kappa_{DB}(\mathbf{k}\times\mathbf{E}) + \mathbf{k}\times\mathbf{H} + \omega\mathbf{E}, \tag{3.43c}$$

$$\mathbf{0} = \kappa_{DB}(\mathbf{k}\times\mathbf{E}) + \mathbf{k}\times(\kappa_{DB}\mathbf{E}+\mathbf{B}) + \omega\mathbf{E}, \tag{3.43d}$$

$$\mathbf{0} = \kappa_{DB}(\mathbf{k}\times\mathbf{E}) + \mathbf{k}\times(\kappa_{DB}\mathbf{E}) + \frac{1}{\omega}\mathbf{k}\times(\mathbf{k}\times\mathbf{E}) + \omega\mathbf{E}. \tag{3.43e}$$

Inserting the explicit vectors and performing a subsequent multiplication with ω leads to the following system in matrix form:

$$\begin{pmatrix} 0 \\ 0 \\ 0 \end{pmatrix} = (A+B)\begin{pmatrix} E^1 \\ E^2 \\ E^3 \end{pmatrix}, \tag{3.44a}$$

$$A = \begin{pmatrix} \omega^2-(k_2^2+k_3^2) & k_1k_2 & k_1k_3 \\ k_1k_2 & \omega^2-(k_1^2+k_3^2) & k_2k_3 \\ k_1k_3 & k_2k_3 & \omega^2-(k_1^2+k_2^2) \end{pmatrix}, \tag{3.44b}$$

$$B = \omega\begin{pmatrix} -2(\tilde{\kappa}^{31}_{o+}k_2+\tilde{\kappa}^{12}_{o+}k_3) & \tilde{\kappa}^{31}_{o+}k_1+\tilde{\kappa}^{23}_{o+}k_2 & \tilde{\kappa}^{12}_{o+}k_1+\tilde{\kappa}^{23}_{o+}k_3 \\ \tilde{\kappa}^{31}_{o+}k_1+\tilde{\kappa}^{23}_{o+}k_2 & -2(\tilde{\kappa}^{23}_{o+}k_1+\tilde{\kappa}^{12}_{o+}k_3) & \tilde{\kappa}^{12}_{o+}k_2+\tilde{\kappa}^{31}_{o+}k_3 \\ \tilde{\kappa}^{12}_{o+}k_1+\tilde{\kappa}^{23}_{o+}k_3 & \tilde{\kappa}^{12}_{o+}k_2+\tilde{\kappa}^{31}_{o+}k_3 & -2(\tilde{\kappa}^{23}_{o+}k_1+\tilde{\kappa}^{31}_{o+}k_2) \end{pmatrix}. \tag{3.44c}$$

The total system can be completely decomposed into the standard part of A and a Lorentz-violating contribution comprised in B. Note that here B gets a global minus sign when lowering the indices of the $\mathbf{k}$ components. Therefore the determinant condition results in the following equation for the photon energy:

$$\omega^2(\omega^2 - 2\omega\boldsymbol{\zeta}\cdot\mathbf{k} - \mathbf{k}^2)[(\omega-\boldsymbol{\zeta}\cdot\mathbf{k})^2 - (1+\boldsymbol{\zeta}^2)\mathbf{k}^2] = 0. \tag{3.45}$$

Here $\boldsymbol{\zeta} \equiv (\tilde{\kappa}^{23}_{o+}, \tilde{\kappa}^{31}_{o+}, \tilde{\kappa}^{12}_{o+})^T$ is the spatial part of the second preferred spacetime direction and $\mathbf{k}$ is understood to have lower components. The second and the third of the three factors can be solved for the energy giving two distinct dispersion relations:

$$\omega_1 = \boldsymbol{\zeta}\cdot\mathbf{k} + \sqrt{\mathbf{k}^2 + (\boldsymbol{\zeta}\cdot\mathbf{k})^2}, \tag{3.46a}$$

$$\omega_2 = \boldsymbol{\zeta}\cdot\mathbf{k} + \sqrt{1+\boldsymbol{\zeta}^2}|\mathbf{k}|, \tag{3.46b}$$

$$\cos\vartheta = \hat{\boldsymbol{\zeta}}\cdot\hat{\mathbf{k}}, \qquad \hat{\boldsymbol{\zeta}} \equiv \frac{\boldsymbol{\zeta}}{\mathcal{E}}, \qquad \hat{\mathbf{k}} \equiv \frac{\mathbf{k}}{|\mathbf{k}|},$$
$$\mathcal{E} \equiv |\boldsymbol{\zeta}| = \sqrt{(\tilde{\kappa}^{23}_{o+})^2 + (\tilde{\kappa}^{31}_{o+})^2 + (\tilde{\kappa}^{12}_{o+})^2}. \tag{3.46c}$$

For convenience, it is again reasonable to set up the coordinate system such that $\boldsymbol{\zeta}$ points along its third axis where ϑ is the angle between the wave vector $\mathbf{k}$ and the spatial direction. Dividing the first factor of Eq. (3.45) by $\mathbf{k}^2$ then leads to

$$v_{\mathrm{ph}}^2 - 2\mathcal{E}v_{\mathrm{ph}}\cos\vartheta - 1 = 0. \tag{3.47}$$

Introducing spherical polar coordinates with $v_{\mathrm{ph}} = |\mathbf{u}|$ results in

$$\mathbf{u}^2 - 2\mathcal{E}u^3 - 1 = 0. \tag{3.48}$$

This is the indicatrix for the first Finsler space that can be associated with the parity-odd case. We can employ Okubo's technique to obtain

$$0 = \mathbf{u}^2 - 2\mathcal{E}F(\mathbf{u})u^3 - F(\mathbf{u})^2, \tag{3.49a}$$

$$F(\mathbf{u})|_{\otimes}^{(1)\pm} = -\mathcal{E}u^3 \pm \sqrt{\mathbf{u}^2 + (\mathcal{E}u^3)^2}, \tag{3.49b}$$

$$F(\mathbf{u})|_{\otimes}^{\boldsymbol{\zeta}(1)\pm} = -\boldsymbol{\zeta}\cdot\mathbf{u} \pm \sqrt{\mathbf{u}^2 + (\boldsymbol{\zeta}\cdot\mathbf{u})^2}, \tag{3.49c}$$

where Eq. (3.49c) is the generalization of Eq. (3.49b) for $\boldsymbol{\zeta}$ pointing along an arbitrary direction and the symbol $\otimes$ denotes "parity-odd." Without loss of generality, the properties of the Finsler structure can be investigated with $\boldsymbol{\zeta}$ pointing along the third axis of the coordinate system, which simplifies the calculations. The derived metric is again lengthy and does not seem to provide any deeper understanding. The derived metric contracted with the spatial velocity components leads to the square of Eq. (3.49c):

$$g_{\otimes,ij}^{(1)\pm}u^iu^j = (F(\mathbf{u})|_{\otimes}^{(1)\pm})^2, \qquad g_{\otimes,ij}^{(1)\pm} \equiv \frac{1}{2}\frac{\partial^2(F(\mathbf{u})|_{\otimes}^{(1)\pm})^2}{\partial u^i\partial u^j}. \tag{3.50}$$

The following properties of $F(\mathbf{u})|_{\otimes}^{(1)\pm}$ in Eq. (3.49c) can be deduced:

(1) $F(\mathbf{u})|_{\otimes}^{(1)+} > 0$ for $\mathbf{u} \in TM\backslash\{0\}$ and $\mathcal{E}$ sufficiently small,
(2) $F(\mathbf{u})|_{\otimes}^{(1)\pm} \in C^\infty$ for $\mathbf{u} \in TM\backslash\{0\}$,
(3) $F(\lambda\mathbf{u})|_{\otimes}^{(1)\pm} = \lambda F(\mathbf{u})|_{\otimes}^{(1)\pm}$ for $\lambda > 0$, and
(4) the derived metric of $F(\mathbf{u})|_{\otimes}^{(1)\pm}$ is positive definite for $\mathbf{u} \in TM\backslash\{0\}$ and $\mathcal{E}$ sufficiently small.

Due to the first item, only $F(\mathbf{u})|_{\otimes}^{(1)+}$ is a Finsler structure. Its Matsumoto torsion vanishes, whereas the Cartan torsion does not. Furthermore when taking into account its form, $F(\mathbf{u})|_{\otimes}^{(1)+}$ must be a Randers structure. This particular type of geometry was introduced by Randers to account for the fact that particles always move on timelike trajectories pointing forwards in time [92]. In contrast to general relativity, his framework incorporates an additional four-vector into the metric. However, this four-vector should not be considered as a preferred spacetime direction since it can be changed by a kind of gauge transformation without affecting the arc length traveled by a particle. In the Lorentz-violating case considered here $\boldsymbol{\zeta}$ is a preferred direction, indeed.

The parity-odd framework is characterized by both a preferred timelike and a spacelike direction; cf. Eq. (2.21b). For the isotropic and anisotropic cases, which are parity-even, the corresponding Finsler structures are expected to involve only bilinear expressions such as $a_{ij}u^iu^j$, since these are invariant under $u^i \mapsto u'^i = -u^i$. Due to parity violation the Finsler structure of the parity-odd case is expected to involve terms such as b_iu^i, though. The Randers structure is a very natural possibility with this property, but it is not the only one as we shall see below.

The Finsler structure of Eq. (3.49c) has the same form as the corresponding dispersion relation of Eq. (3.46a) not taking into account additional minus signs. Such structures could be called "automorphic." They seem to appear when the dispersion equation [here Eq. (3.45)] involves one additional parity-odd contribution.

The parity-odd case of modified Maxwell theory has a second indicatrix, which follows from the second factor of Eq. (3.45) using the same procedure:

$$v_{\mathrm{ph}}^2 - 2\mathcal{E}v_{\mathrm{ph}}\cos\vartheta + \mathcal{E}^2\cos^2\vartheta - (1+\mathcal{E}^2) = 0, \tag{3.51a}$$

$$\mathbf{u}^2 - 2\mathcal{E}u^3 + \frac{\mathcal{E}^2(u^3)^2}{\mathbf{u}^2} - (1+\mathcal{E}^2) = 0. \tag{3.51b}$$

Okubo's technique leads to

$$F(\mathbf{u})|_{\otimes}^{(2)\pm} = \frac{-\mathcal{E}u^3 \pm \sqrt{1+\mathcal{E}^2}|\mathbf{u}|}{1+\mathcal{E}^2-(\mathcal{E}u^3)^2/\mathbf{u}^2}, \tag{3.52a}$$

$$F(\mathbf{u})|_{\otimes}^{(2)\zeta\pm} = \frac{-\boldsymbol{\zeta}\cdot\mathbf{u} \pm \sqrt{1+\mathcal{E}^2}|\mathbf{u}|}{1+\mathcal{E}^2-(\boldsymbol{\zeta}\cdot\mathbf{u})^2/\mathbf{u}^2}. \tag{3.52b}$$

Let us investigate the characteristics of Eq. (3.52a). We again obtain

$$g_{\otimes,ij}^{(2)\pm}u^iu^j = (F(\mathbf{u})|_{\otimes}^{(2)\pm})^2, \qquad g_{\otimes,ij}^{(2)\pm} \equiv \frac{1}{2}\frac{\partial^2(F(\mathbf{u})|_{\otimes}^{(2)\pm})^2}{\partial u^i\partial u^j}. \tag{3.53}$$

Hence, for $F(\mathbf{u})|_{\otimes}^{(2)+}$, analog properties hold such as for Eq. (3.49c), which makes it to a Finsler structure for sufficiently small $\mathcal{E}$. Note that the latter is not automorphic, since its off-shell dispersion relation in Eq. (3.45) does not exclusively involve additional parity-odd terms, but also contributions like $(\boldsymbol{\zeta}\cdot\mathbf{k})^2$. For this structure the Matsumoto torsion does not vanish, which is why it is neither a Randers nor a Kropina structure. The deviation from a Randers structure is of second order in the controlling coefficients:

$$F(\mathbf{u})|_{\otimes}^{\boldsymbol{\zeta}(2)\pm} = -\boldsymbol{\zeta}\cdot\mathbf{u} \pm \sqrt{1+\mathcal{E}^2}|\mathbf{u}| + \mathcal{O}(\tilde{\kappa}_{o+}^2). \tag{3.54}$$

Recall that the massive-photon dispersion equation of this mode, Eq. (2.23), was not quadratic, but quartic. For this reason, it was challenging to derive a classical point-particle Lagrange function corresponding to the second photon polarization. It is also interesting to note that a large number

of complications arise in the quantum field theory based on the parity-odd framework due to the behavior of this mode [24]. On the contrary, the first mode is much easier to handle. The Finsler structures obtained seem to reflect these properties. The first, given by Eq. (3.49c), is a well-understood Randers structure, whereas the second deviates from such a structure at second order in Lorentz violation, which makes its properties much more involved to analyze.

The studies carried out in the current section will prove to be useful when describing photons in the geometric-optics approximation. Thereby the eikonal equation will play an important role. How all these concepts are linked to each other will be clarified in the forthcoming part of the article.

IV. CLASSICAL RAY EQUATIONS

Propagating electromagnetic waves can be treated in the geometric-optics approximation as long as their wave lengths can be neglected in comparison to other physical length scales. For example, this is possible for waves with low energies propagating over large distances when physical phenomena related to the wave character (such as diffraction) do not play a role. This physical regime could be called "classical" and the wave then corresponds to a geometric ray. The goal of the current section is to establish *ray equations* that describe the physical behavior of propagating rays.

Each electromagnetic pulse has a wavefront, which separates the region with nonzero electromagnetic fields from the region with vanishing fields. At any instant of time the wavefront can be considered as a two-dimensional surface in three-dimensional space, i.e., it can be described by an equation of the form $\psi(\mathbf{x}) = t$ where $\mathbf{x}$ are spatial coordinates and t is the time. The gradient $\boldsymbol{\nabla}\psi$ points along the propagation direction. There is a relation between $\boldsymbol{\nabla}\psi$ and the refractive index n of the medium; it reads $|\boldsymbol{\nabla}\psi| = n$. The latter is called the *eikonal equation* in a subset of the literature. In what follows, n is assumed to depend on the position $\mathbf{x}$ only, but not on the velocity $\mathbf{u}$, i.e., $n = n(\mathbf{x})$.

Consider a wave propagating along a trajectory $\mathbf{x}(s)$ where s is the arc length of the curve. In this parametrization, the tangent vector has magnitude 1, which is why the ray equations read as follows:

$$\frac{\mathrm{d}\mathbf{x}}{\mathrm{d}s} = \frac{\boldsymbol{\nabla}\psi}{|\boldsymbol{\nabla}\psi|}, \qquad n\frac{\mathrm{d}\mathbf{x}}{\mathrm{d}s} = \boldsymbol{\nabla}\psi. \tag{4.1}$$

Computing an additional derivative of the latter with respect to s, its right-hand side can be expressed in terms of the refractive index as well:

$$\begin{aligned}\frac{\mathrm{d}}{\mathrm{d}s}\boldsymbol{\nabla}\psi &= \left(\frac{\mathrm{d}\mathbf{x}}{\mathrm{d}s}\cdot\boldsymbol{\nabla}\right)\boldsymbol{\nabla}\psi \\ &= \frac{1}{n}\boldsymbol{\nabla}\psi\cdot[\boldsymbol{\nabla}(\boldsymbol{\nabla}\psi)] = \frac{1}{2n}\boldsymbol{\nabla}(\boldsymbol{\nabla}\psi)^2 = \frac{1}{2n}\boldsymbol{\nabla}n^2 = \boldsymbol{\nabla}n.\end{aligned} \tag{4.2}$$

Trajectories may not necessarily be parametrized by arc length. For an arbitrary parametrization with parameter t we obtain

$$\frac{\mathrm{d}}{\mathrm{d}s} = \frac{\mathrm{d}t}{\mathrm{d}s}\frac{\mathrm{d}}{\mathrm{d}t} = \left(\frac{\mathrm{d}s}{\mathrm{d}t}\right)^{-1}\frac{\mathrm{d}}{\mathrm{d}t} = \frac{1}{|\mathbf{u}|}\frac{\mathrm{d}}{\mathrm{d}t}. \tag{4.3}$$

Now the ray equations (4.1) can be cast into the following final form:

$$\frac{\mathrm{d}}{\mathrm{d}s}\left(n\frac{\mathrm{d}\mathbf{x}}{\mathrm{d}s}\right) = \boldsymbol{\nabla}n, \tag{4.4a}$$

$$\frac{\mathrm{d}}{\mathrm{d}t}(\boldsymbol{\nabla}\psi) = |\mathbf{u}|\boldsymbol{\nabla}n, \qquad \boldsymbol{\nabla}\psi = n\frac{\mathbf{u}}{|\mathbf{u}|}. \tag{4.4b}$$

The literature seems to be discordant about which equation should actually be called the eikonal equation. Some sources call the first one of Eq. (4.4b) the eikonal equation, whereas others denote it as the vector magnitude of the second one. Note that the latter leads us back to $|\boldsymbol{\nabla}\psi| = n$ (cf. the beginning of this section). In the current paper whenever referring to the eikonal equation, we will be talking about the first one of Eq. (4.4b). For clarity, the vector magnitude of the second one will be called the *wavefront equation*. Equation (4.4b) can be understood as the Euler-Lagrange equations resulting from the condition that the following functional becomes stationary:

$$\begin{aligned}L[\mathbf{x},\mathbf{u}] &= \int_A^B \mathrm{d}s n(\mathbf{x}) = \int_{T_A}^{T_B}\mathrm{d}t V, \\ V &= V(\mathbf{x},\mathbf{u}) = n(\mathbf{x})|\mathbf{u}|.\end{aligned} \tag{4.5}$$

The integrand of this functional is the infinitesimal optical path length and the functional itself gives the total optical path length traveled by a ray along its trajectory between two points A and B. Here T_A is the departure time of the ray at A and T_B the arrival time at B. The optical path length is defined to be the path length equivalent that light has to travel *in vacuo* to take the same time as for a given path in a medium with refractive index $n(\mathbf{x})$. The functional of Eq. (4.5) can be understood as the base of the Fermat principle, cf. [93,94], where V is a velocity.

A. Wavefront and eikonal equation in modified Maxwell theory

The analog of the wavefront equation in Eq. (4.4b) in the context of modified Maxwell theory was partially studied

in [95]. The authors of the latter reference chose the coefficients contained in κ_{DE} and κ_{HB} as nonvanishing where both the trace of these matrices and the matrices mixing electric and magnetic fields were assumed to be zero. The trace components can be restored without any effort by just replacing their β_E by κ_{DE} and their β_B by κ_{HB}. The wavefront equation then follows from the matrix M_e in their Eq. (38):

$$M_e^{ij} = (1-|\nabla\psi|^2)\delta^{ij} + \partial^i\psi\partial^j\psi + \kappa_{DE}^{ij} - \kappa_{HB}^{kl}\varepsilon^{ink}\varepsilon^{jml}\partial^n\psi\partial^m\psi, \tag{4.6}$$

where ε^{ijk} is the totally antisymmetric Levi-Civita symbol in three dimensions with $\varepsilon^{123}=1$. This matrix is multiplied with the time derivatives of the fields, which are singular on the wavefront. Therefore their Eq. (33) can only have nontrivial solutions if the determinant of M_e vanishes. This condition directly leads to the wavefront equation within the framework considered. For the isotropic case (cf. Sec. III B), the anisotropic, nonbirefringent case (cf. Sec. III C), and the anisotropic, birefringent sector (cf. Sec. III D) we obtain

$$1 = \mathcal{A}^2|\nabla\psi|^2, \tag{4.7a}$$

$$1 = (\partial^1\psi)^2 + (\partial^2\psi)^2 + \mathcal{B}^2(\partial^3\psi)^2, \tag{4.7b}$$

$$1-\mathcal{G}^2 = |\nabla\psi|^2 + \mathcal{G}\{(\partial^1\psi)^2[1-\cos(2\eta)] - (\partial^3\psi)^2[1+\cos(2\eta)]\} - \mathcal{G}^2\{(\partial^2\psi)^2 + [(\partial^1\psi)^2 - (\partial^3\psi)^2]\cos(2\eta)\}, \tag{4.7c}$$

$$1+\mathcal{G}\cos(2\eta) = |\nabla\psi|^2 + \mathcal{G}\{(\partial^1\psi)^2 + (\partial^2\psi)^2\cos(2\eta) - (\partial^3\psi)^2\}. \tag{4.7d}$$

These are the analogs of the wavefront equation $|\nabla\psi|^2 = n^2$ in modified Maxwell theory. Following the lines in connection to Eq. (2.30) classical Hamilton functions can be obtained as parts of the Hamilton-Jacobi equation describing a classical ray. For the sectors considered a few lines above they read as follows:

$$H|_{\odot} = -\mathcal{A}\sqrt{\mathbf{k}^2}, \tag{4.8a}$$

$$H|_{\oplus} = -\sqrt{k_1^2 + k_2^2 + \mathcal{B}^2 k_3^2}, \tag{4.8b}$$

$$\sqrt{1-\mathcal{G}^2}H|_{\circledcirc}^{(1)} = -\{\mathbf{k}^2 + \mathcal{G}\{k_1^2[1-\cos(2\eta)] - k_3^2[1+\cos(2\eta)]\} - \mathcal{G}^2[k_2^2 + (k_1^2-k_3^2)\cos(2\eta)]\}^{1/2},$$
$$H|_{\circledcirc}^{(1)} = -\sqrt{\mathcal{G}_1 k_1^2 + k_2^2 + \mathcal{G}_2 k_3^2}, \tag{4.8c}$$

$$\sqrt{1+\mathcal{G}\cos(2\eta)}H|_{\circledcirc}^{(2)} = -\sqrt{\mathbf{k}^2 + \mathcal{G}[k_1^2 + k_2^2\cos(2\eta) - k_3^2]},$$
$$H|_{\circledcirc}^{(2)} = -\sqrt{\tilde{\mathcal{G}}_1 k_1^2 + k_2^2 + \tilde{\mathcal{G}}_2 k_3^2}, \tag{4.8d}$$

with $\mathcal{G}_1, \mathcal{G}_2$ of Eq. (3.34c) and $\tilde{\mathcal{G}}_1, \tilde{\mathcal{G}}_2$ taken from Eq. (3.34d). These Hamilton functions are directly linked to the modified dispersion relations, cf. the paragraph below Eq. (3.11) for the isotropic case, Eq. (3.20) for the anisotropic (nonbirefringent) sector, and Eq. (3.34) for the anisotropic (birefringent) case. This nicely demonstrates that all computations are consistent with each other.

The wavefront equations (4.7) are not suitable for our calculations since they involve first derivatives of the wavefront that are unclear how to be treated. Having the eikonal equations involving the refractive indices and velocity components only would be of advantage. As a cross check with the previously obtained results, the refractive indices can be derived from Eq. (4.7). For the isotropic case, using the second of Eq. (4.4b) we obtain $|\nabla\psi|^2 = n^2$, which by inserting into Eq. (4.7a) directly leads to the isotropic result $n|_{\odot} = 1/\mathcal{A}$. In Eq. (4.7b) of the anisotropic (nonbirefringent) sector we can introduce

$$(\partial^1\psi)^2 + (\partial^2\psi)^2 = n^2\sin^2\vartheta, \qquad \partial^3\psi = n\cos\vartheta, \tag{4.9}$$

leading to $n|_{\oplus} = 1/\sqrt{\sin^2\vartheta + \mathcal{B}^2\cos^2\vartheta}$. The latter depends on the angle ϑ between the propagation direction and the preferred direction $\boldsymbol{\zeta}$. For the anisotropic (birefringent) sector we insert

$$\partial^1\psi = n\frac{\cos\theta_1 - \cos\theta_2}{2\sin\eta}, \qquad \partial^3\psi = n\frac{\cos\theta_1 + \cos\theta_2}{2\cos\eta},$$
$$\partial^2\psi = \sqrt{n^2 - (\partial^1\psi)^2 - (\partial^3\psi)^2}, \tag{4.10}$$

both in Eq. (4.7d) and Eq. (4.7c) to obtain two refractive indices differing at second order in Lorentz violation:

$$n|_{\circledcirc}^{(1)} = \sqrt{\frac{1-\mathcal{G}^2}{1+\mathcal{G}\{(\mathcal{G}/2)[\cos(2\theta_1)+\cos(2\theta_2)] - 2\cos\theta_1\cos\theta_2\}}}, \tag{4.11a}$$

$$n|^{(2)}_{\textcircled{v}} = \sqrt{\frac{1+\mathcal{G}\cos(2\eta)}{1+\mathcal{G}[\cos(2\eta)-2\cos\theta_1\cos\theta_2]}}. \tag{4.11b}$$

Based on these refractive indices the integrands of the action functional in Eq. (4.5) can be computed. The results are consistent with Eqs. (3.14b), (3.27):

$$V(\mathbf{u})|_{\textcircled{o}} = n|_{\textcircled{o}}|\mathbf{u}| = \frac{1}{\mathcal{A}}\sqrt{\mathbf{u}^2} = F(\mathbf{u})|^{+}_{\textcircled{o}}, \tag{4.12a}$$

$$\begin{aligned} V(\mathbf{u})|_{\textcircled{d}} &= n|_{\textcircled{d}}|\mathbf{u}| = \frac{\sqrt{(u^1)^2+(u^2)^2+(u^3)^2}}{\sqrt{\sin^2\vartheta+\mathcal{B}^2\cos^2\vartheta}} \\ &= \frac{(u^1)^2+(u^2)^2+(u^3)^2}{\sqrt{(u^1)^2+(u^2)^2+\mathcal{B}^2(u^3)^2}} \\ &= F(\mathbf{u})|^{+}_{\textcircled{d}}, \end{aligned} \tag{4.12b}$$

$$\begin{aligned} V(\mathbf{u})|^{(1)}_{\textcircled{v}} &= n|^{(1)}_{\textcircled{v}}|\mathbf{u}| = F(\mathbf{u})|^{(1)+}_{\textcircled{v}}, \\ V(\mathbf{u})|^{(2)}_{\textcircled{v}} &= n|^{(2)}_{\textcircled{v}}|\mathbf{u}| = F(\mathbf{u})|^{(2)+}_{\textcircled{v}}, \end{aligned} \tag{4.12c}$$

where for the latter two Eq. (3.38) has to be employed. The refractive indices obtained from the wavefront equations correspond to the refractive indices computed directly from their definitions via the inverse phase velocity: $n \equiv v_{\mathrm{ph}}^{-1} = |\mathbf{k}|/\omega$.

$$n|_{\textcircled{o}} = v_{\mathrm{ph}}|^{-1}_{\textcircled{o}} = \frac{|\mathbf{k}|}{\omega|_{\textcircled{o}}} = \frac{1}{\mathcal{A}}, \tag{4.13a}$$

$$\begin{aligned} n|_{\textcircled{d}} &= v_{\mathrm{ph}}|^{-1}_{\textcircled{d}} = \frac{|\mathbf{k}|}{\omega|_{\textcircled{d}}} = \sqrt{\frac{\mathbf{k}^2}{k_\perp^2+\mathcal{B}^2k_\parallel^2}} \\ &= \frac{1}{\sqrt{\sin^2\vartheta+\mathcal{B}^2\cos^2\vartheta}}, \end{aligned} \tag{4.13b}$$

$$\begin{aligned} n|^{(1)}_{\textcircled{v}} &= (v_{\mathrm{ph}}|^{(1)}_{\textcircled{v}})^{-1} = \frac{|\mathbf{k}|}{\omega_1|_{\textcircled{v}}}, \\ n|^{(2)}_{\textcircled{v}} &= (v_{\mathrm{ph}}|^{(2)}_{\textcircled{v}})^{-1} = \frac{|\mathbf{k}|}{\omega_2|_{\textcircled{v}}}. \end{aligned} \tag{4.13c}$$

The studies previously performed do not reveal any inconsistencies. The essential conclusion is that it should be warranted to describe the isotropic, anisotropic (nonbirefringent), and anisotropic (birefringent) sectors of modified Maxwell theory (in the geometric-optics approximation) with an adapted version of the eikonal equation, Eq. (4.4b).

Last but not least the parity-odd sector of Sec. III E shall be elaborated on. The wavefront equations for the parity-odd case were not derived in [95] since in the latter reference all controlling coefficients mixing electric and magnetic fields were set to zero. Adapting the procedure used allows one to derive them nevertheless. The authors of [95] consider the values of the fields directly on the wavefront, e.g., for the electric field: $\mathbf{E}_0(\mathbf{x}) = \mathbf{E}(t,\mathbf{x})|_{t=\psi(\mathbf{x})}$. In what follows, all fields evaluated on the wavefront will be denoted by an additional "0" as an index. The spatial derivative on the wavefront is then given by

$$\frac{\partial \mathbf{E}_0}{\partial x^j} = \frac{\partial \mathbf{E}}{\partial x^j} + \dot{\mathbf{E}}\frac{\partial \psi}{\partial x^j}. \tag{4.14}$$

Based on this procedure, from Maxwell's equations four equations can be derived that involve field components on the wavefront and field derivatives only:

$$\boldsymbol{\nabla}\times\mathbf{E}_0 = -\dot{\mathbf{B}} + \boldsymbol{\nabla}\psi\times\dot{\mathbf{E}}, \qquad \boldsymbol{\nabla}\times\mathbf{H}_0 = \dot{\mathbf{D}} + \boldsymbol{\nabla}\psi\times\dot{\mathbf{H}}, \tag{4.15a}$$

$$\boldsymbol{\nabla}\cdot\mathbf{D}_0 = \boldsymbol{\nabla}\psi\cdot\dot{\mathbf{D}}, \qquad \boldsymbol{\nabla}\cdot\mathbf{B}_0 = \boldsymbol{\nabla}\psi\cdot\dot{\mathbf{B}}, \tag{4.15b}$$

$$\mathbf{D} = \mathbf{E} + \kappa_{DB}\mathbf{B}, \qquad \mathbf{H} = \kappa_{DB}\mathbf{E} + \mathbf{B}. \tag{4.15c}$$

These must be combined to obtain an equation that involves the time derivatives of only a single field, e.g., the electric field and field values on the wavefront that may not necessarily include only a single field. This can be carried out via the following chain of steps:

$$\boldsymbol{\nabla}\times\mathbf{E}_0 = -\dot{\mathbf{H}} + \kappa_{DB}\dot{\mathbf{E}} + \boldsymbol{\nabla}\psi\times\dot{\mathbf{E}}, \tag{4.16a}$$

$$\begin{aligned} &\boldsymbol{\nabla}\psi\times(\boldsymbol{\nabla}\times\mathbf{E}_0) \\ &\quad = -\boldsymbol{\nabla}\psi\times\dot{\mathbf{H}} + \boldsymbol{\nabla}\psi\times\kappa_{DB}\dot{\mathbf{E}} + \boldsymbol{\nabla}\psi\times(\boldsymbol{\nabla}\psi\times\dot{\mathbf{E}}), \end{aligned} \tag{4.16b}$$

$$\begin{aligned} &\boldsymbol{\nabla}\psi\times(\boldsymbol{\nabla}\times\mathbf{E}_0) \\ &\quad = \dot{\mathbf{D}} - \boldsymbol{\nabla}\times\mathbf{H}_0 + \boldsymbol{\nabla}\psi\times\kappa_{DB}\dot{\mathbf{E}} + \boldsymbol{\nabla}\psi\times(\boldsymbol{\nabla}\psi\times\dot{\mathbf{E}}), \end{aligned} \tag{4.16c}$$

$$\begin{aligned} &\boldsymbol{\nabla}\psi\times(\boldsymbol{\nabla}\times\mathbf{E}_0) \\ &\quad = \dot{\mathbf{E}} + \kappa_{DB}\dot{\mathbf{B}} - \boldsymbol{\nabla}\times\mathbf{H}_0 + \boldsymbol{\nabla}\psi\times\kappa_{DB}\dot{\mathbf{E}} \\ &\qquad + \boldsymbol{\nabla}\psi\times(\boldsymbol{\nabla}\psi\times\dot{\mathbf{E}}), \end{aligned} \tag{4.16d}$$

$$\begin{aligned} &\boldsymbol{\nabla}\psi\times(\boldsymbol{\nabla}\times\mathbf{E}_0) \\ &\quad = \dot{\mathbf{E}} + \kappa_{DB}(\boldsymbol{\nabla}\psi\times\dot{\mathbf{E}} - \boldsymbol{\nabla}\times\mathbf{E}_0) - \boldsymbol{\nabla}\times\mathbf{H}_0 \\ &\qquad + \boldsymbol{\nabla}\psi\times\kappa_{DB}\dot{\mathbf{E}} + \boldsymbol{\nabla}\psi\times(\boldsymbol{\nabla}\psi\times\dot{\mathbf{E}}). \end{aligned} \tag{4.16e}$$

The resulting equation then reads

$$\dot{\mathbf{E}} + \kappa_{DB}\boldsymbol{\nabla}\psi \times \dot{\mathbf{E}} + \boldsymbol{\nabla}\psi \times \kappa_{DB}\dot{\mathbf{E}} + \boldsymbol{\nabla}\psi \times (\boldsymbol{\nabla}\psi \times \dot{\mathbf{E}}) = \boldsymbol{\nabla}\psi \times (\boldsymbol{\nabla} \times \mathbf{E}_0) + \boldsymbol{\nabla} \times \mathbf{H}_0 + \kappa_{DB}\boldsymbol{\nabla} \times \mathbf{E}_0. \tag{4.17}$$

The condition for a vanishing determinant of the matrix on the left-hand side for the existence of nontrivial solutions leads to the wavefront equation for the parity-odd case:

$$(1 + 2\boldsymbol{\zeta}\cdot\boldsymbol{\nabla}\psi - |\boldsymbol{\nabla}\psi|^2)[1 - (1+\boldsymbol{\zeta}^2)|\boldsymbol{\nabla}\psi|^2 + 2(\boldsymbol{\zeta}\cdot\boldsymbol{\nabla}\psi) + (\boldsymbol{\zeta}\cdot\boldsymbol{\nabla}\psi)^2] = 0. \tag{4.18}$$

Inserting the second of Eq. (4.4b) into the first factor of Eq. (4.18) results in

$$1 + 2\boldsymbol{\zeta}\cdot\boldsymbol{\nabla}\psi - |\boldsymbol{\nabla}\psi|^2 = 1 - 2n\boldsymbol{\zeta}\cdot\hat{\mathbf{u}} - n^2 \overset{!}{=} 0. \tag{4.19}$$

The latter can be solved with respect to the refractive index n to give

$$n|_{\otimes}^{\zeta(1)} = -\boldsymbol{\zeta}\cdot\hat{\mathbf{u}} + \sqrt{1 + (\boldsymbol{\zeta}\cdot\hat{\mathbf{u}})^2} = -\mathcal{E}\cos\vartheta + \sqrt{1 + \mathcal{E}^2\cos^2\vartheta}, \tag{4.20}$$

where only the positive-sign solution delivers a physically meaningful refractive index. Hence, the result obtained from the eikonal equation is consistent with Eq. (3.49c), which can be seen upon close inspection:

$$V(\mathbf{u})|_{\otimes}^{\zeta(1)} = n|_{\otimes}^{\zeta(1)}|\mathbf{u}| = -\boldsymbol{\zeta}\cdot\mathbf{u} + \sqrt{\mathbf{u}^2 + (\boldsymbol{\zeta}\cdot\mathbf{u})^2} = F(\mathbf{u})|_{\otimes}^{\zeta(1)+}. \tag{4.21}$$

The same procedure applied to the second factor of Eq. (4.18) leads to

$$1 - (1+\mathcal{E}^2)n^2 - 2n(\boldsymbol{\zeta}\cdot\hat{\mathbf{u}}) + n^2(\boldsymbol{\zeta}\cdot\hat{\mathbf{u}})^2 = 0. \tag{4.22}$$

Therefore, the refractive index reads

$$n|_{\otimes}^{\zeta(2)} = \frac{-\boldsymbol{\zeta}\cdot\hat{\mathbf{u}} + \sqrt{1+\mathcal{E}^2}}{1 + \mathcal{E}^2 - (\boldsymbol{\zeta}\cdot\hat{\mathbf{u}})^2} = \frac{-\mathcal{E}\cos\vartheta + \sqrt{1+\mathcal{E}^2}}{1 + \mathcal{E}^2\sin^2\vartheta}, \tag{4.23}$$

which is consistent with Eq. (3.52)

$$V(\mathbf{u})|_{\otimes}^{\zeta(2)} = n|_{\otimes}^{\zeta(2)}|\mathbf{u}| = \frac{-\boldsymbol{\zeta}\cdot\mathbf{u} + \sqrt{1+\mathcal{E}^2}|\mathbf{u}|}{1 + \mathcal{E}^2 - (\boldsymbol{\zeta}\cdot\mathbf{u})^2/\mathbf{u}^2} = F(\mathbf{u})|_{\otimes}^{\zeta(2)+}. \tag{4.24}$$

The refractive indices obtained from the wavefront equations for the isotropic and anisotropic cases, Eqs. (4.7a)–(4.7d), respectively, are consistent with the usual definition of the refractive index via the inverse phase velocity [cf. Eqs (4.13a)–(4.13c)]. However, this does not seem to be the case for the parity-odd sector. Inspecting Eqs. (3.46a), (3.46b) and the latter results for the refractive indices of Eqs. (4.20), (4.23) reveals the inconsistency:

$$\frac{|\mathbf{k}|}{\omega_1|_{\otimes}} = \frac{1}{\mathcal{E}\cos\vartheta + \sqrt{1 + \mathcal{E}^2\cos^2\vartheta}} \neq n|_{\otimes}^{\zeta(1)}, \tag{4.25a}$$

$$\frac{|\mathbf{k}|}{\omega_2|_{\otimes}} = \frac{1}{\mathcal{E}\cos\vartheta + \sqrt{1 + \mathcal{E}^2}} \neq n|_{\otimes}^{\zeta(2)}. \tag{4.25b}$$

The definition of the refractive index via the inverse of the phase velocity rests on the existence of a nonzero permeability and permittivity. However, for the parity-odd case they both vanish and the electric fields even mix with the magnetic fields, which is why the ordinary definition of the refractive index does not seem to be reasonable. A further origin of the issue may be that Okubo's method does not produce Finsler structures in a unique manner. We conclude that it may be problematic to treat the parity-odd case of modified Maxwell theory with the eikonal equation. Finding a solution to this clash is an interesting open problem.

B. Usefulness of Finsler structures

The quantity V that was dealt with on the last few pages is a velocity, which is not to be confused with the phase or group velocity in a Lorentz-violating vacuum. It is the integrand of the path length functional in a nontrivial medium with refractive index $n(\mathbf{x})$. In the previous sections it was clarified that V can be understood as a Finsler structure. These Finsler structures are the analogs of classical Lagrangians in the fermion sector obtained in [63–67]. It was shown that they are directly connected to the refractive indices of the corresponding Lorentz-violating vacua that are comprised in the eikonal equation. Both the eikonal equation and Finsler structures will play an essential role for phenomenology in Sec. V and for the discussion of explicit Lorentz violation in Secs. VI, VII.

In [62] slightly different conventions are used and such a Finsler structure is interpreted as a phase describing the state of evolution of a wave. The reason is due to the form of a plane wave: $\exp(\mathrm{i}\varphi)$ with $\varphi = \omega(n\hat{\mathbf{k}}\cdot\mathbf{x} - t)$ where $\hat{\mathbf{k}}$ is the wave unit vector and $\mathbf{x}$ a vector in configuration space. Note that a product of the refractive index and a spatial distance (optical path length) is comprised both in the latter phase φ and the integrand of the path length functional in Eq. (4.5).

Having such a Finsler structure V at hand, their lines of constant value in two spatial dimensions can be investigated. If the Finsler structure is purely Riemannian these lines are either concentric circles, cf. Eq. (3.14b), or ellipses whose axes may not be aligned with the coordinate axes [Fig. 1(a)]. In contrast, Finsler structures that are not Riemannian have a vast number of novel properties. For

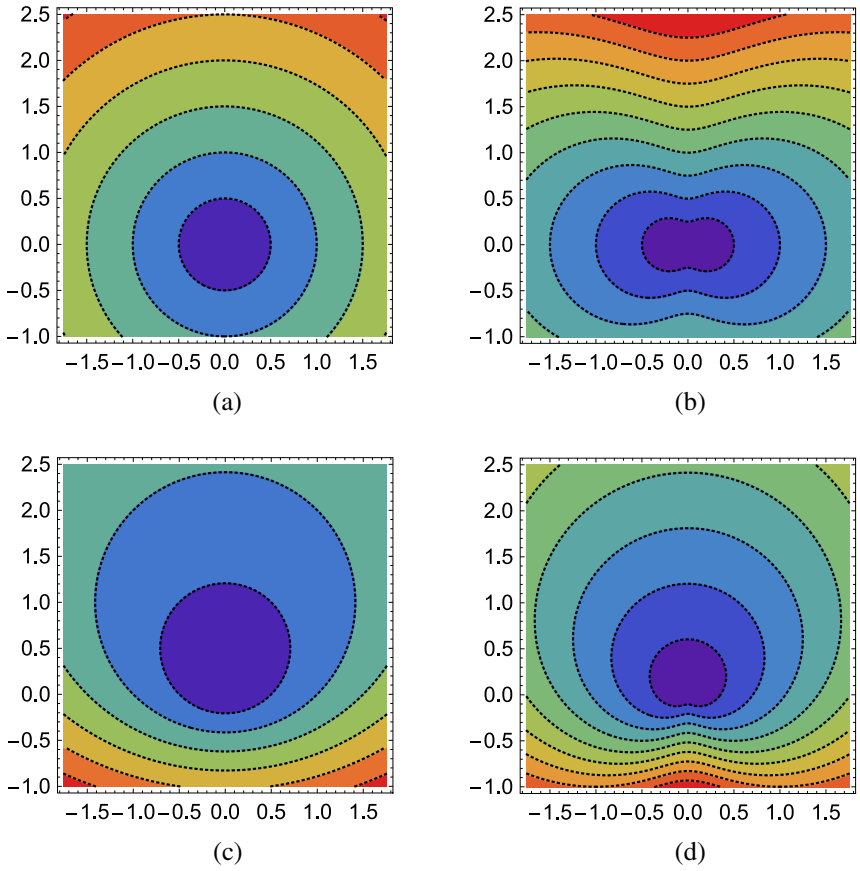

FIG. 1 (color online). Lines of constant V for the isotropic Finsler structure of Eq. (3.14b) (a), the anisotropic structure of Eq. (3.27) (b) for $\mathcal{B} = 1$, the first parity-odd structure in Eq. (3.49c) for $\mathcal{E} = 1$ (c), and the second parity-odd structure in Eq. (3.52b) for $\mathcal{E} = 1$ (d).

the structure of Eq. (3.27) the previously mentioned lines may have notches, i.e., regions of negative (extrinsic) curvature. These lines look like two merged circles that have been smoothed out at their intersections [Fig. 1(b)]. In the case of a Randers structure, Eq. (3.39), we have circles whose centers are displaced from the coordinate origin [Fig. 1(c)]. For the second-order deviation of a Randers structure, Eq. (3.40), each displaced circle has an additional notch [Fig. 1(d)]. At such notches the density of lines is larger compared to other regions, which means that these regions are very steep in a three-dimensional plot of V. Thus, plenty of physical information is comprised in the Finsler structure V: the shape of the state of wave development (shapes other than circles and ellipses for non-Riemmanian structures), how quickly the state of development changes in different directions (steep regions near notches versus flat regions otherwise), and whether the centers of these states lie on a point or a curve (the latter, e.g., for Randers structures).

Reducing the notion of waves to the picture of rays, V delivers information on whether it suffices to describe the dynamics of the corresponding ray with Riemannian geometry. An isotropic theory is characterized by a preferred timelike direction and it can be interpreted as a Riemannian framework. This is not entirely surprising since such a theory can only involve a scaling factor (denoted as $\mathcal{A}$ in Sec. III B) that affects all spatial directions equivalently. For an anisotropic framework, the situation is already different (cf. the anisotropic, nonbirefringent or the parity-odd theory). The corresponding classical analogs are connected to Finsler structures. Promoting the refractive index to a position-dependent function and computing the extremal traveling time of a light ray between two points, the geodesic equation of Riemannian geometry is not sufficient anymore. In fact, such setups are closely linked to the Zermelo navigation problem of a ship or plane in a current [96] and the related geodesics are no longer Riemannian. To compute geodesics based on the functional of Eq. (4.5), the Finsler structures of Eqs. (3.14b), (3.27), (3.39), (3.40), (3.49c), and (3.52b) will be needed. It is reasonable to have them at hand for future purpose.

Last but not least, the Finsler spaces associated with the minimal SME photon sector may be of interest to mathematicians investigating their properties. Note that b space [63,64,67], which is connected to the fermonic b_μ coefficient, has raised some mathematical interest; cf. [72]. Although its form is quite simple it has a rich set of interesting properties. This may also be the case for the "second-order Kropina structures" of Eqs. (3.27), (3.39), (3.40).

V. GRAVITATIONAL BACKGROUNDS

The physics for a classical point-particle equivalent to a massive fermion rests on its Lagrangian. The procedure of deriving those within the framework of the SME works for massive particles only where in the limit of a vanishing particle mass the Lagrangian goes to zero. So far we have demonstrated that the important quantity to describe the physics of electromagnetic waves in the geometric-optics approximation is the refractive index. The reason is that the motion of photons is much more restricted than the motion of a massive particle. After all, for a particle with mass moving in a potential the initial position, direction, and velocity can be chosen freely. On the contrary, for a photon the initial position and direction only are not fixed, whereas its initial speed is determined by the refractive index at its starting point.

In the previous sections, it was shown how to establish connections between various cases of the minimal SME photon sector and certain Finsler geometries. The Finsler geometries found were discovered to be closely related to the various refractive indices where only for the parity-odd case of the CPT-even sector such a connection is not manifest. The refractive indices found are independent of the spacetime position just as the controlling coefficients, which corresponds to the analog of a homogeneous medium in optics. However, the refractive index can depend on the three spatial velocity components. In other words, in such cases the refractive index depends on angles enclosed between the propagation direction and preferred directions. This situation is reminiscent of anisotropic media in optics. Hence, Finsler structures related to the CPT-even photon sector are three-dimensional in contrast to the Finsler structures obtained from Wick-rotating classical Lagrangians of massive particles. Besides, note that in the photon case no Wick rotation is necessary since the intrinsic metric involved is already of a Euclidean signature.

These results shall serve as a base for studying light rays in the geometric-optics approximation in the presence of Lorentz violation. As we saw, for most cases these can be described by the eikonal equation; cf. Eq. (4.4b):

$$\frac{\mathrm{d}}{\mathrm{d}s}\left[n\frac{\mathrm{d}\mathbf{x}}{\mathrm{d}s}\right]=\boldsymbol{\nabla}_{\mathbf{x}}n, \tag{5.1}$$

where n is the refractive index of the medium considered. On the right-hand side, the gradient is understood to be computed with respect to the position vector $\mathbf{x}$. The photon trajectory is given by $\mathbf{x}=\mathbf{x}(s)$ and it is parametrized by the arc length s. For an isotropic and homogeneous medium, the refractive index is a mere constant. In this case, one immediately sees that the resulting ray equation is

$$\frac{\mathrm{d}^2\mathbf{x}}{\mathrm{d}s^2}=\mathbf{0}, \tag{5.2}$$

whose solution is a straight line as expected. For homogeneous, but anisotropic, media the refractive index depends on at least one angle, $n=n(\vartheta)$, where further angles are suppressed for brevity. For a straight-ray trajectory, the angle ϑ is fixed by the initial direction and it does not change during propagation, i.e., it is not a function of s. Furthermore due to homogeneity the refractive index does not change along the trajectory as well, which is why $\boldsymbol{\nabla}_{\mathbf{x}}n(\vartheta)=0$ for points on the trajectory. Therefore in this case we again end up with Eq. (5.2). For inhomogeneous media with $n=n(\mathbf{x})$ the eikonal equation cannot have straight-line solutions, though.

In what follows the formalism and knowledge attained shall be applied to propagating light rays in curved spacetimes with metric $g_{\mu\nu}=g_{\mu\nu}(x)$. The trajectory of a ray in a spacetime is described by a four-vector $x^\mu=x^\mu(s)$ and it propagates with the four-velocity $u^\mu\equiv\mathrm{d}x^\mu/\mathrm{d}s$. Propagation occurs along geodesics combined with the nullcone condition $g_{\mu\nu}u^\mu u^\nu=0$ that has to hold locally at each spacetime point. For practical reasons, which will become clear in the course of the current section, all forthcoming investigations will be performed in a spacetime characterized by a line interval of the form

$$\begin{aligned}\mathrm{d}\tau^2=&\frac{1}{A(r,\theta,\phi)}\mathrm{d}t^2\\&-A(r,\theta,\phi)(\mathrm{d}r^2+r^2\mathrm{d}\theta^2+r^2\sin^2\theta\mathrm{d}\phi^2).\end{aligned} \tag{5.3}$$

Here t is the time, (r,θ,ϕ) are spherical coordinates, and A is a time-independent function. Such metrics were proposed in [97] and they are denoted as "generally isotropic" where metrics with $A=A(r)$ are called "spherically symmetric." The parentheses in the spatial part of Eq. (5.3) give the volume element of a three-dimensional ball and it is multiplied by $A(r,\theta,\phi)$. The choice $A(r,\theta,\phi)=1$ in Eq. (5.3) describes Minkowski spacetime in three-dimensional spherical coordinates. In this case, the spatial coordinate surfaces with constant r are two-spheres. For arbitrary $A(r,\theta,\phi)$ these surfaces are still two-spheres topologically, but their local geometry depends on r, θ, and ϕ. Note that the metric describing a weak gravitational field can be brought into the generally isotropic form:

$$\begin{aligned}(g_{\mu\nu})&=\mathrm{diag}((1+2\Phi),-(1-2\Phi),-(1-2\Phi),-(1-2\Phi))\\&=\mathrm{diag}\left(\frac{1}{1-2\Phi},-(1-2\Phi),-(1-2\Phi),\right.\\&\quad\left.-(1-2\Phi)\right)+\mathcal{O}(\Phi^2).\end{aligned} \tag{5.4}$$

Here $\Phi=\Phi(r)=-GM/r\ll 1$ is the Newtonian potential.

In the latter paper [97] it was shown that there is a link between the eikonal equation of the geometric-optics approximation and the null geodesic equations of a spacetime based on a line interval of Eq. (5.3). A suitable combination of the geodesic equations leads to

$$\frac{\mathrm{d}}{\mathrm{d}s}\left[A(r,\theta,\phi)\frac{\mathrm{d}\mathbf{x}}{\mathrm{d}s}\right] = \boldsymbol{\nabla}A(r,\theta,\phi), \tag{5.5}$$

i.e., $A(r,\theta,\phi)$ of Eq. (5.3) can be understood as an inhomogeneous and anisotropic refractive index. Therefore as long as weak gravitational fields are considered, light behaves according to the geometric-optics approximation. The approximation is expected to break down as soon as strong gravitational forces appear such as in the direct vicinity of a black hole. In this case the original geodesic equations have to be studied instead of the eikonal approach. Note that the converse is true as well. If the eikonal equation is known to be valid (also in flat spacetime) this corresponds to a propagating ray in a generally isotropic spacetime of Eq. (5.3).

A. Isotropic case

The eikonal approach has a great potential to be applied to the propagation of light rays in a weak gravitational field permeated by a Lorentz-violating background field. It is reasonable to start with the simplest case, which is the isotropic one investigated in Sec. III B. With the constant refractive index $n = 1/\mathcal{A}$ (in Minkowski spacetime) given by Eq. (3.8) or Eq. (4.13a) the eikonal equation and the corresponding spacetime, Eq. (5.3), read as follows:

$$\frac{\mathrm{d}}{\mathrm{d}s}\left[\frac{1}{\mathcal{A}}\frac{\mathrm{d}\mathbf{x}}{\mathrm{d}s}\right] = \boldsymbol{\nabla}\left(\frac{1}{\mathcal{A}}\right), \tag{5.6a}$$

$$\mathrm{d}\tau^2 = \mathcal{A}\mathrm{d}t^2 - \frac{1}{\mathcal{A}}(\mathrm{d}r^2 + r^2\mathrm{d}\theta^2 + r^2\sin^2\theta\mathrm{d}\phi^2). \tag{5.6b}$$

The coordinate surfaces of the associated spacetime are spheres whose radii are scaled by $1/\sqrt{\mathcal{A}}$. This intermediate result can now be used to introduce a gravitational background. Via the principle of minimal coupling the flat Minkowski metric is replaced by a curved spacetime metric, $\eta_{\mu\nu} \mapsto g_{\mu\nu}(x)$, and the constant refractive index n is promoted to a spacetime-position dependent function: $n \mapsto n(r,\theta,\phi)$. The curved spacetime metric is taken to be Eq. (5.4) for a weak gravitational field. Since the latter is spherically symmetric, it is reasonable to assume spherical symmetry for the position-dependent refractive index, i.e., $n(r) = 1/\mathcal{A}(r)$. The corresponding eikonal equation and the line interval then read as follows:

$$\frac{\mathrm{d}}{\mathrm{d}s}\left[n(r)\frac{\mathrm{d}\mathbf{x}}{\mathrm{d}s}\right] = \boldsymbol{\nabla}n(r), \qquad n(r) \equiv \frac{1-2\Phi(r)}{\mathcal{A}(r)}, \tag{5.7a}$$

$$\mathrm{d}\tau^2 = \frac{1}{n(r)}\mathrm{d}t^2 - n(r)(\mathrm{d}r^2 + r^2\mathrm{d}\theta^2 + r^2\sin^2\theta\mathrm{d}\phi^2). \tag{5.7b}$$

Hence, the minimal-coupling principle amounts to a refractive index that is the product of a spatial component of the weak gravitational field metric and the spacetime-position dependent refractive index $1/\mathcal{A}(r)$ associated with the isotropic Lorentz-violating framework considered.

The approach introduced has a paramount advantage. The physics of a Lorentz-violating photon in a (weak) gravity field can be studied without field theory and the geodesic equations in a curved spacetime. Instead, a classical method is used replacing photons by light rays and working in the geometric-optics approximation with the eikonal equation. In this context, Lorentz symmetry violation is treated as explicit, which is known to clash with the existence of gravitational backgrounds [41]. The latter Secs. VI and VII will be dedicated to this issue where for now we will delve into phenomenology.

One possible application of the used approach lies in the (modified) deflection of light in the vicinity of a massive body (cf. Fig. 2), which is an important test of gravitational theories. From a technical point of view the eikonal equation is nonlinear, which makes it challenging to solve analytically in general. However, for the isotropic case, i.e., a refractive index only depending on the radial coordinate r, the formula of Bouguer follows from the eikonal equation (see, e.g., Sec. 3.2.1 of [98]):

$$n(r)r\sin\alpha = C. \tag{5.8}$$

Here C is a constant and α the angle between the tangent vector of the trajectory and the radial vector pointing from the coordinate origin to a particular point on the trajectory. The latter relationship is the equivalent of energy and angular momentum conservation for a massive particle in classical mechanics. Since both the distance r of a particular point from the origin and the angle α associated with this point does not depend on the parametrization of the trajectory, we choose to parametrize it by spherical coordinates. Thereby the problem is restricted to the

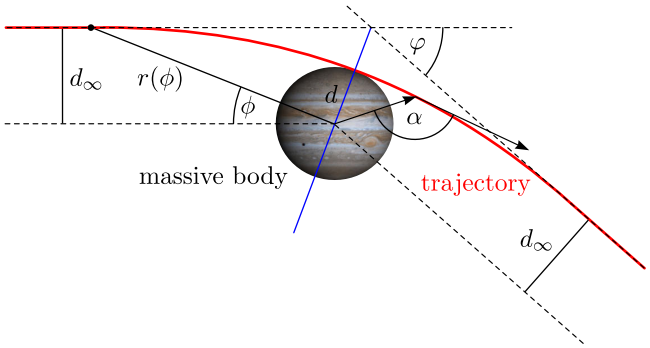

FIG. 2 (color online). Deflection of light near a massive body, e.g., the planet Jupiter. (The picture of Jupiter was taken by the Cassini spacecraft; cf. http://www.nasa.gov/audience/forstudents/5-8/features/nasa-knows/what-is-jupiter-58.html.)

$x-z$-plane with $\theta=\pi/2$. The trajectory then reads $\mathbf{x}=r\hat{\mathbf{e}}_r$ where $r=r(\phi)$ and $\hat{\mathbf{e}}_r=\hat{\mathbf{e}}_r(\phi)$ is the unit vector pointing in radial direction. The angle α is given as follows:

$$\sin\alpha=\frac{r(\phi)}{\sqrt{r^2(\phi)+\dot{r}^2(\phi)}},\qquad \dot{r}\equiv\frac{\mathrm{d}r}{\mathrm{d}\phi}. \tag{5.9}$$

Now the formula of Bouguer delivers a differential equation for $\phi(r)$. Its solution is obtained by solving the latter with respect to $\mathrm{d}\phi/\mathrm{d}r$ and by performing a subsequent integration:

$$\phi(r)=C\int_d^r\frac{\mathrm{d}r}{r\sqrt{n(r)^2r^2-C^2}}, \tag{5.10}$$

where d is the distance of minimal proximity and the condition $\phi(d)=0$ has been set. By doing so, solving the eikonal equation has been reduced to computing a one-dimensional integral. Now consider a classical light ray approaching a massive body with impact parameter d_∞, which is the distance between the particle propagation direction in the asymptotically flat region and the parallel going through the center of mass of the body (at the coordinate origin). The photon will travel such that its distance to the body steadily decreases until reaching a minimum where it increases again afterwards. At the minimum distance d we have that $\dot{r}=0$ and therefore $\alpha=\pi/2$. The minimum distance corresponds to the impact parameter to a very good approximation: $d\approx d_\infty$. This is why Eq. (5.8) immediately tells us that

$$C=n(d)d\approx n(d_\infty)d_\infty. \tag{5.11}$$

Without the massive body, the change $\Delta\phi$ in the angle would be equal to π for a photon coming from an asymptotically flat region, passing near the coordinate origin, and propagating back to infinity. Due to the body there is a deflection, which changes $\Delta\phi$ to an angle that is slightly larger than π. Performing the integration in Eq. (5.10) from $r=d$ to infinity gives half of this contribution since it only takes into account the second half of the trajectory. Therefore, the deflection angle φ is given by

$$\varphi=\Delta\phi-\pi=2C\int_d^\infty\frac{\mathrm{d}r}{r\sqrt{n(r)^2r^2-C^2}}-\pi. \tag{5.12}$$

It can be checked that Eq. (5.12) gives $\varphi=0$ for $n(r)=1$ as expected. For a constant refractive index n it holds that $C=nd$. By inspecting Eq. (5.12) it follows immediately that a constant n does not lead to any deflection. This is in contrast to [99] where for certain Lorentz-violating frameworks with *constant* Lorentz-violating coefficient it was shown that there is a change in the deflection angle caused by Lorentz violation, indeed. However, note that in the latter reference a Schwarzschild black hole was considered whose line interval had not been cast into generally isotropic form; cf. Eq. (5.3). A discussion of this difference leading to more insight into Bouguer's formula is relegated to Appendix B, since it is quite technical and probably not of relevance for all readers.

B. Phenomenology for the isotropic framework

With the technique further developed, we are ready to carry out phenomenological calculations. The goal is to obtain predictions for the change of the light deflection angle caused by particular Lorentz-violating frameworks. These predictions will be compared to experiment with obtaining sensitivities on controlling coefficients in the minimal SME photon sector. As the most important example, light deflection at the Sun will be discussed first. However, light can be deflected at any other massive bodies such as planets.

First of all, we intend to recapitulate the standard result. For vanishing Lorentz violation the deflection angle of Eq. (5.12) can be computed analytically. Thereby the integral 2.266 of [100] is helpful:

$$\int\frac{\mathrm{d}x}{x\sqrt{\alpha+\beta x+\gamma x^2}}=\frac{1}{\sqrt{-\alpha}}\arcsin\left(\frac{2\alpha+\beta x}{x\sqrt{\beta^2-4\alpha\gamma}}\right),\qquad \alpha<0,\qquad \beta^2-4\alpha\gamma>0. \tag{5.13}$$

For the Lorentz-invariant case we have

$$\alpha=-\frac{d}{R_S}\left(\frac{d}{R_S}+2\right),\qquad \beta=2,\qquad \gamma=1, \tag{5.14}$$

with the Schwarzschild radius $R_S=2GM/c^2$ of the massive body. Here G is the gravitational constant, M the mass of the body, and c the speed of light. The conditions for α,β, and γ stated in Eq. (5.13) are fulfilled and the full analytical result for the deflection angle is given as follows:

$$\varphi=\frac{1+2\xi}{\sqrt{1+4\xi}}\left[\pi+2\arcsin\left(\frac{2\xi}{1+2\xi}\right)\right]-\pi=4\xi+\mathcal{O}(\xi^2),\qquad \xi=\frac{R_S}{2d}, \tag{5.15}$$

where the latter is the first-order expansion in the dimensionless parameter $\xi\ll1$. Now considering a light ray directly passing the surface of the Sun (scraping incidence), d is given by the radius $r_\odot$ of the Sun. Using the values of Table I and multiplying the previous equation with $180\times60^2/\pi$ leads to the well-known result $\varphi\approx1.75''$, which lies within few standard deviations from the mean value observed during the total eclipse in 1919 [101,102].

Now the refractive index is modified due to Lorentz violation according to Eq. (5.7a). Therefore the isotropic Lorentz-violating coefficient $\tilde{\kappa}_{\mathrm{tr}}$ is promoted to a spacetime-position dependent function (cf. Fig. 3). It is assumed to

TABLE I. Gravitational constant, masses, and radii of the Sun (⊙), Jupiter (♃), and Saturn (♄). For Jupiter and Saturn the average of the pole and equatorial radii is used.

Quantity	Unit	Value
G	$\mathrm{m}^3/(\mathrm{kg}\cdot\mathrm{s}^2)$	6.67384×10^{-11}
$M_\odot$	kg	1.98910×10^{30}
$M_♃$	kg	1.89813×10^{27}
$M_♄$	kg	5.68319×10^{26}
$r_\odot$	m	6.95508×10^{8}
$r_♃$	m	6.99110×10^{7}
$r_♄$	m	5.82320×10^{7}

only depend on the radial coordinate r to keep the framework isotropic:

$$\tilde{\kappa}_{tr} \mapsto \tilde{\kappa}_{tr}(r) = \tilde{\kappa}_{tr}[1 - f(r)], \tag{5.16}$$

with a function f having special properties. The latter shall be constructed such that $1 - f \geq 0$ for $r/d \geq 1$. This means that the sign of $\tilde{\kappa}_{tr}(r)$ is fixed by the sign of the constant prefactor $\tilde{\kappa}_{tr}$. Furthermore $\lim_{r\mapsto\infty}\tilde{\kappa}_{tr}(r) = \tilde{\kappa}_{tr}$, whereby in the asymptotically flat region the position-dependent controlling coefficient is identified with the corresponding SME photon coefficient $\tilde{\kappa}_{tr}$ in Minkowski spacetime. The refractive index then reads as

$$n(r) = \sqrt{\frac{1+\tilde{\kappa}_{tr}(r)}{1-\tilde{\kappa}_{tr}(r)}}\left(1+\frac{R_S}{r}\right). \tag{5.17}$$

From Eq. (5.7b) the coordinate velocity of light in this framework is given by

$$c = \frac{|\mathrm{d}\mathbf{r}|}{\mathrm{d}t} = \frac{1}{n(r)}, \tag{5.18}$$

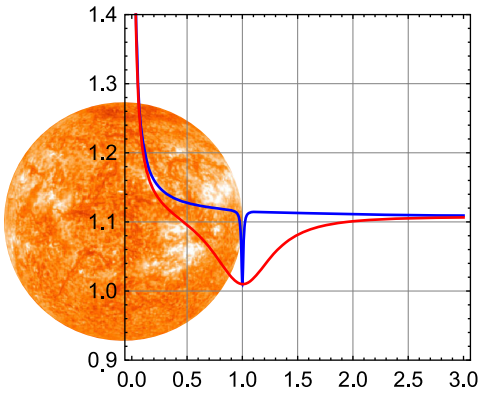

FIG. 3 (color online). Spacetime-position dependent refractive index (and controlling coefficient) as a function of the dimensionless parameter r/d where d corresponds to the Sun radius $r_\odot$ in this example. (The picture of the Sun was taken by SOHO—EIT Consortium, ESA, NASA; cf. http://science.nasa.gov/science-news/science-at-nasa/2003/22apr_currentsheet/.)

i.e., for $\tilde{\kappa}_{tr} > 0$ it is reduced in comparison to the Lorentz-invariant case.

The position dependence shall reflect the properties of the gravitational background. The curvature radius R_S is the physical scale of the background, i.e., it is reasonable to associate it with $\tilde{\kappa}_{tr}(r)$ as well. Note that we are only interested in the behavior of the function outside of the massive body, which means $r \geq d$. Generic functions with these properties are

$$f(r) \equiv \left[1 + a\left(\frac{r-d}{R_S}\right)^2\right]^{-1}, \tag{5.19a}$$

$$g(r) \equiv \frac{2\arctan\{a[1-(r-d)^2/R_S^2]\}+\pi}{2\arctan(a)+\pi}, \tag{5.19b}$$

where $a \leq 1$ is a free, dimensionless parameter. Therefore for these particular sample functions it holds that $f(d) = 1$ and $\lim_{r\mapsto\infty} f(r) = 0$. Whatever the underlying theory for a possible violation of Lorentz invariance looks like, it is reasonable to assume that the amount of Lorentz violation is influenced by a gravitational background field. Referring to a small-scale structure of spacetime where simple models were shown to produce Lorentz-violating particle dispersion relations [14,15] the argument could be along the following lines. A gravitational field has an energy density associated with it; cf. [103] for the case of spheres and black holes. Since a spacetime foam is caused by energy fluctuations, an additional contribution of energy density associated with a gravitational field may have some influence on it. This would render the effective controlling coefficients for Lorentz violation spacetime-position dependent. Hence, for the isotropic framework considered the refractive index directly at the surface of the Sun may have a dip for $\tilde{\kappa}_{tr} > 0$ or a peak for $\tilde{\kappa}_{tr} < 0$ in its position dependence (cf. Fig. 3). As long as the underlying description is not available, it is challenging to deliver a more rigorous argumentation. Thus, a $\tilde{\kappa}_{tr}(r)$ including Eq. (5.19) with the parameter a controlling the width of the dip/peak must be interpreted as a phenomenological description of such effects.

Now the modified deflection angle can be calculated in two different ways. The first is to compute the integral according to Bouguer's formula of Eq. (5.12). The second is to solve the eikonal equation directly. In Appendix C the eikonal equation is brought into a form that is suitable for solving it. For a refractive index that has a radial dependence only, Eq. (C5) results in

$$0 = (r^2+\dot{r}^2)r\frac{\partial n}{\partial r} + n(r^2+2\dot{r}^2-r\ddot{r}). \tag{5.20}$$

Bouguer's formula is a first integral of the eikonal equation that follows from angular momentum conservation. Therefore using it allows us to avoid the computation of one integral. Nevertheless as a cross check it is reasonable

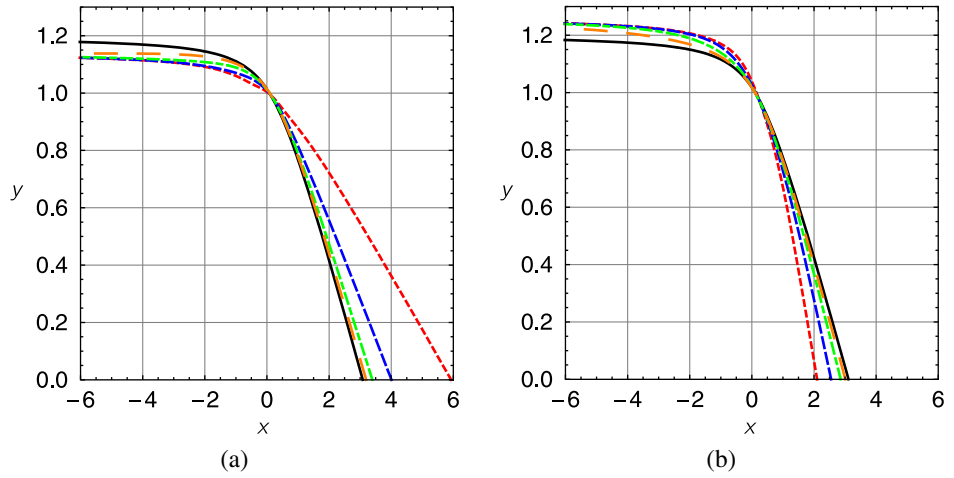

FIG. 4 (color online). Solutions of the eikonal equation in the x-y plane (in dimensions of d) for $\tilde{\kappa}_{tr} = 1/20$ (a) and for $\tilde{\kappa}_{tr} = -1/20$ (b). The massive body resides in the origin and the hypothetical value $d/R_S = 5$ has been chosen. The black (plain) curve shows standard light deflection where for the remaining [red (dotted), blue (dashed), green (dashed-dotted), orange (dashed with large spaces)] curve $a = \{1, 1/10, 1/10^2, 1/10^3\}$ has been taken successively.

to carry out the computation with the two techniques. Both the integral of Eq. (5.12) and the eikonal equation are challenging to be solved analytically for a refractive index that is modified by Lorentz violation. Therefore we attempt to treat both cases numerically with *Mathematica*.

To gain some physical understanding, the eikonal equation is solved numerically for hypothetical values of R_S and $\tilde{\kappa}_{tr}$ first. At the distance of minimal proximity d the sample functions of Eq. (5.19) vanish by construction. Therefore $n(d) = 1 + R_S/d$, which is why $C = n(d)d$ and the impact parameter is given by

$$d_\infty = \frac{C}{n(r=\infty)} = \sqrt{\frac{1-\tilde{\kappa}_{tr}}{1+\tilde{\kappa}_{tr}}}(d + R_S). \qquad (5.21)$$

For realistic situations, i.e., light bending at stars, the Schwarzschild radius is much smaller than the distance of minimal proximity. Note that for scraping incidence, d corresponds to the radius of the star. Since bounds on the isotropic coefficient $\tilde{\kappa}_{tr}$ in flat, asymptotic spacetime are strict, it holds that $d \approx d_\infty$ to a good approximation. For the hypothetical values that we choose for illustration purposes this is not necessarily warranted. Taking $d/R_S = 5$ and $\tilde{\kappa}_{tr} = 1/20$ we obtain the results depicted in Fig. 4(a). The curves show the solutions of the eikonal equation where the refractive index has been modeled according to Eq. (5.17) using the sample function $f(r)$ of Eq. (5.19a) for different choices of the parameter a. Recall that the latter characterizes the width of the dip/peak in the refractive index directly at the surface of the massive body, which is caused by Lorentz violation. Since for comparison all curves should meet at a single point, the impact parameters d_∞ have to be adapted properly, which is why they differ from each other.

The observation is that for increasing a and $\tilde{\kappa}_{tr} > 0$ the deflection angle is reduced. As long as the light ray is far away from the massive body it experiences a refractive index that increases when the distance to the body decreases. This is the standard behavior of the refractive index whose origin lies in nonvanishing Riemann curvature components. Upon approaching the massive body, the light ray suddenly experiences the dip where the refractive index becomes smaller for decreasing distance. The ray then behaves contrary to the standard case and tends to be bent away from the body, which can be clearly seen in Fig. 4(a). Note that for $\tilde{\kappa}_{tr} < 0$ the dip in the refractive index turns into a peak. Hence, the behavior is opposite and the ray is bent towards the body even stronger; cf. Fig. 4(b).

From a technical point of view to solve the eikonal equation, proper initial conditions have to be considered. Since the ray is assumed to arrive from an asymptotically flat region, the initial angle is $\phi_0 = \pi$. In practice, an angle lying close to π must be chosen where the direction of the ray initially is assumed to point along the positive horizontal axis. We express the solution of the eikonal equation as $r(\phi) = d\xi(\phi)$ with the dimensionless function $\xi(\phi)$. The initial conditions are then fixed to be $\xi(\phi_0) = \Delta$ and $\xi'(\phi_0) = -\cot(\phi_0)\Delta$ where $\phi_0 = \pi - \arcsin(d_\infty/\Delta)$. Here Δ is a length scale with the property $\Delta \gg d$, which is tuned to increase the precision of the numerical result. Theoretically Δ should approach infinity, which is not a possible value to choose in practice, though. Setting the final angle in the numerical integration to $\phi_1 \lesssim 0$ leads to numerical instabilities, which is why ϕ_1 is taken to be only slightly smaller than zero. This is supposed to be sufficient for small bending angles that appear in realistic scenarios. Note that $\phi_1 = -\pi/2$ would correspond to the upper infinite integration limit in Bouguer's formula. Since it is impossible to choose the latter value for ϕ_1 there is a (maximum) systematic error of around 8×10^{-10} μarcs between angles obtained in both methods. This systematic

TABLE II. Numerical results for modified light deflection angles at Jupiter (scraping incidence) in the isotropic framework. The first column states (ranges of) the parameter a used in Eq. (5.19). The second column gives the value of the isotropic coefficient. In the third and fourth columns differences between the standard deflection angle $\varphi_{\text{+}}^{*} \approx 16.6$ marcs and the modified angle $\varphi_{\text{+}}$ are shown in suitable units. For the third column the modeling function $f(r)$ of Eq. (5.19a) is used and for the fourth column we employ $g(r)$ of Eq. (5.19b). Each number is understood to be associated with the proper parameter a in the first column where both lists are in order. The results for a negative $\tilde{\kappa}_{\text{tr}}$ are (almost) equal to the corresponding numbers for a positive $\tilde{\kappa}_{\text{tr}}$ where the global sign of $\varphi_{\text{+}}^{*} - \varphi_{\text{+}}$ is reversed. The deviation in the absolute values shows up in the third digit for almost all differences.

$-\log_{10}(a)$	$-\log_{10}(\tilde{\kappa}_{\text{tr}})$	$f(r)$ $\varphi_{\text{+}}^{*} - \varphi_{\text{+}}$ [10 μarcs]	$g(r)$ $\varphi_{\text{+}}^{*} - \varphi_{\text{+}}$ [10 μarcs]
0	14	1.61	1.40
1…4	13	9.07; 5.10; 2.87; 1.61	8.80; 4.97; 2.80; 1.57
5…8	12	9.07; 5.10; 2.87; 1.61	8.84; 4.97; 2.80; 1.57
9…12	11	9.07; 5.10; 2.86; 1.60	8.84; 4.97; 2.79; 1.56
13…15	10	8.81; 4.70; 2.34	8.58; 4.57; 2.26

deviation cancels when angle differences of both techniques are compared to each other leaving back purely numerical uncertainties. To reduce those as much as possible the working precision is set to a large number and the maximum number of steps is taken to be infinite.

There are at least two space-based missions available that could test gravity based on light deflection. Two of the most promising ones are GAIA and LATOR. In what follows we will discuss the perspective of these missions in obtaining constraints on Lorentz violation in the (isotropic) photon sector by performing measurements of light deflection at massive bodies. Thereby the theoretical tools developed so far will be of great use.

1. Sensitivity of GAIA

GAIA[2] [104] is a space probe that was launched in December 2013 by ESA. The mission goal is to perform measurements of positions and radial velocities of about 1% of the galactic stellar population, which shall generate a three-dimensional map of our galaxy. This is supposed to give information on the galactic history, dark matter as well as extra-solar planetary systems. GAIA can measure angles with a sensitivity of around 10 μarcs, which is why it can test deflection of light at massive bodies to a high precision. However, the mission parameters do not allow light to be measured grazing the surface of the Sun. Such measurements will be possible for Jupiter and Saturn only (see Table III in [104]).

Now we intend to perform phenomenology of light bending in an isotropic Lorentz-violating framework based on the possibilities of GAIA. Thereby sample functions are taken according to Eq. (5.19) with different values for the parameter $a = 1/10^{i}$ and the range $i = 0…15$. Choosing a particular controlling coefficient $\tilde{\kappa}_{\text{tr}}$, the deflection angle of light in the vicinity of Jupiter is computed with two methods. The first uses the formula of Bouguer, Eq. (5.12). The second solves the eikonal equation (5.20) numerically in analogy to what was described above. The bending angle is then computed via the scalar product of the initial and final normalized tangent vectors. This gives an excellent cross check for the results since the two methods are independent of each other.

The bending angle obtained is then compared to the standard result. This procedure is repeated for a decreasing isotropic coefficient $\tilde{\kappa}_{\text{tr}}$ until the difference between the modified and the standard result approximately matches the precision that GAIA can measure angles with. This sets the sensitivity of the experiment with respect to $\tilde{\kappa}_{\text{tr}}$ in a curved background. However, it is challenging to compute the integral or to solve the eikonal equation with a high precision. We use the difference of the results obtained from the two methods as a measure for how meaningful they are. For a conservative estimate of the sensitivity one should keep results only if this theoretical uncertainty is much smaller than the difference between the modified and the standard bending angle.

First of all for $\tilde{\kappa}_{\text{tr}} > 0$ the difference between the standard bending angle $\varphi_{\text{+}}^{*}$ and the modified bending angle is positive, which shows that the bending angle is reduced by a positive Lorentz-violating coefficient $\tilde{\kappa}_{\text{tr}}$ (see the third column of Table II). For $\tilde{\kappa}_{\text{tr}} < 0$ the behavior is vice versa and the absolute numbers mainly deviate in the third digit, which is why they are omitted in the table. We stated all differences $\varphi_{\text{+}}^{*} - \varphi_{\text{+}}$ that are larger than and lie in the vicinity of the experimental precision of GAIA, i.e., 10 μarcs. Such modifications can be expected to be detectable by this mission. From the results it becomes clear that the sensitivity of the isotropic coefficient reduces when the width of the dip, which is controlled by the parameter a, decreases. If the width lies in the order of magnitude of Jupiter's radius the sensitivity for $|\tilde{\kappa}_{\text{tr}}|$ is 10^{-14}. In case the width lies 15 orders of magnitude below

[2]The acronym originally meant "Global Astrometric Interferometer for Astrophysics." Although the foreseen measurement technique was changed upon construction of the apparatus, the acronym was kept.

TABLE III. Numerical results for modified light deflection at the Sun in the isotropic framework (see Table II for the meaning of each column). The standard deflection angle for scraping incidence at the Sun is $\varphi^*_\odot \approx 1.75$ arcs [see Eq. (5.15) and the subsequent paragraph]. In the second line $a = 0$ is associated with the first value in the fourth column.

$-\log_{10}(a)$	$-\log_{10}(\tilde{\kappa}_{tr})$	$f(r)$ $\varphi^*_\odot - \varphi_\odot$ [10^{-2} μarcs]	$g(r)$ $\varphi^*_\odot - \varphi_\odot$ [10^{-2} μarcs]
0	16	1.57	—
(0)1…4	15	8.84; 4.97; 2.80; 1.57	13.6; 8.58; 4.84; 2.72; 1.53
5…8	14	8.84; 4.97; 2.79; 1.56	8.61; 4.84; 2.72; 1.52
9…11	13	8.57; 4.56; 2.26	8.35; 4.43; 2.18
12…13	12	9.99; 3.91	9.49; 3.64
14…15	11	13.9; 4.64	12.7; 4.21

that the sensitivity of $|\tilde{\kappa}_{tr}|$ is still 10^{-10}. Hence, the sensitivity does not decrease as quickly as the parameter a. The numbers are meaningful, since the difference of the results obtained with Bouguer's formula and by solving the eikonal equation directly is around 4×10^{-9} μarcs at the maximum. The latter is interpreted as the theoretical uncertainty and it is much smaller than $|\varphi^*_{♄} - \varphi_{♄}|$.

Obtaining the modified deflection angles for Saturn works completely analogously. The sensitivity on $\tilde{\kappa}_{tr}$ lies in the same order of magnitude. The only difference is that even smaller a could be probed based on a modeling according to Eq. (5.19). The reason is that

$$\frac{d_{♄}}{R_{S,♄}} \approx 2.78 \frac{d_{♄}}{R_{S,♄}}, \tag{5.22}$$

whereby the additional dimensionless factor increases the contribution of a.

2. Sensitivity of LATOR

LATOR (Laser Astrometric Test of Relativity) [105,106] is a mission that is being planned by a collaboration of NASA and ESA. It is a Michelson-Morley-type experiment that shall perform curvature measurements in our solar system to determine the Eddington post-Newtonian parameter γ with a precision of 1 part in 10^8. It is considered to be a test mission for general relativity and it is supposed to detect the frame-dragging effect and to determine the solar quadrupole moment. The primary objective will be to measure the gravitational deflection of light by the Sun to an accuracy of 0.02 μarcs. Such an astounding precision shall be made possible by an improved laser ranging and a long-baseline optical interferometry system.

We carry out phenomenology as we did before by choosing different parameters a for the sample functions of Eq. (5.19). The calculations are completely analogous to before where the only difference is that they are carried out for the Sun using the appropriate parameters of Table I. The essential numerical results are stated in Table III. The bending angle behaves similarly to before, i.e., it is reduced for $\tilde{\kappa}_{tr} > 0$ and it increases for $\tilde{\kappa}_{tr} < 0$. The differences $\varphi^*_\odot - \varphi_\odot$ are listed that lie in the vicinity of the experimental precision expected for LATOR, i.e., 0.02 μarcs. If the width of the dip/peak in the refractive index of the Lorentz-violating vacuum lies in the order of magnitude of the Sun's radius the sensitivity for the isotropic coefficient $|\tilde{\kappa}_{tr}|$ is 10^{-16}. The lowest sensitivity in case of a very narrow dip/peak is 10^{-11}. Comparing the results determined from Bouguer's formula to the results from the numerical solution of the eikonal equation reveals differences of ca. 6×10^{-12} μarcs. Therefore, the theoretical uncertainty is still much smaller than $|\varphi^*_\odot - \varphi_\odot|$. Note that for the model function $g(r)$ the modification of the deflection angle for $|\tilde{\kappa}_{tr}| = 10^{-16}$ is smaller than 1.50×10^{-2} μarcs. Therefore assuming this model function, the sensitivity of LATOR will not be sufficient to detect a $|\tilde{\kappa}_{tr}|$ lying in the order of magnitude of 10^{-16}.

3. Discussion

According to the current (2015) version of the data tables [5] the strictest lower bounds on $\tilde{\kappa}_{tr}$ lie in the order of magnitude of -10^{-16} where the best upper bounds are around 10^{-20}. The isotropic coefficient of modified Maxwell theory is challenging to be constrained in laboratory experiments, which is why these bounds are related to ultrahigh energy cosmic rays. With the precision of LATOR there would be a space-based experiment performed under controlled conditions that could have a sensitivity comparable to the best current constraints on a negative $\tilde{\kappa}_{tr}$. This is astonishing taking into account that the precision of a man-made experiment may match the sensitivity reached by the most energetic particles propagating through interstellar space for distances of many light-years. It illustrates the versatility of the technique presented to constrain Lorentz violation in the photon sector by precise measurements of light bending at massive bodies. Note that the sensitivity does not largely depend on the model function used. This independence could be checked for further model functions, which can be regarded as an interesting future project.

C. Anisotropic (nonbirefringent) case

The anisotropic case of modified Maxwell theory exhibiting a single modified dispersion relation was discussed in Sec. III C. This particular case is characterized by a preferred spacelike direction (chosen to point along the positive z axis) and one controlling coefficient. The refractive index was found in Eq. (4.13b) and it was expressed in terms of the angle ϑ enclosed between the propagation direction and the preferred axis. The possible trajectory of a light ray is parametrized by $\mathbf{r}(\phi) = r(\phi)\hat{\mathbf{e}}_\phi$ such as for the isotropic case. The angle ϑ in the refractive index is then given by the scalar product of the tangent vector $\mathbf{t}$ and the preferred direction $\boldsymbol{\zeta}$ where it is sufficient to work in two spatial dimensions:

$$\cos\vartheta = \frac{\mathbf{t}\cdot\boldsymbol{\zeta}}{|\mathbf{t}|} = \frac{r(\phi)\cos\phi + \dot{r}(\phi)\sin\phi}{\sqrt{r(\phi)^2 + \dot{r}(\phi)^2}}. \tag{5.23}$$

Note that for the anisotropic case angular momentum is not conserved and Bouguer's formula loses its meaning. Hence, there does not seem to be an alternative to solving the eikonal equation directly, which is carried out numerically for hypothetical values of R_S and the controlling coefficient $\tilde{\kappa}^{11}_{e-}$. The results are shown in Fig. 5. In contrast to the isotropic case, cf. Fig. 4, where the trajectory is not modified for a spacetime position independent $\tilde{\kappa}_{\mathrm{tr}}$ this is not the case here. For the anisotropic sector, the shape of the trajectory gets distorted where the final impact parameter decreases for $\tilde{\kappa}^{11}_{e-} > 0$. Physically this means that the ray loses angular momentum. An interesting future research project would be to perform a similar kind of phenomenological analysis as we did for the isotropic case.

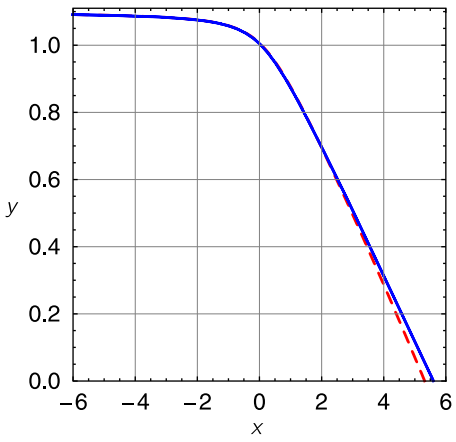

FIG. 5 (color online). Solution of the eikonal equation in the x-y plane (in dimensions of d) with $d/R_S = 5$. The blue (plain) curve shows the solution for the Lorentz-invariant case, whereas the red (dashed) curve depicts the solution for the anisotropic case with $\tilde{\kappa}^{11}_{e-} = 0.65$. The massive body resides in the coordinate center.

VI. MODIFIED ENERGY-MOMENTUM CONSERVATION

The phenomenology in the previous section was carried out in an explicitly Lorentz-violating framework, which is known to cause tensions in a gravitational background [41]. The purpose of the current section is to investigate where exactly these problems occur in our classical description and how they can be interpreted from the point of view of an inhomogeneous medium. Therefore the energy-momentum tensor and its conservation law will be derived for the isotropic case. The (Belinfante-Rosenfeld) energy-momentum tensor follows from varying the corresponding Lagrangian with respect to the metric. The Finsler structure $F(\mathbf{u})|^{+}_{\circledcirc}$ of Eq. (3.14b) is the equivalent to a Lagrangian, since it appears as the integrand of the path length functional that is stationary for the trajectory travelled by the light ray. Instating an auxiliary metric tensor $\psi_{\mu\nu}$ leads to the following result:

$$F = n|\mathbf{u}| = \sqrt{\frac{1+\tilde{\kappa}_{\mathrm{tr}}\psi_{\mu\nu}\xi^\mu\xi^\nu}{1-\tilde{\kappa}_{\mathrm{tr}}\psi_{\rho\sigma}\xi^\rho\xi^\sigma}}\sqrt{-\psi_{ij}u^iu^j}. \tag{6.1}$$

Note that in Minkowski spacetime it holds that $\eta_{\mu\nu}\xi^\mu\xi^\nu = \xi^2 = 1$ and $-\eta_{ij}u^iu^j = \mathbf{u}^2$ where the minus sign in the latter term is due to the signature of the metric chosen. Variation has to be carried out for all independent degrees of freedom. A useful formula is

$$\begin{aligned}\delta(A_\mu A^\mu) &= \delta(\psi_{\mu\nu}A^\mu A^\nu)\\ &= \psi_{\mu\nu}\delta A^\mu A^\nu + \psi_{\mu\nu}A^\mu\delta A^\nu + \delta\psi_{\mu\nu}A^\mu A^\nu\\ &= 2A_\nu\delta A^\nu + \delta\psi_{\mu\nu}A^\mu A^\nu,\end{aligned} \tag{6.2}$$

which states the variation of a scalar product of fields. Employing this rule, the variation of F can then be computed as follows:

$$\begin{aligned}\delta F &= (\delta n)\sqrt{-\psi_{ij}u^iu^j} + n\delta\left(\sqrt{-\psi_{ij}u^iu^j}\right)\\ &= \frac{\tilde{\kappa}_{\mathrm{tr}}}{n(1-\tilde{\kappa}_{\mathrm{tr}})^2}\delta(\psi_{\mu\nu}\xi^\mu\xi^\nu)\sqrt{-\psi_{ij}u^iu^j}\\ &\quad + \frac{n}{2\sqrt{-\psi_{ij}u^iu^j}}\delta(-\psi_{ij}u^iu^j)\\ &= \frac{\tilde{\kappa}_{\mathrm{tr}}}{n(1-\tilde{\kappa}_{\mathrm{tr}})^2}\sqrt{-\psi_{ij}u^iu^j}(2\xi_\nu\delta\xi^\nu + \delta\psi_{\mu\nu}\xi^\mu\xi^\nu)\\ &\quad - \frac{n}{2\sqrt{-\psi_{ij}u^iu^j}}(2u_j\delta u^j + \delta\psi_{ij}u^iu^j).\end{aligned} \tag{6.3}$$

Now everything is available to obtain the energy-momentum tensor from δF by considering all terms comprising a variation of the metric. An additional prefactor containing the metric has to be taken into account in the definition. However, we are interested in the covariant conservation law of $T^{\mu\nu}$ for Minkowski spacetime, i.e., for a spacetime-position dependent refractive index without an additional gravitational field. In this case $\psi_{\mu\nu} = \eta_{\mu\nu}$ whereby

$$T^{\mu\nu} \equiv \frac{2}{\sqrt{|\psi|}} \frac{\delta(\sqrt{|\psi|}F)}{\delta\psi_{\mu\nu}}\bigg|_{\psi_{\mu\nu}=\eta_{\mu\nu}}$$
$$= \frac{2\tilde{\kappa}_{\mathrm{tr}}}{n(1-\tilde{\kappa}_{\mathrm{tr}})^2}\sqrt{u_i u^i}\,\xi^\mu\xi^\nu - \frac{n}{\sqrt{u_i u^i}}\tilde{u}^\mu\tilde{u}^\nu$$
$$= n\sqrt{u_i u^i}\left[\frac{1}{2}\left(n^2-\frac{1}{n^2}\right)\xi^\mu\xi^\nu - \frac{\tilde{u}^\mu\tilde{u}^\nu}{u_i u^i}\right]. \tag{6.4}$$

Here $\psi \equiv \det(\psi_{\mu\nu})$ and $(\tilde{u}^\mu) \equiv (0, \mathbf{u})^T$, i.e., $\tilde{u}^\mu$ involves the spatial velocity and its zeroth component vanishes. Upon inspection of the latter result we see that the 00-component of $T^{\mu\nu}$ is made up by the preferred timelike spacetime direction ξ^μ and it vanishes for $n = 1$, i.e., in a Lorentz-invariant vacuum. The spatial part solely comprises products of three-velocity components and the mixed components vanish. Now the partial derivative of the energy-momentum tensor in Minkowski spacetime leads to

$$\partial_\mu T^{\mu\nu} = (\partial_\mu n)\sqrt{\mathbf{u}^2}\left[\frac{1}{2}\left(n^2-\frac{1}{n^2}\right)\xi^\mu\xi^\nu - \frac{\tilde{u}^\mu\tilde{u}^\nu}{\mathbf{u}^2}\right]$$
$$+ n\sqrt{\mathbf{u}^2}\partial_\mu\left[\frac{1}{2}\left(n^2-\frac{1}{n^2}\right)\right]\xi^\mu\xi^\nu$$
$$= \frac{T^{\mu\nu}}{n}\partial_\mu n + \left(n^2+\frac{1}{n^2}\right)\sqrt{\mathbf{u}^2}\xi^\mu\xi^\nu(\partial_\mu n)$$
$$= \sqrt{\mathbf{u}^2}\left[\frac{1}{2}\left(3n^2+\frac{1}{n^2}\right)\xi^\mu\xi^\nu - \frac{\tilde{u}^\mu\tilde{u}^\nu}{\mathbf{u}^2}\right](\partial_\mu n). \tag{6.5}$$

An interesting observation is that the timelike contribution can be expressed in terms of the metric $\tilde{g}_{\mu\nu}$ appearing in Eq. (5.7b):

$$(\tilde{g}^2)^\mu{}_\mu = 3n^2 + \frac{1}{n^2}, \tag{6.6a}$$
$$\tilde{g}_{\mu\nu}(r) \equiv \mathrm{diag}\left(\frac{1}{n(r)}, -n(r), -n(r), -n(r)\right)_{\mu\nu}. \tag{6.6b}$$

Note that $\tilde{g}_{\mu\nu}$ is not associated with a gravity field but only with a nonconstant refractive index. The result obtained in Eq. (6.5) describes the conservation of energy and momentum of a light ray. Its properties are in order. First, it vanishes for a constant refractive index, i.e., energy and momentum of the ray are conserved in a homogeneous medium, in the Lorentz-invariant vacuum, and a Lorentz-violating vacuum with a constant controlling coefficient. Second, in an inhomogeneous medium or in a Lorentz-violating vacuum with spacetime-dependent controlling coefficient the energy-momentum tensor is not conserved, since the partial derivative of the refractive index does not vanish in this case. As long as the refractive index is not time-dependent, $\partial_0 n = 0$, which is why $\partial_\mu T^{\mu 0} = 0$. Since the case under consideration is isotropic, the controlling coefficient and the refractive index, respectively, can only depend on the radial coordinate: $\tilde{\kappa}_{\mathrm{tr}} = \tilde{\kappa}_{\mathrm{tr}}(r)$, $n = n(r)$. Thus, $\partial_\mu n$ has a nonvanishing component along the radial basis vector only, i.e., $\partial_r n \neq 0$ and $\partial_\theta n = \partial_\phi n = 0$. Decomposing the spatial velocity into a radial part u^r and transverse components u^θ, u^ϕ,

$$\mathbf{u} = u^r\mathbf{e}_r + u^\theta\mathbf{e}_\theta + u^\phi\mathbf{e}_\phi, \tag{6.7}$$

the spatial part of the conservation law reads as

$$\partial_\mu T^{\mu i} = -\frac{1}{\sqrt{\mathbf{u}^2}}(\boldsymbol{\nabla} n\cdot\mathbf{u})u^i = -\sqrt{\mathbf{u}^2}(\boldsymbol{\nabla} n\cdot\hat{\mathbf{u}})\hat{u}^i$$
$$= -\sqrt{\mathbf{u}^2}(\partial_r n)\hat{u}^r\hat{u}^i, \qquad \hat{\mathbf{u}} = \frac{\mathbf{u}}{|\mathbf{u}|}. \tag{6.8}$$

Several observations can be made upon inspecting the result. For a constant refractive index, the right-hand side of the latter equation is zero, which means that the spatial part of the energy-momentum conservation law is valid as well in this case. For $\partial_r n \neq 0$ it even holds when the radial velocity component vanishes: $u^r = 0$. This is a special situation that can occur for a light ray in an inhomogeneous, isotropic medium whose refractive index has a particular r-dependence and when the ray is emitted tangentially to a circle with its center lying in the coordinate origin (cf. [107] for a beautiful paper on geometric-ray optics and its implications for certain optical systems). The trajectory of the ray is then a circle where the refractive index is constant. The magnitude of the three-momentum vector does not change, but only its direction. So momentum is not exchanged between the light ray and the medium because any momentum transfer would change the magnitude of the momentum vector. For any other case with nonzero $\partial_r n$, momentum has to be exchanged, which is why $T^{\mu\nu}$ of the ray cannot be conserved. The net term obtained above points in the direction $\hat{\mathbf{u}}$ of the ray at the point considered. However, the total energy-momentum tensor with $T^{\mu\nu}_{\mathrm{med}}$ of the medium included is expected to be conserved because any momentum change of the light ray will cause a momentum change of the medium itself.

In general relativity local diffeomorphism invariance is tightly linked to energy-momentum conservation. In [41] it was shown that explicit Lorentz violation in gravity leads to a loss of diffeomorphism invariance, which then causes the energy-momentum tensor to be no longer covariantly conserved. Note that in the latter reference the energy-momentum tensor $T^{\mu\nu}_e$ is considered that follows by varying the Lagrangian with respect to the vierbein instead of with respect to the metric tensor. It is different from the Belinfante-Rosenfeld energy-momentum tensor considered here even in case there is no Lorentz violation [108]. The covariant derivative of $T^{\mu\nu}_e$ in [41] involves the covariant derivative of the Lorentz-violating controlling coefficients, i.e., a term of the structure $J^x D_\nu k_x$. Here k_x is a generic controlling coefficient with a particular Lorentz index structure x contracted with an appropriate operator J^x. For general, curved manifolds there is no spacetime-position dependent function satisfying $D_\nu k_x = 0$, but only for parallelizable manifolds such as the circle S^1 or the

two-torus $T^2 = S^1 \times S^1$. In four dimensions, such manifolds are rare, though, and they do not seem to be of particular interest in the context of general relativity.

The conservation law without gravitational fields is given by $\partial_\mu(\Theta_c)^{\mu\nu} = J^x\partial^\nu k_x$ with the canonical energy-momentum tensor $(\Theta_c)^{\mu\nu}$ [41]. Therefore, if the controlling coefficient k_x is dependent on spacetime position the conservation law is modified even in flat spacetime. From a physical perspective, this is not surprising since such a controlling coefficient implies that the vacuum behaves like an effective, inhomogeneous medium. In general, the magnitude of the three-momentum of a light ray is not conserved as was argued above. Therefore momentum has to be exchanged between the ray and the medium. When considering explicit Lorentz violation the effective medium is considered to be nondynamical, which is why it can neither absorb nor deliver momentum to the light ray.

Interestingly the situation is different when spontaneous violations of diffeomorphism invariance and local Lorentz symmetry are considered. In these cases, the ground state violates these symmetries dynamically by an emergent vacuum expectation value of a vector or tensor field in a potential [7,41,42,54–58]. Such models have in common that they involve massless (Nambu-Goldstone) modes where the latter appear when any global, continuous symmetry is broken spontaneously. When the symmetry is local there can be an additional Higgs-type mechanism absorbing the massless modes to produce massive gauge fields. Since for spontaneous Lorentz violation the dynamics of the Lorentz-violating background field is taken into account, the energy-momentum conservation law is restored in these theories. In the corresponding equation, there is no contribution $J^x\partial^\nu k_x$.

From the perspective of an inhomogeneous medium translational and rotational symmetry are violated spontaneously by the atomic lattice. The Nambu-Goldstone modes (gapless excitations) linked to the spontaneous violation of these symmetries are the two transverse and the longitudinal types of phonons.[3] Since the medium is now dynamical, it can absorb momentum from the ray upon producing phonons. Hence, the conservation law for the light ray remains valid in this case.

VII. PROPERTIES OF THE ISOTROPIC FINSLER SPACE

In the previous section, the modified conservation law for the Belinfante-Rosenfeld energy-momentum tensor for a light ray in an isotropic, inhomogeneous medium was considered and discussed. It was found that the energy-momentum tensor is not conserved since the nontrivial medium is nondynamical corresponding to a background violating Lorentz symmetry explicitly. This issue persists even in Minkowski spacetime since in inhomogeneous media light rays behave similarly to rays propagating in gravitational backgrounds. The most prominent example for a common effect is light bending.

The conservation law of the energy-momentum tensor for a medium with spherically symmetric refractive index, Eq. (6.8), involves both the first derivative of the refractive index and the propagation direction of the ray at a given point. Recall that in gravitational theories with explicit Lorentz violation nonconservation of the energy-momentum tensor clashes with the Bianchi identities of Riemannian geometry [41]. Although we work with an effective Lorentz-violating theory for light rays based on a nontrivial refractive index, this issue can be encountered here as well.

The purpose of the current section is to figure out whether explicit (isotropic) Lorentz violation can be considered in a weak gravity field in the framework of Finsler geometry such that no inconsistencies arise. As a basis, we use the spacetime metric of Eq. (5.7b), which was shown to be closely linked to the isotropic case. The properties of the latter metric shall be studied from a Finslerian point of view where we use the conventions of [61] for all geometrical quantities. The latter are treated based on the indefinite signature of the metric in Eq. (5.7b). As a starting point, an appropriate Finsler structure has to be constructed whose derived metric should correspond to Eq. (5.7b). This works for the following choice; cf. the similarity to Eq. (3.14b):

$$F(r,\mathbf{y}) = \sqrt{\mathbf{y}^2},$$
$$\mathbf{y}^2 = \frac{1}{n}(y^t)^2 - n(y^r)^2 - n[(y^\theta)^2 + (y^\phi)^2\sin^2\theta]r^2, \tag{7.1}$$

where the refractive index solely has a radial dependence. In what follows we write $n(r) = n$ for brevity, i.e., the argument of the refractive index will be omitted. The vector $\mathbf{y} \in TM$ is expressed in three-dimensional spherical coordinates as $\mathbf{y} = y^t\mathbf{e}_t + y^r\mathbf{e}_r + y^\theta\mathbf{e}_\theta + y^\phi\mathbf{e}_\phi$ with suitable basis vectors, so is the spatial part of the Finsler structure. The corresponding Finsler metric is then computed according to the usual definition and it corresponds to the result of Eq. (5.7b) (with the spatial part transformed to spherical coordinates):

$$g_{\mu\nu} \equiv \frac{1}{2}\frac{\partial^2 F^2}{\partial y^\mu \partial y^\nu} = \mathrm{diag}\left(\frac{1}{n}, -n, -nr^2, -nr^2\sin^2\theta\right)_{\mu\nu}. \tag{7.2a}$$

The inverse metric simply reads as

[3]The number of spontaneously broken translational and rotational generators is six. However, as they are not independent from each other, the total number of Nambu-Goldstone bosons is reduced by these constraints to be three. Relations between broken symmetries and Nambu-Goldstone bosons in certain nonrelativistic systems such as crystals, ferromagnets, and superfluids are nicely described in [109].

$$g^{\mu\nu} = \mathrm{diag}\left(n, -\frac{1}{n}, -\frac{1}{nr^2}, -\frac{1}{nr^2\sin^2\theta}\right)^{\mu\nu}. \tag{7.2b}$$

Since the metric does not depend on $\mathbf{y}$, the Cartan connection [61] vanishes:

$$A_{\mu\nu\varrho} \equiv \frac{F}{2}\frac{\partial g_{\mu\nu}}{\partial y^{\varrho}} = \frac{F}{4}\frac{\partial^3 F^2}{\partial y^{\mu}\partial y^{\nu}\partial y^{\varrho}} = 0. \tag{7.3}$$

Therefore according to Deicke's theorem [86] the Finsler space considered is Riemannian. Now the base has been set up to study the geometry of the space defined by Eq. (7.1). The first step is the obtain the coefficients of the affine connection (Christoffel symbols of the second kind) that are defined in analogy to the Christoffel symbols in Riemannian geometry:

$$\gamma^{\mu}{}_{\nu\rho} = \frac{1}{2}g^{\mu\alpha}\left(\frac{\partial g_{\alpha\nu}}{\partial x^{\rho}} - \frac{\partial g_{\nu\rho}}{\partial x^{\alpha}} + \frac{\partial g_{\rho\alpha}}{\partial x^{\nu}}\right). \tag{7.4}$$

Note that summation over equal indices is understood based on Einstein's convention. The nonzero contributions read as follows:

$$\gamma^{t}{}_{tr} = -\frac{n'}{2n}, \qquad \gamma^{r}{}_{tt} = -\frac{n'}{2n^3}, \qquad \gamma^{r}{}_{rr} = \frac{n'}{2n},$$
$$\gamma^{r}{}_{\theta\theta} = -\frac{r(2n+rn')}{2n}, \tag{7.5a}$$

$$\gamma^{r}{}_{\phi\phi} = -\frac{r(2n+rn')}{2n}\sin^2\theta, \qquad \gamma^{\theta}{}_{r\theta} = \frac{1}{r} + \frac{n'}{2n},$$
$$\gamma^{\theta}{}_{\phi\phi} = -\sin\theta\cos\theta, \tag{7.5b}$$

$$\gamma^{\phi}{}_{r\phi} = \frac{1}{r} + \frac{n'}{2n}, \qquad \gamma^{\phi}{}_{\theta\phi} = \cot\theta. \tag{7.5c}$$

Since torsion is assumed to vanish, the Christoffel symbols are symmetric in the latter two indices. The connection coefficients with at least one index equal to the radial coordinate r involve the first derivative of the refractive index. Furthermore they do not involve the angle ϕ as expected for spherically symmetric metrics. As a next step, the geodesic spray coefficients are needed: $G^{\mu} \equiv \gamma^{\mu}{}_{\nu\varrho}y^{\nu}y^{\varrho}$. The latter appear in the geodesic equations in Finsler geometry:

$$G^{t} = -y^{t}y^{r}\frac{n'}{n}, \tag{7.6a}$$

$$G^{r} = -(y^{t})^2\frac{n'}{2n^3} + \frac{1}{2n}\{(y^{r})^2 n' - r(2n+rn')[(y^{\theta})^2 + (y^{\phi})^2\sin^2\theta]\}, \tag{7.6b}$$

$$G^{\theta} = y^{r}y^{\theta}\left(\frac{2}{r} + \frac{n'}{n}\right) - (y^{\phi})^2\sin\theta\cos\theta,$$
$$G^{\phi} = y^{\phi}\left[2y^{\theta}\cot\theta + y^{r}\left(\frac{2}{r} + \frac{n'}{n}\right)\right]. \tag{7.6c}$$

The geodesic spray coefficients can be used to define the nonlinear connection [61] on $TM\backslash\{0\}$:

$$N^{\mu}{}_{\nu} \equiv \frac{1}{2}\frac{\partial G^{\mu}}{\partial y^{\nu}}. \tag{7.7}$$

The reasons for introducing these connection coefficients is as follows. On the one hand, the basis vectors $\partial/\partial x^{\nu}$ and $\partial/\partial y^{\nu}$ are unsuitable to be chosen as a local basis of TTM since the $\partial/\partial x^{\nu}$ transform in a complicated way. On the other hand, if $\{\mathrm{d}x^{\mu}, \mathrm{d}y^{\mu}\}$ is chosen as a local basis of the cotangent bundle T^*TM the transformation properties of $\mathrm{d}y^{\mu}$ are involved. To have the desired transformation properties for the basis of the tangent and the cotangent bundle of $TM\backslash\{0\}$ the following basis vectors can be introduced using the nonlinear connection:

$$\left\{\frac{\delta}{\delta x^{\nu}}, F\frac{\partial}{\partial y^{\nu}}\right\}, \qquad \frac{\delta}{\delta x^{\nu}} \equiv \frac{\partial}{\partial x^{\nu}} - N^{\mu}{}_{\nu}\frac{\partial}{\partial y^{\mu}}, \tag{7.8a}$$

$$\left\{\mathrm{d}x^{\mu}, \frac{\delta y^{\mu}}{F}\right\}, \qquad \delta y^{\mu} \equiv \mathrm{d}y^{\mu} + N^{\mu}{}_{\nu}\mathrm{d}x^{\nu}. \tag{7.8b}$$

For the particular case studied here the nonlinear connection coefficients can be comprised in a (3×3) matrix that reads as

$$(N^{\mu}{}_{\nu}) = \frac{1}{2}\begin{pmatrix} -y^{r}n'/n & -y^{t}n'/n & 0 & 0 \\ -y^{t}n'/n^3 & y^{r}n'/n & -y^{\theta}r(2n+rn')/n & -y^{\phi}r\sin^2\theta(2n+rn')/n \\ 0 & y^{\theta}(2/r+n'/n) & y^{r}(2/r+n'/n) & -y^{\phi}\sin(2\theta) \\ 0 & y^{\phi}(2/r+n'/n) & 2y^{\phi}\cot\theta & y^{r}(2/r+n'/n)+2y^{\theta}\cot\theta \end{pmatrix}. \tag{7.9}$$

To compute directional derivatives of tensor fields on Finsler manifolds, a further connection has to be found to define a covariant derivative. It was shown that the pulled-back bundle π^*TM has a linear connection associated with it, which is called the Chern connection $\Gamma^{\mu}{}_{\nu\varrho}$. Explicitly it can be obtained from the Finsler metric using the nonlinear connection $N^{\mu}{}_{\nu}$:

$$\Gamma^{\mu}{}_{\nu\varrho} = \frac{1}{2} g^{\mu\alpha}\left(\frac{\delta g_{\alpha\nu}}{\delta x^{\varrho}} - \frac{\delta g_{\nu\varrho}}{\delta x^{\alpha}} + \frac{\delta g_{\varrho\alpha}}{\delta x^{\nu}}\right)$$
$$= \frac{1}{2} g^{\mu\alpha}\left(\frac{\partial g_{\alpha\nu}}{\partial x^{\varrho}} - N^{\beta}{}_{\varrho}\frac{\partial g_{\alpha\nu}}{\partial y^{\beta}} - \left[\frac{\partial g_{\nu\varrho}}{\partial x^{\alpha}} - N^{\beta}{}_{\alpha}\frac{\partial g_{\nu\varrho}}{\partial y^{\beta}}\right] + \frac{\partial g_{\varrho\alpha}}{\partial x^{\nu}} - N^{\beta}{}_{\nu}\frac{\partial g_{\varrho\alpha}}{\partial y^{\beta}}\right). \quad (7.10)$$

The Chern connection is unique and formally it has the same index structure as the formal Christoffel symbols. The difference to the latter is that the derivative $\delta/\delta x^{\mu}$ is used instead of the ordinary partial derivative $\partial/\partial x^{\mu}$. However, in the particular case studied here, $\Gamma^{\mu}{}_{\nu\varrho} = \gamma^{\mu}{}_{\nu\varrho}$, since the Finsler metric $g_{\mu\nu}$ does not depend on the components of $\mathbf{y}$. Finally the Chern connection is needed to define a Finslerian version of the Riemann curvature tensor:

$$R_{\nu}{}^{\mu}{}_{\varrho\sigma} = \frac{\delta\Gamma^{\mu}{}_{\nu\sigma}}{\delta x^{\varrho}} - \frac{\delta\Gamma^{\mu}{}_{\nu\varrho}}{\delta x^{\sigma}} + \Gamma^{\mu}{}_{\alpha\varrho}\Gamma^{\alpha}{}_{\nu\sigma} - \Gamma^{\mu}{}_{\alpha\sigma}\Gamma^{\alpha}{}_{\nu\varrho}$$
$$= \frac{\partial\Gamma^{\mu}{}_{\nu\sigma}}{\partial x^{\varrho}} - N^{\beta}{}_{\varrho}\frac{\partial\Gamma^{\mu}{}_{\nu\sigma}}{\partial y^{\beta}} - \left(\frac{\partial\Gamma^{\mu}{}_{\nu\varrho}}{\partial x^{\sigma}} - N^{\beta}{}_{\sigma}\frac{\partial\Gamma^{\mu}{}_{\nu\varrho}}{\partial y^{\beta}}\right) + \Gamma^{\mu}{}_{\alpha\varrho}\Gamma^{\alpha}{}_{\nu\sigma} - \Gamma^{\mu}{}_{\alpha\sigma}\Gamma^{\alpha}{}_{\nu\varrho}. \quad (7.11)$$

Since the Chern connection coefficients correspond to the formal Christoffel symbols and the latter are independent of y^{μ}, the curvature components correspond to the Riemannian ones. They involve an additional derivative of the Christoffel symbols, which is why they comprise second derivatives of the refractive index. Explicitly the independent curvature tensor components are stated as follows:

$$R_{t}{}^{r}{}_{tr} = \frac{nn'' - 2n'^2}{2n^4}, \qquad R_{t}{}^{\theta}{}_{t\theta} = \frac{n'(2n + rn')}{4rn^4} = R_{t}{}^{\phi}{}_{t\phi}, \quad (7.12a)$$

$$R_{r}{}^{t}{}_{tr} = \frac{nn'' - 2n'^2}{2n^2}, \qquad R_{\theta}{}^{t}{}_{t\theta} = \frac{rn'(2n + rn')}{4n^2},$$
$$R_{\theta}{}^{\phi}{}_{\theta\phi} = \frac{rn'(4n + rn')}{4n^2}, \quad (7.12b)$$

$$R_{\phi}{}^{t}{}_{t\phi} = \frac{rn'(2n + rn')}{4n^2}\sin^2\theta,$$
$$R_{\phi}{}^{\theta}{}_{\theta\phi} = -\frac{rn'(4n + rn')}{4n^2}\sin^2\theta. \quad (7.12c)$$

The components related by symmetries are omitted. Since the Finsler structure of Eq. (7.1) is Riemannian according to Deicke's theorem, we will first use the Riemannian definitions of the Ricci tensor $\mathcal{R}ic_{\mu\nu} \equiv R_{\mu}{}^{\alpha}{}_{\alpha\nu}$ and the curvature scalar (Ricci scalar) $\mathcal{R}ic$. These are denoted by calligraphic letters and they follow from suitable contractions of the Riemann curvature tensor. The Ricci tensor components with equal indices deliver nonzero contributions only:

$$\mathcal{R}ic_{tt} = \frac{1}{2rn^4}[rn'^2 - n(2n' + rn'')],$$
$$\mathcal{R}ic_{rr} = -\frac{1}{2rn}(2n' + rn''), \quad (7.13a)$$

$$\mathcal{R}ic_{\theta\theta} = \frac{r}{2n^2}[rn'^2 - n(2n' + rn'')],$$
$$\mathcal{R}ic_{\phi\phi} = \frac{r}{2n^2}[rn'^2 - n(2n' + rn'')]\sin^2\theta, \quad (7.13b)$$

$$\mathcal{R}ic \equiv \mathcal{R}ic^{\mu}{}_{\mu} = g^{\mu\nu}\mathcal{R}ic_{\mu\nu} = \frac{1}{2rn^3}[2n(2n' + rn'') - rn'^2]. \quad (7.13c)$$

In Riemannian geometry, the curvature tensor obeys the first and the second Bianchi identities. Especially the second one,

$$0 \equiv D_{\eta}R_{\lambda}{}^{\mu}{}_{\nu\kappa} + D_{\kappa}R_{\lambda}{}^{\mu}{}_{\eta\nu} + D_{\nu}R_{\lambda}{}^{\mu}{}_{\kappa\eta}, \quad (7.14a)$$

$$D_{\lambda}R_{\mu}{}^{\nu}{}_{\rho\sigma} = \partial_{\lambda}R_{\mu}{}^{\nu}{}_{\rho\sigma} - \Gamma^{\alpha}{}_{\mu\lambda}R_{\alpha}{}^{\nu}{}_{\rho\sigma} + \Gamma^{\nu}{}_{\alpha\lambda}R_{\mu}{}^{\alpha}{}_{\rho\sigma} - \Gamma^{\alpha}{}_{\rho\lambda}R_{\mu}{}^{\nu}{}_{\alpha\sigma} - \Gamma^{\alpha}{}_{\sigma\lambda}R_{\mu}{}^{\nu}{}_{\rho\alpha}, \quad (7.14b)$$

is important in the context of general relativity, because it leads to the statement that the Einstein tensor $G^{\mu\nu}$ is covariantly constant:

$$D_{\mu}G^{\mu}{}_{\nu} = \partial_{\mu}G^{\mu}{}_{\nu} + \Gamma^{\mu}{}_{\alpha\mu}G^{\alpha}{}_{\nu} - \Gamma^{\alpha}{}_{\nu\mu}G^{\mu}{}_{\alpha} \equiv 0,$$
$$G^{\mu\nu} \equiv \mathcal{R}ic^{\mu\nu} - \frac{\mathcal{R}ic}{2}g^{\mu\nu}, \quad (7.15a)$$

which was checked to be valid for the particular metric $g_{\mu\nu}$ of Eq. (7.2a). This identity is the reason why explicit Lorentz violation is incompatible with Riemannian geometry. Due to the Einstein equations it forces the energy-momentum tensor to be covariantly conserved as well, which does not necessarily hold when there is a space-time-dependent background. At this point it is reasonable to wonder how Finsler geometry can help us to solve that problem. For the isotropic metric considered the identity $D_{\mu}G^{\mu}{}_{\nu} \equiv 0$ is inherited from the Riemannian to the Finslerian framework, since the Finsler metric of Eq. (7.2a) does not comprise any dependence on y^{μ}. Assuming that Finsler geometry provides the necessary tools to circumvent the no-go theorem of [41] in a general explicitly Lorentz-violating setting, then it should also work for the special isotropic case studied here.

One possible approach (there may be others) might be to consider a suitable equivalent of the Einstein equations in Finsler geometry. Such an equivalent can be based on an

alternative definition of the Einstein tensor $G^{\mu\nu}$ constructed from curvature-related tensors in the Finsler framework. These objects will be introduced in what follows. The first is obtained from the curvature tensor by contracting the latter with two vectors y^μ/F according to

$$R^\mu{}_\varrho \equiv \frac{y^\nu}{F} R_\nu{}^\mu{}_{\varrho\sigma} \frac{y^\sigma}{F}. \tag{7.16}$$

Note that this construction does not correspond to the Ricci tensor of Riemannian geometry. In particular, it is sometimes referred to as the predecessor of flag curvature, which is a generalization of sectional curvature in Finsler geometry. For the special case here $R^\mu{}_\varrho$ are the components of a (4×4) matrix. The trace of this matrix is taken to obtain the generalization of the Ricci scalar in Finsler geometry: $Ric \equiv R^\varrho{}_\varrho$. Since the explicit expressions for $R^\mu{}_\varrho$ and Ric are complicated and not illuminating, they will not be stated.

The flag curvature in Finsler geometry is computed similarly to the sectional curvature in Riemannian geometry. The latter is defined in a tangent space at a point x of the manifold where two arbitrary, linearly independent directions are needed for its computation. The resulting quantity only depends on the plane considered, but not on the particular choice of the directions. The flag curvature in Finsler geometry carries the same spirit where one direction is chosen to correspond to $\mathbf{y}$ and the other one, say $\mathbf{L}$, is supposed to be orthogonal to $\mathbf{y}$. These vectors are then suitably contracted with the curvature tensor of Eq. (7.11). Note that $\mathbf{y}$ and the vector orthogonal to it can be considered to span a flag where $\mathbf{y}$ is assumed to point along the flag pole. This explains the name for the curvature. For an n-dimensional Finsler manifold R is the sum of $n-1$ flag curvatures. It only depends on r and $\mathbf{y}$, but not on the direction $\mathbf{L}$ chosen orthogonal to $\mathbf{y}$.

Although $R_{\mu\varrho}$ of Eq. (7.16) is not understood to be the generalization of the Ricci tensor in Finsler geometry, it is still possible to define the latter. The definition (cf. Eq. (7.6.4) in [61]) involves both the Finsler structure F and the Finslerian version of the Ricci scalar Ric:

$$Ric_{\mu\nu} \equiv \frac{1}{2} \frac{\partial^2 (F^2 Ric)}{\partial y^\mu \partial y^\nu}. \tag{7.17}$$

For Finsler metrics that are Riemannian, i.e., for the isotropic metric considered in Eq. (7.2a) it also holds that $\mathrm{Ric}_{\mu\nu} = R_\mu{}^\alpha{}_{\alpha\nu}$. Hence, in our case the Finslerian definition of the Ricci tensor corresponds to the Riemannian expression, computing an appropriate trace of the curvature tensor. The expression of Eq. (7.17) can be used to obtain the Ricci scalar in Finsler geometry by contracting the Ricci tensor with two vectors y^μ/F (cf. (7.6.5) in [61]):

$$Ric \equiv Ric_{\mu\nu} \frac{y^\mu}{F} \frac{y^\nu}{F}. \tag{7.18}$$

Recall that the latter corresponds to $R^\varrho{}_\varrho$ that is obtained from tracing Eq. (7.16). This object is distinguished from the Ricci scalar $\mathcal{R}ic$ in a Riemannian setting, which follows from tracing the Ricci curvature tensor $\mathcal{R}ic_{\mu\nu}$; cf. Eq. (7.13c). Note that the quantity of Eq. (7.18) is the direct Finslerian equivalent of the Ricci scalar. Since the Finsler metric considered is Riemannian, $\mathcal{R}ic$ only involves dependences on r, whereas Ric depends on y^μ as well. In general and especially here $\mathcal{R}ic \neq \mathrm{Ric}$.

At this stage, there are several possibilities of defining the Einstein tensor $G_{\mu\nu}$ in a Finsler framework using different combinations of $\mathcal{R}ic_{\mu\nu}$, $\mathcal{R}ic$, $R_{\mu\nu}$, $Ric_{\mu\nu}$, and Ric. The following have been tried:

$$(G^\mu{}_\nu)^{(1)} \equiv \mathcal{R}ic^\mu{}_\nu - \frac{1}{2}\delta^\mu{}_\nu Ric, \tag{7.19a}$$

$$(G^\mu{}_\nu)^{(2)} \equiv R^\mu{}_\nu - \frac{1}{2}\delta^\mu{}_\nu Ric, \tag{7.19b}$$

$$(G^\mu{}_\nu)^{(3)} \equiv R^\mu{}_\nu - \frac{1}{2}\delta^\mu{}_\nu \mathcal{R}ic. \tag{7.19c}$$

A reasonable test of whether one of these choices is suitable requires computing their covariant derivatives, i.e., $D_\mu (G^\mu{}_\nu)^{(i)}$ for $i = 1 \ldots 3$. The wishful result would be a nonvanishing covariant derivative bearing resemblance to the modified covariant conservation law of the energy-momentum tensor in Eq. (6.8). This makes sense when we assume that the modified Einstein tensor (in a Finslerian framework) is linked to the energy-momentum tensor in an explicitly Lorentz-violating theory. The corresponding covariant derivative to be used involves both the nonminimal connection $N^\mu{}_\nu$ and the Chern connection $\Gamma^\mu{}_{\nu\varrho}$ being equal to the Christoffel symbols $\Gamma^\mu{}_{\nu\varrho}$ in this case:

$$D_\mu (G^\mu{}_\nu)^{(i)} = \frac{\partial (G^\mu{}_\nu)^{(i)}}{\partial x^\mu} - N^\beta{}_\mu \frac{(G^\mu{}_\nu)^{(i)}}{\partial y^\beta} + \Gamma^\mu{}_{\alpha\mu} (G^\alpha{}_\nu)^{(i)} - \Gamma^\alpha{}_{\nu\mu} (G^\mu{}_\alpha)^{(i)}. \tag{7.20}$$

Starting from the Finsler metric of Eq. (7.2a) there have been up to three derivatives with respect to the coordinates involved, which is why in Eq. (7.20) the third derivative of the refractive index appears in general.

The more of the higher derivatives of a Taylor expansion of $n(r)$ are taken into account, the smaller are the structures in changes of $n(r)$ to be resolved. Therefore relying on the geometric-optics approximation it is reasonable to consider only the first-order change of $n(r)$ incorporated in its first derivative and to neglect the higher-order derivatives, which describe small-scale changes of $n(r)$. Within this approximation it makes sense to set $n(r) = 1$, since modifications lead to higher-order contributions.

Furthermore the Finsler structure that the isotropic case was identified with is three-dimensional; cf. Eq. (3.14b),

and it involves spatial velocity components only. Hence, y^t can be considered as auxiliary and will be set to zero at the end. With this physical input the covariant derivative of each Einstein tensor proposed in Eq. (7.19) can be computed. The final result for the third possibility looks rather promising:

$$D_\mu(G^\mu{}_\nu)^{(3)}|_{y^t=0} = \frac{1}{(y^r)^2 + r^2[(y^\theta)^2 + (y^\phi)^2\sin^2\theta]}\frac{n'}{r^2} \times \begin{pmatrix} 0 \\ (y^r)^2 \\ y^r y^\theta r^2 \\ y^r y^\phi r^2 \sin^2\theta \end{pmatrix}_\nu + \ldots, \tag{7.21}$$

where terms of $\mathcal{O}(n'', n''', n'^2, n'^3)$ have been neglected. Using the inverse metric $g^{\mu\nu}$ of Eq. (7.2b) the second index can be raised. Besides we identify the spatial components of $\mathbf{y}$ with the spatial components of the physical velocity, i.e., $y^r = u^r$, $y^\theta = u^\theta$, and $y^\phi = u^\phi$ where the spatial flat metric in spherical polar coordinates is given by $(r_{ij}) = \mathrm{diag}(1, r^2, r^2\sin^2\theta)$. This leads to the final result

$$D_\mu(G^{\mu\nu})^{(3)}|_{y^t=0} = -\frac{n'}{\mathbf{u}^2 r^2}\begin{pmatrix} 0 \\ (u^r)^2 \\ u^r u^\theta \\ u^r u^\phi \end{pmatrix}^\nu + \ldots, \tag{7.22a}$$

$$D_\mu(G^{\mu i})^{(3)}|_{y^t=0} = -\frac{n'}{r^2}\hat{u}^r\hat{u}^i + \ldots, \tag{7.22b}$$

with the normalized three-velocity vector $\hat{\mathbf{u}} = \mathbf{u}/|\mathbf{u}|$. Comparing the obtained result to Eq. (6.8) reveals that the structure of both expressions is very similar. The difference is a global prefactor of the form $r^2\sqrt{\mathbf{u}^2}$. The dimensionful factor of r^2 is not surprising. Both the Riemann curvature tensor and the (modified) Einstein tensor involve two derivatives, which is why their mass dimensions is -2. However, the energy-momentum tensor is based on the "Lagrangian" of a classical light ray, Eq. (6.1), which is a dimensionless quantity. The discrepancy in mass dimensions is compensated by the only dimensionful length scale available, which is r. It seems that an alternative definition of the Einstein tensor in the framework of Finsler geometry can compensate for the modified energy-momentum conservation law when explicit Lorentz violation is considered. This result is interesting and deserves further study, e.g., whether it holds for anisotropic theories as well.

VIII. CONCLUSIONS AND OUTLOOK

In this work classical-ray analogs to the photon sector of the minimal Standard-Model extension were discussed. It was shown that a nonvanishing photon mass allows for deriving classical point-particle Lagrangians in analogy to the fermion sector. However, in case the photon mass vanishes the standard method used for the fermion sector is not applicable. The reason is that a light ray does not have as many degrees of freedom as a massive particle.

Instead, for the photon sector an alternative technique had to be employed which made it possible to derive a Lagrangian-type function for a classical ray directly from the modified photon dispersion relation. This was carried out for several interesting cases of the minimal, *CPT*-even photon sector, which is characterized by dimensionless controlling coefficients. Subsequently it was shown that the results obtained are consistent with the eikonal equation approach that describes the geometric-optics limit of an electromagnetic wave. Mathematically the Lagrangian-type functions can be interpreted as Finsler structures. In contrast to the fermion sector, they only involve the spatial velocity components and they are closely linked to an effective refractive index of the Lorentz-violating vacuum.

It has been known for some time that there is a connection between the geodesic equations for a light ray in a gravitational background and the eikonal equations. This link is warranted for weak gravitational fields at least, e.g., in the solar system. It was crucial to set up a phenomenological description of light rays subject to Lorentz violation in a weak gravitational field. This description made it possible to obtain sensitivities on the isotropic controlling coefficient $\tilde{\kappa}_{\mathrm{tr}}$ that could be probed by the space missions GAIA and LATOR employing measurements of light deflection at massive bodies. The upshot is that the planned mission LATOR may have a sensitivity on $|\tilde{\kappa}_{\mathrm{tr}}|$ in the order of magnitude of 10^{-16} where the running mission GAIA can reach 10^{-14}. The difference in sensitivity originates from the different precision of measuring angles for both missions.

The final part of the paper was dedicated to investigating the properties of the (isotropic) curved spacetime, which the phenomenological studies were based on, from a Finslerian point of view. It was demonstrated that in the classical limit (neglecting higher spacetime derivatives of the refractive index) an Einstein tensor can be defined that is not subject to the usual Bianchi identities in Riemannian geometry. Therefore its covariant derivative is nonzero and it has a form that is related to the modified conservation law of the energy-momentum tensor based on the classical Lagrangian-type function studied in this context. Hence, it seems that Finsler geometry provides new geometrical degrees of freedom that can serve as a kind of "buffer" to allow for a momentum transfer whenever the momentum of the light ray changes. These geometrical degrees of freedom take the role of the Nambu-Goldstone modes appearing when spontaneous Lorentz violation is considered.

To summarize, the current article provides a technique in treating Lorentz-violating photons in a curved background in a geometric-optics approximation. As an outlook, it will be interesting to apply the setup to anisotropic frameworks, first to obtain sensitivities on related controlling coefficients and second to study the properties of the underlying Finsler geometry.

ACKNOWLEDGMENTS

It is a pleasure to thank V. A. Kostelecký for suggesting this line of research and for having fruitful discussions. Furthermore, the author is indebted to N. Russell for giving helpful advice on improving the language. Last but not least the author is happy to thank the anonymous referee for further suggestions that helped to improve the article. This work was performed with financial support from the Deutsche Akademie der Naturforscher Leopoldina within Grant No. LPDS 2012-17.

APPENDIX A: CLASSICAL LAGRANGIANS FOR MASSIVE LORENTZ-VIOLATING PHOTONS

The first part of the appendix shall briefly demonstrate how to derive the classical Lagrange functions in Sec. II C from the set of equations (2.2), (2.4), and (2.5). The demonstration will be performed for the nonbirefringent, anisotropic case of the *CPT*-even sector and for a particular choice of the *CPT*-odd framework. The calculation is easier for the *CPT*-even theory, which is why it will be studied first.

1. *CPT*-even minimal photon sector

The base is Eq. (2.19) where for convenience we set $(3/2)\tilde{\kappa}_{e-}^{11} \equiv \kappa$. For the remaining *CPT*-even cases, the procedure works analogously. First of all the modified dispersion relation for a massive photon subject to this particular Lorentz-violating framework reads

$$(1+\kappa)(k_0^2 - k_1^2 - k_2^2) - (1-\kappa)k_3^2 = m_\gamma^2. \tag{A1}$$

To obtain the group velocity components it is often reasonable not to solve the dispersion relation to obtain k_0 directly, but to differentiate it implicitly with respect to the spatial momentum components:

$$2(1+\kappa)k_0\frac{\partial k_0}{\partial k_1} - 2(1+\kappa)k_1 = 0 \Leftrightarrow \frac{\partial k_0}{\partial k_1} = \frac{k_1}{k_0}, \tag{A2a}$$

$$2(1+\kappa)k_0\frac{\partial k_0}{\partial k_2} - 2(1+\kappa)k_2 = 0 \Leftrightarrow \frac{\partial k_0}{\partial k_2} = \frac{k_2}{k_0}, \tag{A2b}$$

$$2(1+\kappa)k_0\frac{\partial k_0}{\partial k_3} - 2(1-\kappa)k_3 = 0 \Leftrightarrow \frac{\partial k_0}{\partial k_3} = \frac{1-\kappa}{1+\kappa}\frac{k_3}{k_0}. \tag{A2c}$$

For the particular case studied, Eq. (2.4) leads to the following three equations:

$$\frac{k_1}{k_0} = -\frac{u^1}{u^0}, \qquad \frac{k_2}{k_0} = -\frac{u^2}{u^0}, \qquad \frac{1-\kappa}{1+\kappa}\frac{k_3}{k_0} = -\frac{u^3}{u^0}. \tag{A3}$$

Evidently only the third one is modified by Lorentz violation mirroring the spatial anisotropy. These relations can be solved directly to express the spatial momentum components via k_0:

$$k_1 = -\frac{k_0 u^1}{u^0}, \qquad k_2 = -\frac{k_0 u^2}{u^0}, \qquad k_3 = -\frac{1+\kappa}{1-\kappa}\frac{k_0 u^3}{u^0}. \tag{A4}$$

We can now use Eq. (2.5) and express the spatial momentum components by taking into account the previously obtained results of Eq. (A4):

$$\begin{aligned} L &= -(k_0 u^0 + k_1 u^1 + k_2 u^2 + k_3 u^3) \\ &= \frac{k_0}{u^0}\left[-(u^0)^2 + (u^1)^2 + (u^2)^2 + \frac{1+\kappa}{1-\kappa}(u^3)^2\right]. \end{aligned} \tag{A5}$$

The latter is solved with respect to k_0 giving an expression comprising the (unknown) Lagrange function and the four-velocity components:

$$k_0 = -L\frac{(1-\kappa)u^0}{(1-\kappa)[(u^0)^2 - (u^1)^2 - (u^2)^2] - (1+\kappa)(u^3)^2}. \tag{A6}$$

Now all four-momentum components in the dispersion relation can be eliminated via Eq. (A4) and a subsequent insertion of Eq. (A6):

$$\begin{aligned} 0 = \frac{1+\kappa}{1-\kappa}\frac{k_0^2}{(u^0)^2}\{&(1-\kappa)[(u^0)^2 - (u^1)^2 - (u^2)^2] \\ &- (1+\kappa)(u^3)^2\} - m_\gamma^2, \end{aligned} \tag{A7a}$$

$$0 = L^2\frac{(1-\kappa)(1+\kappa)}{(1-\kappa)[(u^0)^2 - (u^1)^2 - (u^2)^2] - (1+\kappa)(u^3)^2} - m_\gamma^2. \tag{A7b}$$

The final equation comprises a polynomial of the Lagrangian whose coefficients depend on four-velocity components only. The polynomial must be solved to give L:

$$L^\pm = \pm m_\gamma\sqrt{\frac{1}{1+\kappa}[(u^0)^2 - (u^1)^2 - (u^2)^2] - \frac{1}{1-\kappa}(u^3)^2}. \tag{A8}$$

The result corresponds to Eq. (2.25a). The procedure shown is typically applied to derive classical Lagrangians. Four of the five equations are employed to eliminate all four-momentum components and to obtain a polynomial equation in L that only comprises the four-velocity. The latter is then solved with respect to L finally.

2. *CPT*-odd minimal photon sector

Due to observer Lorentz invariance without a loss of generality $(k_{AF})^\kappa = (0,0,0,1)^\kappa$ will be chosen for the spacelike case. The modified dispersion relation involves an isotropic contribution and a second term that does not comprise the momentum component parallel to the preferred spacetime direction:

$$(k_0^2 - \mathbf{k}^2)^2 - 4m_{\mathrm{CS}}^2(k_0^2 - k_1^2 - k_2^2) = 0. \tag{A9}$$

The group velocity components are obtained by implicit differentiation of Eq. (A9) with respect to the spatial momentum components:

$$\begin{aligned} 0 &= 4(k_0^2 - \mathbf{k}^2)\left[k_0\frac{\mathrm{d}k_0}{\mathrm{d}k_1} - k_1\right] - 8m_{\mathrm{CS}}^2\left(k_0\frac{\mathrm{d}k_0}{\mathrm{d}k_1} - k_1\right) \\ &= 4(k_0^2 - \mathbf{k}^2 - 2m_{\mathrm{CS}}^2)\left[k_0\frac{\mathrm{d}k_0}{\mathrm{d}k_1} - k_1\right], \end{aligned} \tag{A10a}$$

$$0 = 4(k_0^2 - \mathbf{k}^2 - 2m_{\mathrm{CS}}^2)\left[k_0\frac{\mathrm{d}k_0}{\mathrm{d}k_2} - k_2\right], \tag{A10b}$$

$$\begin{aligned} 0 &= 4(k_0^2 - \mathbf{k}^2)\left[k_0\frac{\mathrm{d}k_0}{\mathrm{d}k_3} - k_3\right] - 8m_{\mathrm{CS}}^2 k_0\frac{\mathrm{d}k_0}{\mathrm{d}k_3} \\ &= 4(k_0^2 - \mathbf{k}^2 - 2m_{\mathrm{CS}}^2)k_0\frac{\mathrm{d}k_0}{\mathrm{d}k_3} - 4(k_0^2 - \mathbf{k}^2)k_3. \end{aligned} \tag{A10c}$$

Since the preferred spacetime direction points along the third axis of the coordinate system, the first and second group velocity components remain standard where only the third one is modified:

$$\frac{\mathrm{d}k_0}{\mathrm{d}k_1} = \frac{k_1}{k_0}, \qquad \frac{\mathrm{d}k_0}{\mathrm{d}k_2} = \frac{k_2}{k_0}, \qquad \frac{\mathrm{d}k_0}{\mathrm{d}k_3} = \frac{k_3(k_0^2 - \mathbf{k}^2)}{k_0(k_0^2 - \mathbf{k}^2 - 2m_{\mathrm{CS}}^2)}. \tag{A11}$$

Therefore Eq. (2.4) results in

$$\frac{k_1}{k_0} = -\frac{u^1}{u^0}, \qquad \frac{k_2}{k_0} = -\frac{u^2}{u^0}, \qquad \frac{k_3(k_0^2 - \mathbf{k}^2)}{k_0(k_0^2 - \mathbf{k}^2 - 2m_{\mathrm{CS}}^2)} = -\frac{u^3}{u^0}. \tag{A12}$$

The first two of these relationships allow for writing k_1 and k_2 in terms of k_0. However, the third equation would lead to a cumbersome third-order polynomial to be solved, which is not a reasonable step to take. It is better to insert the first two of Eq. (A12) into Eq. (2.5) and to solve the latter with respect to k_3. Then it is possible to express k_3 via k_0 only:

$$k_3 = \frac{1}{u^0 u^3}\{k_0[(u^1)^2 + (u^2)^2 - (u^0)^2] - Lu^0\}. \tag{A13}$$

Now we can express all spatial momentum components via k_0. Thus, we can eliminate all of them in Eq. (A9) to obtain an equation that only involves k_0. This can be solved to write k_0 in terms of four-velocity components and the Lagrangian where one of the solutions reads

$$k_0 = -u^0\frac{L\sqrt{u_\perp^2} + m_{\mathrm{CS}}(u^3)^2 + |u^3|\sqrt{L^2 + 2m_{\mathrm{CS}}\sqrt{u_\perp^2}L + m_{\mathrm{CS}}^2(u^3)^2}}{u^2\sqrt{u_\perp^2}}, \tag{A14a}$$

$$(u_\perp^\mu) = (u^0, u^1, u^2, 0)^T. \tag{A14b}$$

Here $u^0 > 0$ has been assumed for simplicity. The last step is to eliminate all four-momentum components in the third of Eq. (A12) to obtain a polynomial equation for L:

$$L^2 + 2m_{\mathrm{CS}}\sqrt{u_\perp^2}L + m_{\mathrm{CS}}^2(u^3)^2 = 0, \tag{A15}$$

which leads to the Lagrange functions

$$L^\pm = m_{\mathrm{CS}}[\pm\sqrt{u^2} - \sqrt{u_\perp^2}]. \tag{A16}$$

Reinstating the preferred spacetime direction, it is possible to write the latter in the form of Eq. (2.14). Using the other solution of k_0 similar to Eq. (A14) the Lagrangians with the opposite signs are obtained. A computation for $u^0 < 0$ leads to analogous results. Due to observer Lorentz invariance the form of the Lagrangian stays the same for general spacelike k_{AF}.

APPENDIX B: LIGHT DEFLECTION IN SCHWARZSCHILD SPACETIMES

In [99] it was found that a constant refractive index $n \neq 1$ due to Lorentz violation leads to a change in light deflection. This result is in contrast to what we obtain

from Bouguer's formula in Sec. VA. A rough explanation is that Bouguer's formula relies on the eikonal equation, which is equivalent to the null geodesic equations only for a weak gravitational field. However, the latter reference is based on a Schwarzschild metric,

$$\mathrm{d}\tau^2 = \left(1-\frac{2GM}{r}\right)\mathrm{d}t^2 - \left(1-\frac{2GM}{r}\right)^{-1}\mathrm{d}r^2 - r^2(\mathrm{d}\theta^2+\sin^2\theta\mathrm{d}\phi^2), \tag{B1}$$

which in this form is not generally isotropic. To get a more profound understanding, consider the geodesic equations for a photon in a generally isotropic spacetime of Eq. (5.3) with $A = A(r)$. The Christoffel symbols are computed in Riemannian geometry according to Eq. (7.4) and the geodesic equations read

$$\frac{\mathrm{d}x^\mu}{\mathrm{d}\lambda} + \gamma^\mu{}_{\nu\varrho}\frac{\mathrm{d}x^\nu}{\mathrm{d}\lambda}\frac{\mathrm{d}x^\varrho}{\mathrm{d}\lambda} = 0, \qquad (x^\mu) = (t,r,\theta,\phi)^T. \tag{B2}$$

In what follows, differentiation with respect to the curve parameter λ and with respect to r, respectively, will be denoted by a dot and a prime. The geodesic equations can then be cast into the following form:

$$0 = \ddot{t} - \frac{A'}{A}\dot{r}\,\dot{t}, \tag{B3a}$$

$$0 = \ddot{r} + \frac{A'}{2A}\dot{r}^2 - \frac{A'}{2A^3}\dot{t}^2 - \left(1+\frac{A'}{2A}r\right)r\dot{\theta}^2 - \left(1+\frac{A'}{2A}r\right)r\sin^2(\theta)\dot{\phi}^2, \tag{B3b}$$

$$0 = \ddot{\theta} + \left(\frac{2}{r}+\frac{A'}{A}\right)\dot{r}\,\dot{\theta} - \sin(\theta)\cos(\theta)\dot{\phi}^2, \tag{B3c}$$

$$0 = \ddot{\phi} + \left(\frac{2}{r}+\frac{A'}{A}\right)\dot{r}\,\dot{\phi} + 2\cot(\theta)\dot{\theta}\,\dot{\phi}, \tag{B3d}$$

$$0 = \frac{1}{A}\dot{t}^2 - A\dot{r}^2 - Ar^2[\dot{\theta}^2+\sin^2(\theta)\dot{\phi}^2], \tag{B3e}$$

where the fifth of those is the condition for a null-trajectory. They correspond to the equations stated in [97] in case that A is a function of the radial coordinate r only. Now the right-hand side of Eq. (B3a) can be written as the derivative of a conserved quantity that is denoted as K_0 in [97]:

$$0 = A\frac{\mathrm{d}}{\mathrm{d}\lambda}\left(\frac{\dot{t}}{A}\right) \Rightarrow K_0 = \frac{\dot{t}}{A}, \qquad \dot{t} = K_0 A. \tag{B4}$$

With the choice of $\theta = \pi/2$ Eq. (B3c) is fulfilled automatically. Using the previous results, Eq. (B3d) can be expressed as the time-derivative of another conserved quantity K_1:

$$0 = \frac{1}{Ar^2}\frac{\mathrm{d}}{\mathrm{d}\lambda}(Ar^2\dot{\phi}) \Rightarrow K_1 = Ar^2\dot{\phi}, \qquad \dot{\phi} = \frac{K_1}{Ar^2}. \tag{B5}$$

Looking at Eq. (B16) we see that both K_0 and K_1 correspond to the conserved quantities that are obtained via the Killing vectors; cf. Appendix B 1. From now on the trajectory shall be parameterized with respect to proper time: $\lambda = \tau$. Since K_0 is then linked to infinitesimal time translations, it is reasonable to identify it with the total photon energy E. Furthermore K_1 is connected to infinitesimal changes in the angle ϕ, which is why it corresponds to the angular momentum L. When these conserved quantities are compared to Eqs. (5.7a, b) in [99] we see that the energy is the same, but the angular momentum differs by an additional factor of A. Finally Eq. (B3b) can be written as follows:

$$0 = \frac{1}{2A\dot{r}}\frac{\mathrm{d}}{\mathrm{d}\tau}\left(A\dot{r}^2 - E^2A + \frac{L^2}{r^2A}\right)$$
$$\Rightarrow K_2 = A\dot{r}^2 - E^2A + \frac{L^2}{r^2A}. \tag{B6}$$

Therefore the latter comprises even another conserved quantity K_2. Setting $K_2 = 0$ is in accordance with the null-trajectory condition of Eq. (B3e). Taking into account that $\dot{r} = (\mathrm{d}r/\mathrm{d}\phi)\dot{\phi}$ where $\dot{\phi}$ is again expressed by the conserved angular momentum, it is possible to solve Eq. (B6) with respect to $\mathrm{d}\phi/\mathrm{d}r$:

$$\frac{\mathrm{d}\phi}{\mathrm{d}r} = \frac{L}{r\sqrt{E^2A(r)^2r^2 - L^2}},$$
$$\phi(r) = L\int_{r_0}^{\infty}\frac{\mathrm{d}r}{r\sqrt{E^2A(r)^2r^2 - L^2}}. \tag{B7}$$

Comparing to Eq. (5.10) we see that $C = L/E$, i.e., the constant appearing in Bouguer's formula can be understood as the ratio of angular momentum and total energy.

Now there are some differences between the final result of Eq. (B7) and the corresponding Eq. (5.9) in [99]. In the latter paper, a black-hole gravitational background is considered in Schwarzschild coordinates. This line interval does not have the form of a generally isotropic metric given in Eq. (5.6a). In fact, there are isotropic coordinates allowing us to write the Schwarzschild solution in the form (see, e.g., page 93 of [102]):

$$\varrho = \frac{1}{2}(r - GM + \sqrt{r(r-2GM)}), \tag{B8a}$$

$$\mathrm{d}\tau^2 = \left(\frac{1-GM/(2\varrho)}{1+GM/(2\varrho)}\right)^2\mathrm{d}t^2 - \left(1+\frac{GM}{2\varrho}\right)^4[\mathrm{d}\varrho^2 + \varrho^2\mathrm{d}\theta^2 + \varrho^2\sin^2\theta\mathrm{d}\phi^2]. \tag{B8b}$$

Using this set of coordinates the equation encoding angular momentum conservation and the change in the angle ϕ with respect to the new radial coordinate ρ read as follows:

$$L = g_{\rho\rho}\rho^2\dot{\phi}, \tag{B9a}$$

$$\frac{\mathrm{d}\phi}{\mathrm{d}\rho} = \frac{L}{\rho}\frac{\sqrt{g_{\rho\rho}g_{tt}}}{\sqrt{E^2 g_{\rho\rho}^2\rho^2 - L^2 g_{\rho\rho}g_{tt}}} = \frac{L}{\rho}\frac{1}{\sqrt{E^2 g_{\rho\rho}^2\rho^2 - L^2}} + \mathcal{O}\left(\frac{GM}{2\rho}\right)^2. \tag{B9b}$$

The first corresponds to Eq. (B5) and the second to Eq. (B7) neglecting second-order gravity effects. Multiplying the modified line interval of Eq. (4.12) in [99] by the constant $\sqrt{1+\epsilon}$ leads to

$$\mathrm{d}\tilde{\tau}^2 = \frac{1}{\sqrt{1+\epsilon}}\left(1-\frac{2GM}{r}\right)\mathrm{d}t^2 - \sqrt{1+\epsilon}\left[\frac{1}{1-2GM/r}\mathrm{d}r^2 + r^2\mathrm{d}\Omega^2\right]. \tag{B10}$$

Since photons move on null-trajectories, $\mathrm{d}\tilde{\tau}^2 = 0$ anyhow, which is why a multiplication of the line element by a constant should not change the physics. In this case, the Lorentz-violating contribution governed by a position-independent ϵ drops out of $\mathrm{d}\phi/\mathrm{d}\rho$ when taking into account Eq. (B9a). Therefore in the isotropic coordinates the particular Lorentz-violating contribution of their case 3 produces second-order gravity effects associated with Lorentz violation. Far away from the black-hole event horizon there are no novel physical effects and this corresponds to the outcome of the eikonal approach.

1. Killing vectors of a spherically symmetric spacetime

In the current paragraph the Killing vectors for a spherically symmetric spacetime, cf. Eq. (5.3) with $A(r,\theta,\phi) = A(r)$, will be listed. The Killing vectors ξ_μ describe infinitesimal isometries for a spacetime and they are linked to underlying symmetries and conserved quantities. In general they are obtained from a set of partial differential equations called the Killing equations:

$$D_\alpha\xi_\beta + D_\beta\xi_\alpha = 0, \qquad D_\nu\xi_\lambda = \partial_\nu\xi_\lambda - \gamma^\mu{}_{\nu\lambda}\xi_\mu, \tag{B11}$$

with the covariant derivative D_α and the Christoffel symbols $\gamma^\mu{}_{\nu\lambda}$. The latter can be directly extracted from Eq. (B3). For the spherically symmetric spacetime, it is possible to solve the Killing equations analytically. To do so, it is reasonable to make a certain *Ansatz*, e.g., one with vanishing spatial components of ξ_μ. This simplifies the set of equations dramatically where several are immediately fulfilled automatically. They are then solved successively to obtain four Killing vectors. Since the metric is isotropic, it is reasonable to make an *Ansatz* for ξ_μ that only involves a nonvanishing timelike component that does not depend on time itself:

$$(\xi_\mu) = \begin{pmatrix} \xi_0(r,\theta,\phi) \\ 0 \\ 0 \\ 0 \end{pmatrix}. \tag{B12}$$

In this case the following three differential equations must to be solved:

$$\xi_0\frac{A'}{A} + \frac{\partial\xi_0}{\partial r} = 0, \qquad \frac{\partial\xi_0}{\partial\theta} = 0, \qquad \frac{\partial\xi_0}{\partial\phi} = 0. \tag{B13}$$

The remaining ones are fulfilled automatically. The latter two tell us immediately that ξ_0 neither depends on θ nor ϕ. Therefore the first differential equation is an ordinary one that can be solved directly by integration:

$$\frac{\xi_0{}'}{\xi_0} = -\frac{A'}{A} \Rightarrow \ln|\xi_0| = -\ln|c_0 A| \Rightarrow \xi_0(r) = \frac{\tilde{c}_0}{A(r)}, \qquad c_0, \tilde{c}_0 \in \mathbb{R}. \tag{B14}$$

A similar approach leads to the remaining Killing vectors. In total one obtains

$$\xi_\mu^{(1)} = \begin{pmatrix} 1/A \\ 0 \\ 0 \\ 0 \end{pmatrix}, \qquad \xi_\mu^{(2)} = r^2 A\begin{pmatrix} 0 \\ 0 \\ \sin\phi \\ \sin\theta\cos\theta\cos\phi \end{pmatrix}, \tag{B15a}$$

$$\xi_\mu^{(3)} = r^2 A\begin{pmatrix} 0 \\ 0 \\ \cos\phi \\ -\sin\theta\cos\theta\sin\phi \end{pmatrix}, \qquad \xi_\mu^{(4)} = r^2 A\begin{pmatrix} 0 \\ 0 \\ 0 \\ \sin^2\theta \end{pmatrix}. \tag{B15b}$$

Suitable contractions of the Killing vectors with $(\dot{x}^\mu) = (\dot{t},\dot{r},\dot{\theta},\dot{\phi})^T$ (and additional linear combinations) lead to conserved quantities. The first conserved quantity follows from a contraction with the first Killing vector:

$$\xi^{(1)}_\mu \dot{x}^\mu = \frac{\dot{t}}{A} = \text{const.} \tag{B16a}$$

The latter corresponds to the result obtained in Eq. (B16a) and it is related to energy conservation. The second conserved quantity involves the remaining Killing vectors where it is understood to be evaluated at $\theta = \pi/2$:

$$\sqrt{\sum_{i=2}^{4} (\xi^{(i)}_\mu \dot{x}^\mu)^2}\Big|_{\theta=\pi/2} = A r^2 \dot{\phi} = \text{const.} \tag{B16b}$$

This conserved quantity is the same as what was obtained in Eq. (B5) and it means angular momentum conservation. Hence, the Killing vectors $\xi^{(i)}$ for $i = 2\ldots4$ are related to rotational symmetry of the spherically symmetric spacetime.

APPENDIX C: EIKONAL EQUATION FOR INHOMOGENEOUS AND ANISOTROPIC MEDIA

The current section serves with providing some general results on the physics of the eikonal equation, which are used in Sec. V extensively. In general, the eikonal equation provides a set of three coupled nonlinear differential equations. In what follows a refractive index bearing a dependence on the radial distance r and an angle ϕ is assumed [cf., e.g., Eq. (5.23)]. The photon trajectory shall be parametrized by the angle ϕ, i.e., $\mathbf{r}(\phi) = r(\phi)\hat{\mathbf{e}}_r(\phi)$. Its first and second derivative read

$$\mathbf{r}' = \dot{r}\hat{\mathbf{e}}_r + r\hat{\mathbf{e}}_\phi, \qquad \mathbf{r}'' = (\ddot{r} - r)\hat{\mathbf{e}}_r + 2\dot{r}\hat{\mathbf{e}}_\phi. \tag{C1a}$$

The arc length depends on ϕ and we obtain a set of useful relationships:

$$\begin{aligned} s(\phi) &= \int^\phi \mathrm{d}\phi' |\mathbf{r}'| = \int^\phi \mathrm{d}\phi' \sqrt{r^2 + \dot{r}^2}, \\ \frac{\mathrm{d}s}{\mathrm{d}\phi} &= \sqrt{r^2 + \dot{r}^2}, \end{aligned} \tag{C1b}$$

$$\begin{aligned} \left(\frac{\mathrm{d}s}{\mathrm{d}\phi}\right)^{-2} &= \frac{1}{r^2 + \dot{r}^2}, \\ \frac{\mathrm{d}}{\mathrm{d}\phi}\left(\frac{\mathrm{d}s}{\mathrm{d}\phi}\right)^{-1} &= \frac{\mathrm{d}}{\mathrm{d}\phi}\left(\frac{1}{\sqrt{r^2 + \dot{r}^2}}\right) = -\frac{(r + \ddot{r})\dot{r}}{(r^2 + \dot{r}^2)^{3/2}}, \end{aligned} \tag{C1c}$$

$$\frac{\mathrm{d}\mathbf{r}}{\mathrm{d}s} = \frac{\mathrm{d}\mathbf{r}}{\mathrm{d}\phi}\left(\frac{\mathrm{d}s}{\mathrm{d}\phi}\right)^{-1}. \tag{C1d}$$

Now the derivative on the left-hand side of the eikonal equation can be computed. Instead of differentiating with respect to the arc length we have to calculate derivatives with respect to ϕ, which leads to three terms:

$$\begin{aligned} \frac{\mathrm{d}}{\mathrm{d}s}\left[n\frac{\mathrm{d}\mathbf{r}}{\mathrm{d}\phi}\left(\frac{\mathrm{d}s}{\mathrm{d}\phi}\right)^{-1}\right] &= \frac{\mathrm{d}n}{\mathrm{d}s}\frac{\mathrm{d}\mathbf{r}}{\mathrm{d}\phi}\left(\frac{\mathrm{d}s}{\mathrm{d}\phi}\right)^{-1} + n\frac{\mathrm{d}^2\mathbf{r}}{\mathrm{d}\phi^2}\left(\frac{\mathrm{d}s}{\mathrm{d}\phi}\right)^{-2} \\ &\quad + \frac{\mathrm{d}}{\mathrm{d}s}\left(\frac{\mathrm{d}s}{\mathrm{d}\phi}\right)^{-1} n\frac{\mathrm{d}\mathbf{r}}{\mathrm{d}\phi} \\ &= \frac{\mathrm{d}n}{\mathrm{d}\phi}\frac{\mathrm{d}\mathbf{r}}{\mathrm{d}\phi}\left(\frac{\mathrm{d}s}{\mathrm{d}\phi}\right)^{-2} + n\frac{\mathrm{d}^2\mathbf{r}}{\mathrm{d}\phi^2}\left(\frac{\mathrm{d}s}{\mathrm{d}\phi}\right)^{-2} \\ &\quad + \frac{\mathrm{d}}{\mathrm{d}\phi}\left[\left(\frac{\mathrm{d}s}{\mathrm{d}\phi}\right)^{-1}\right]\left(\frac{\mathrm{d}s}{\mathrm{d}\phi}\right)^{-1} n\frac{\mathrm{d}\mathbf{r}}{\mathrm{d}\phi}. \end{aligned} \tag{C2}$$

Now employing the derivatives of Eq. (C1a) and the identities given in Eq. (C1b) the eikonal equation can be expressed in terms of the radial coordinate r, the angle ϕ, and the basis vectors:

$$\begin{aligned} &\hat{\mathbf{e}}_r\frac{\partial n}{\partial r} + \frac{1}{r}\frac{\partial n}{\partial \phi}\hat{\mathbf{e}}_\phi \\ &\quad = \frac{1}{r^2 + \dot{r}^2}\left\{\frac{\mathrm{d}n}{\mathrm{d}\phi}(\dot{r}\hat{\mathbf{e}}_r + r\hat{\mathbf{e}}_\phi) + n[(\ddot{r} - r)\hat{\mathbf{e}}_r + 2\dot{r}\hat{\mathbf{e}}_\phi]\right\} \\ &\qquad - n(\dot{r}\hat{\mathbf{e}}_r + r\hat{\mathbf{e}}_\phi)\frac{(r + \ddot{r})\dot{r}}{(r^2 + \dot{r}^2)^2} \end{aligned} \tag{C3}$$

Sorting terms associated with $\hat{\mathbf{e}}_r$ and $\hat{\mathbf{e}}_\phi$, respectively, results in a system of two differential equations:

$$\frac{\partial n}{\partial r} = \frac{1}{r^2 + \dot{r}^2}\left[\frac{\mathrm{d}n}{\mathrm{d}\phi}\dot{r} + n(\ddot{r} - r)\right] - n\frac{(r + \ddot{r})\dot{r}^2}{(r^2 + \dot{r}^2)^2}, \tag{C4a}$$

$$\frac{1}{r}\frac{\partial n}{\partial \phi} = \frac{1}{r^2 + \dot{r}^2}\left[\frac{\mathrm{d}n}{\mathrm{d}\phi}r + 2n\dot{r}\right] - n\frac{(r + \ddot{r})r\dot{r}}{(r^2 + \dot{r}^2)^2}. \tag{C4b}$$

Multiplying the second with $\dot{r}/r$ and subtracting it from the first eliminates various terms, which simplifies the equation drastically:

$$\frac{\partial n}{\partial r} - \frac{\dot{r}}{r^2}\frac{\partial n}{\partial \phi} = \frac{n}{r^2 + \dot{r}^2}\left(\ddot{r} - \frac{2\dot{r}^2}{r} - r\right), \tag{C5a}$$

$$0 = (r^2 + \dot{r}^2)\left[r\frac{\partial n}{\partial r} - \frac{\dot{r}}{r}\frac{\partial n}{\partial \phi}\right] + n(r^2 + 2\dot{r}^2 - r\ddot{r}). \tag{C5b}$$

This is the final result that we are interested in and that shall be used for practical purposes. However, multiplying the latter with $r\dot{r}/(r^2 + \dot{r}^2)^{3/2}$, it can be written in a form that allows for a deeper physical understanding:

$$\frac{\mathrm{d}}{\mathrm{d}\phi}(nr\sin\alpha) - \sqrt{r^2 + \dot{r}^2}\frac{\partial n}{\partial \phi} = 0, \qquad \sin\alpha = \frac{r}{\sqrt{r^2 + \dot{r}^2}}. \tag{C6}$$

If the refractive index only depends on the radial coordinate the second term on the left-hand side vanishes,

which then leads us directly to the formula of Bouguer. Physically this result means angular momentum conservation. For a refractive index that additionally depends on the angle ϕ angular momentum is not a conserved quantity any more. Instead, there is a driving term that modifies the angular momentum. The change is bigger the larger the velocity is and the stronger the refractive index changes with the angle.

[1] D. Colladay and V. A. Kostelecký, Lorentz-violating extension of the standard model, Phys. Rev. D **58**, 116002 (1998).

[2] V. A. Kostelecký and M. Mewes, Electrodynamics with Lorentz-violating operators of arbitrary dimension, Phys. Rev. D **80**, 015020 (2009).

[3] V. A. Kostelecký and M. Mewes, Neutrinos with Lorentz-violating operators of arbitrary dimension, Phys. Rev. D **85**, 096005 (2012).

[4] V. A. Kostelecký and M. Mewes, Fermions with Lorentz-violating operators of arbitrary dimension, Phys. Rev. D **88**, 096006 (2013).

[5] V. A. Kostelecký and N. Russell, Data tables for Lorentz and *CPT* violation, Rev. Mod. Phys. **83**, 11 (2011).

[6] O. W. Greenberg, *CPT* Violation Implies Violation of Lorentz Invariance, Phys. Rev. Lett. **89**, 231602 (2002).

[7] V. A. Kostelecký and S. Samuel, Spontaneous breaking of Lorentz symmetry in string theory, Phys. Rev. D **39**, 683 (1989).

[8] V. A. Kostelecký and R. Potting, *CPT* and strings, Nucl. Phys. **B359**, 545 (1991).

[9] V. A. Kostelecký and R. Potting, *CPT*, strings, and meson factories, Phys. Rev. D **51**, 3923 (1995).

[10] R. Gambini and J. Pullin, Nonstandard optics from quantum space-time, Phys. Rev. D **59**, 124021 (1999).

[11] M. Bojowald, H. A. Morales–Técotl, and H. Sahlmann, Loop quantum gravity phenomenology and the issue of Lorentz invariance, Phys. Rev. D **71**, 084012 (2005).

[12] G. Amelino-Camelia and S. Majid, Waves on noncommutative spacetime and gamma-ray bursts, Int. J. Mod. Phys. A **15**, 4301 (2000).

[13] S. M. Carroll, J. A. Harvey, V. A. Kostelecký, C. D. Lane, and T. Okamoto, Noncommutative Field Theory and Lorentz Violation, Phys. Rev. Lett. **87**, 141601 (2001).

[14] F. R. Klinkhamer and C. Rupp, Spacetime foam, *CPT* anomaly, and photon propagation, Phys. Rev. D **70**, 045020 (2004).

[15] S. Bernadotte and F. R. Klinkhamer, Bounds on length scales of classical spacetime foam models, Phys. Rev. D **75**, 024028 (2007).

[16] S. Hossenfelder, Theory and phenomenology of spacetime defects, Adv. High Energy Phys. **2014**, 950672 (2014).

[17] F. R. Klinkhamer, Z-string global gauge anomaly and Lorentz non-invariance, Nucl. Phys. **B535**, 233 (1998).

[18] F. R. Klinkhamer, A *CPT* anomaly, Nucl. Phys. **B578**, 277 (2000).

[19] V. A. Kostelecký and R. Lehnert, Stability, causality, and Lorentz and *CPT* violation, Phys. Rev. D **63**, 065008 (2001).

[20] C. Adam and F. R. Klinkhamer, Causality and *CPT* violation from an Abelian Chern-Simons-like term, Nucl. Phys. **B607**, 247 (2001).

[21] R. Casana, M. M. Ferreira, A. R. Gomes, and P. R. D. Pinheiro, Gauge propagator and physical consistency of the *CPT*-even part of the standard model extension, Phys. Rev. D **80**, 125040 (2009).

[22] R. Casana, M. M. Ferreira, A. R. Gomes, and F. E. P. dos Santos, Feynman propagator for the nonbirefringent *CPT*-even electrodynamics of the standard model extension, Phys. Rev. D **82**, 125006 (2010).

[23] F. R. Klinkhamer and M. Schreck, Consistency of isotropic modified Maxwell theory: Microcausality and unitarity, Nucl. Phys. **B848**, 90 (2011); F. R. Klinkhamer and M. Schreck, Models for low-energy Lorentz violation in the photon sector: Addendum to "Consistency of isotropic modified Maxwell theory", Nucl. Phys. **B856**, 666 (2012).

[24] M. Schreck, Analysis of the consistency of parity-odd nonbirefringent modified Maxwell theory, Phys. Rev. D **86**, 065038 (2012).

[25] M. Cambiaso, R. Lehnert, and R. Potting, Massive photons and Lorentz violation, Phys. Rev. D **85**, 085023 (2012).

[26] D. Colladay, P. McDonald, and R. Potting, Gupta-Bleuler photon quantization in the standard model extension, Phys. Rev. D **89**, 085014 (2014).

[27] M. Maniatis and C. M. Reyes, Unitarity in a Lorentz symmetry breaking model with higher-order operators, Phys. Rev. D **89**, 056009 (2014).

[28] M. Schreck, Quantum field theory based on birefringent modified Maxwell theory, Phys. Rev. D **89**, 085013 (2014).

[29] M. Schreck, Quantum field theoretic properties of Lorentz-violating operators of nonrenormalizable dimension in the photon sector, Phys. Rev. D **89**, 105019 (2014).

[30] M. Cambiaso, R. Lehnert, and R. Potting, Asymptotic states and renormalization in Lorentz-violating quantum field theory, Phys. Rev. D **90**, 065003 (2014).

[31] M. Schreck, Quantum field theoretic properties of Lorentz-violating operators of nonrenormalizable dimension in the fermion sector, Phys. Rev. D **90**, 085025 (2014).

[32] S. Albayrak and I. Turan, *CPT*-odd photon in vacuum-orthogonal model, arXiv:1505.07584.

[33] M. A. Hohensee, D. F. Phillips, and R. L. Walsworth, Covariant quantization of Lorentz-violating electromagnetism, arXiv:1210.2683.

[34] V. A. Kostelecký, C. D. Lane, and A. G. M. Pickering, One-loop renormalization of Lorentz-violating electrodynamics, Phys. Rev. D **65**, 056006 (2002).
[35] D. Colladay and P. McDonald, One-loop renormalization of pure Yang-Mills theory with Lorentz violation, Phys. Rev. D **75**, 105002 (2007).
[36] D. Colladay and P. McDonald, One-Loop renormalization of QCD with Lorentz violation, Phys. Rev. D **77**, 085006 (2008).
[37] D. Colladay and P. McDonald, One-Loop renormalization of the electroweak sector with Lorentz violation, Phys. Rev. D **79**, 125019 (2009).
[38] A. Ferrero and B. Altschul, Renormalization of scalar and Yukawa field theories with Lorentz violation, Phys. Rev. D **84**, 065030 (2011).
[39] T. R. S. Santos and R. F. Sobreiro, Remarks on the renormalization properties of Lorentz and *CPT* violating quantum electrodynamics, arXiv:1502.06881.
[40] T. R. S. Santos and R. F. Sobreiro, Renormalizability of Yang-Mills theory with Lorentz violation and gluon mass generation, Phys. Rev. D **91**, 025008 (2015).
[41] V. A. Kostelecký, Gravity, Lorentz violation, and the standard model, Phys. Rev. D **69**, 105009 (2004).
[42] Q. G. Bailey and V. A. Kostelecký, Signals for Lorentz violation in post-Newtonian gravity, Phys. Rev. D **74**, 045001 (2006).
[43] V. A. Kostelecký, N. Russell, and J. D. Tasson, Constraints on Torsion from Bounds on Lorentz Violation, Phys. Rev. Lett. **100**, 111102 (2008).
[44] V. A. Kostelecký and J. D. Tasson, Prospects for Large Relativity Violations in Matter-Gravity Couplings, Phys. Rev. Lett. **102**, 010402 (2009).
[45] Q. G. Bailey, Time delay and Doppler tests of the Lorentz symmetry of gravity, Phys. Rev. D **80**, 044004 (2009).
[46] V. A. Kostelecký and J. D. Tasson, Matter-gravity couplings and Lorentz violation, Phys. Rev. D **83**, 016013 (2011).
[47] J. D. Tasson, Gravitational physics with antimatter, Hyperfine Interact. **193**, 291 (2009).
[48] J. D. Tasson, Lorentz violation, gravitomagnetism, and intrinsic spin, Phys. Rev. D **86**, 124021 (2012).
[49] J. D. Tasson, Antimatter, the SME, and gravity, Hyperfine Interact. **213**, 137 (2012).
[50] Y. Bonder, Lorentz violation in a uniform Newtonian gravitational field, Phys. Rev. D **88**, 105011 (2013).
[51] Y. Bonder, Lorentz violation in the gravity sector: The *t* puzzle, Phys. Rev. D **91**, 125002 (2015).
[52] Q. G. Bailey, V. A. Kostelecký, and R. Xu, Short-range gravity and Lorentz violation, Phys. Rev. D **91**, 022006 (2015).
[53] J. C. Long and V. A. Kostelecký, Search for Lorentz violation in short-range gravity, Phys. Rev. D **91**, 092003 (2015).
[54] V. A. Kostelecký and S. Samuel, Phenomenological Gravitational Constraints on Strings and Higher-Dimensional Theories, Phys. Rev. Lett. **63**, 224 (1989).
[55] V. A. Kostelecký and S. Samuel, Gravitational phenomenology in higher-dimensional theories and strings, Phys. Rev. D **40**, 1886 (1989).
[56] R. Bluhm, N. L. Gagne, R. Potting, and A. Vrublevskis, Constraints and stability in vector theories with spontaneous Lorentz violation, Phys. Rev. D **77**, 125007 (2008); **79**, 029902(E) (2009).
[57] C. A. Hernaski, Quantization and stability of bumblebee electrodynamics, Phys. Rev. D **90**, 124036 (2014).
[58] R. Bluhm, Explicit versus spontaneous diffeomorphism breaking in gravity, Phys. Rev. D **91**, 065034 (2015).
[59] P. Finsler, *Über Kurven und Flächen in allgemeinen Räumen, in German* (Gebr. Leemann & Co., Zürich, 1918).
[60] É. Cartan, Sur les espaces de Finsler, in French, C. R. Acad. Sci. (Paris) **196**, 582 (1933).
[61] D. Bao, S.-S. Chern, and Z. Shen, *An Introduction to Riemann-Finsler Geometry* (Springer, New York, 2000).
[62] P. L. Antonelli, R. S. Ingarden, and M. Matsumoto, *The Theory of Sprays and Finsler Spaces with Applications in Physics and Biology* (Springer Science + Business Media, Dordrecht, 1993).
[63] V. A. Kostelecký and N. Russell, Classical kinematics for Lorentz violation, Phys. Lett. B **693**, 443 (2010).
[64] V. A. Kostelecký, Riemann-Finsler geometry and Lorentz-violating kinematics, Phys. Lett. B **701**, 137 (2011).
[65] V. A. Kostelecký, N. Russell, and R. Tso, Bipartite Riemann-Finsler geometry and Lorentz violation, Phys. Lett. B **716**, 470 (2012).
[66] D. Colladay and P. McDonald, Classical Lagrangians for momentum dependent Lorentz violation, Phys. Rev. D **85**, 044042 (2012).
[67] N. Russell, Finsler-like structures from Lorentz-breaking classical particles, Phys. Rev. D **91**, 045008 (2015).
[68] M. Schreck, Classical kinematics and Finsler structures for nonminimal Lorentz-violating fermions, Eur. Phys. J. C **75**, 187 (2015).
[69] M. Schreck, Classical kinematics for isotropic, minimal Lorentz-violating fermion operators, Phys. Rev. D **91**, 105001 (2015).
[70] J. E. G. Silva and C. A. S. Almeida, Kinematics and dynamics in a bipartite-Finsler spacetime, Phys. Lett. B **731**, 74 (2014).
[71] J. Foster and R. Lehnert, Classical-physics applications for Finsler *b* space, Phys. Lett. B **746**, 164 (2015).
[72] D. Colladay and P. McDonald, Singular Lorentz-violating Lagrangians and associated Finsler structures, Phys. Rev. D **92**, 085031 (2015).
[73] H. Hironaka, Resolution of singularities of an algebraic variety over a field of characteristic zero: I, Ann. Math. **79**, 109 (1964); Resolution of singularities of an algebraic variety over a field of characteristic zero: II, Ann. Math. **79**, 205 (1964).
[74] V. A. Kostelecký and M. Mewes, Signals for Lorentz violation in electrodynamics, Phys. Rev. D **66**, 056005 (2002).
[75] Q. G. Bailey and V. A. Kostelecký, Lorentz-violating electrostatics and magnetostatics, Phys. Rev. D **70**, 076006 (2004).
[76] S. M. Carroll, G. B. Field, and R. Jackiw, Limits on a Lorentz- and parity-violating modification of electrodynamics, Phys. Rev. D **41**, 1231 (1990).

[77] R. Jackiw and V. A. Kostelecký, Radiatively Induced Lorentz and *CPT* Violation in Electrodynamics, Phys. Rev. Lett. **82**, 3572 (1999).
[78] J. M. Chung, Radiatively-induced Lorentz and *CPT* violating Chern-Simons term in QED, Phys. Lett. B **461**, 138 (1999).
[79] M. Pérez-Victoria, Exact Calculation of the Radiatively Induced Lorentz and *CPT* Violation in QED, Phys. Rev. Lett. **83**, 2518 (1999).
[80] M. Pérez-Victoria, Physical (ir)relevance of ambiguities to Lorentz and *CPT* violation in QED, J. High Energy Phys. 04 (2001) 032.
[81] B. Altschul, Failure of gauge invariance in the nonperturbative formulation of massless Lorentz-violating QED, Phys. Rev. D **69**, 125009 (2004).
[82] B. Altschul, Gauge invariance and the Pauli-Villars regulator in Lorentz- and *CPT*-violating electrodynamics, Phys. Rev. D **70**, 101701(R) (2004).
[83] M. Gomes, J. R. Nascimento, A. Y. Petrov, and A. J. da Silva, Aetherlike Lorentz-breaking actions, Phys. Rev. D **81**, 045018 (2010).
[84] A. P. Baeta Scarpelli, T. Mariz, J. R. Nascimento, and A. Y. Petrov, Four-dimensional aether-like Lorentz-breaking QED revisited and problem of ambiguities, Eur. Phys. J. C **73**, 2526 (2013).
[85] Z. Shen, Landsberg curvature, *S*-curvature and Riemann curvature, in *A Sampler of Riemann-Finsler Geometry*, edited by D. Bao, R. L. Bryant, S.-S. Chern, and Z. Shen, Math. Sci. Res. Inst. Publ. (Cambridge University Press, Cambridge, New York, Port Melbourne, Madrid, Cape Town, 2004), Vol. 50.
[86] A. Deicke, Über die Finsler-Räume mit $A_i = 0$, in German, Arch. Math. **4**, 45 (1953).
[87] M. Matsumoto and S. Hōjō, A conclusive theorem on C-reducible Finsler spaces, Tensor (N.S.) **32**, 225 (1978).
[88] N. McGinnis, Finsler structures in the photon sector of the Standard Model Extension, Bachelor degree thesis, New College of Florida, 2014.
[89] B. Altschul, Vacuum Čerenkov Radiation in Lorentz-Violating Theories Without *CPT* Violation, Phys. Rev. Lett. **98**, 041603 (2007).
[90] V. Fock, *The Theory of Space Time and Gravitation*, translated from Russian by N. Kemmer (Pergamon Press, New York, 1959).
[91] O. Constantinescu and M. Crasmareanu, Examples of conics arising in two-dimensional Finsler and Lagrange geometries, Analele stiintifice ale Universitatii "Al I Cuza" din Iasi Serie noua Sectiunea 1a, Matematica **17**, 45 (2009).
[92] G. Randers, On an asymmetrical metric in the four-space of general relativity, Phys. Rev. **59**, 195 (1941).
[93] V. Perlick, Fermat principle in Finsler spacetimes, Gen. Relativ. Gravit. **38**, 365 (2006).
[94] R. G. Torromé, P. Piccione, and H. Vitório, On Fermat's principle for causal curves in time oriented Finsler spacetimes, J. Math. Phys. (N.Y.) **53**, 123511 (2012).
[95] Z. Xiao, L. Shao, and B.-Q. Ma, Eikonal equation of the Lorentz-violating Maxwell theory, Eur. Phys. J. C **70**, 1153 (2010).
[96] E. Zermelo, Über das Navigationsproblem bei ruhender oder veränderlicher Windverteilung, in German, Z. Angew. Math. Mech. **11**, 114 (1931).
[97] X.-J. Wu and C.-M. Xu, Null geodesic equation equivalent to the geometric optics equation, Commun. Theor. Phys. **9**, 119 (1988).
[98] M. Born and E. Wolf, *Electromagnetic Theory of Propagation Interference and Diffraction of Light*, 7th ed. (Cambridge University Press, Cambridge, England, 2005).
[99] G. Betschart, E. Kant, and F. R. Klinkhamer, Lorentz violation and black-hole thermodynamics, Nucl. Phys. **B815**, 198 (2009).
[100] I. S. Gradshteyn and I. M. Ryzhik, *Table of Integrals, Series, and Products*, 7th ed. (Academic Press, Burlington, San Diego, London, 2007).
[101] F. W. Dyson, A. S. Eddington, and C. Davidson, A determination of the deflection of light by the Sun's gravitational field, from observations made at the total eclipse of May 29, 1919, Phil. Trans. R. Soc. A **220**, 291 (1920).
[102] A. S. Eddington, *The Mathematical Theory of Relativity* (Cambridge University Press, London, 1923).
[103] D. Lynden-Bell and J. Katz, Gravitational field energy density for spheres and black holes, Mon. Not. R. Astron. Soc. **213**, 21 (1985).
[104] M. A. C. Perryman, K. S. de Boer, G. Gilmore, E. Høg, M. G. Lattanzi, L. Lindegren, X. Luri, F. Mignard, O. Pace, and P. T. de Zeeuw, GAIA: Composition, formation and evolution of the galaxy, Astron. Astrophys. **369**, 339 (2001).
[105] S. G. Turyshev, M. Shao, and K. L. Nordtvedt, Jr., Experimental design for the LATOR mission, Int. J. Mod. Phys. D **13**, 2035 (2004).
[106] S. G. Turyshev, M. Shao, K. L. Nordtvedt, Jr., H. Dittus, C. Lämmerzahl, S. Theil, C. Salomon, S. Reynaud *et al.*, Advancing fundamental physics with the laser astrometric test of relativity, Exp. Astron. **27**, 27 (2009).
[107] J. Evans and M. Rosenquist, "$F = ma$" optics, Am. J. Phys. **54**, 876 (1986).
[108] F. J. Belinfante, On the current and the density of the electric charge, the energy, the linear momentum and the angular momentum of arbitrary fields, Physica (Amsterdam) **7**, 449 (1940).
[109] H. Watanabe and H. Murayama, Redundancies in Nambu-Goldstone Bosons, Phys. Rev. Lett. **110**, 181601 (2013).